In situ blocked force measurement in gearboxes with potential application for condition monitoring

ALSDEG ABOHNIK

A thesis submitted in partial fulfilment of the requirements of the Salford University for the degree of Doctor of Philosophy

Acoustics Research Centre

School of Computing, Science and Engineering

University of Salford

Salford, UK

February 2018

Abstract

The use of gearboxes for power transfer is widespread throughout industry. However, machines today are operating at higher speeds than ever before and gear failures such as wear or tooth breakage is serious and legitimate concerns. Incipient fault detection in gears has thus become the subject of intensive investigation and at this stage of development, there are many competing condition monitoring methods based on vibration signal analysis.

This thesis summarizes the research steps taken after a review of (i) current maintenance strategies, (ii) gearbox condition monitoring techniques and gear vibration fundamental and common gearbox failure modes, (iii) new approach called in-situ blocked force.

A test rig was built, designed and fabricated for experimental data collection. The experimental work was carried out using a healthy spur gear and one suffering from tooth breakage with two levels of faults; 25% and 85%.

This study reports the use of the blocked force to characterize the gear mesh interactions; the advantage is to remove the effect of the housing, and to get a signal, which is more representative of the source mechanisms from which it is generated. Under certain assumptions the blocked forces are an intrinsic property of the vibration source. For example, a given vibration source, such as gear, hypothetically operating in the same conditions could produce different vibration signals when installed in different housings, however, the blocked forces theoretically are the same in both cases.

The blocked force represents a property independent of the noise generating mechanisms and is therefore invariant to the gearbox housing. It is proposed that this invariance yields a signal more amenable to fault detection.

In this thesis, assessment of the condition of a gearbox in a test rig is based on vibration analysis but, contrary to standard condition monitoring techniques, this research uses the blocked force signal instead of acceleration signals.

FFT has applied to transform the time domain signal to frequency domain and identify the spectrum of the shaft and mesh frequency. However, the low pass filter has been applied to filter the signal above the 1000 Hz and subjected to statistical parameters.

Conventional parameters using the time domain of the vibration signal (kurtosis, RMS, crest factor and skewness) were used for detecting and diagnosing the faults by applying them to filtered signals. As a result, the noise might be removed or reduced but the effect of the housing remains. Then, the total energy was also applied to detect the presence of the faults by combination with EMD, and the results compared with those obtained by the conventional parameters.

However, the blocked force signal obtained through the inverse procedure was filtered using the same filter which was used for fault detection alternatively to conventional signal. Moreover, the aim was to use BF as a signal for condition monitoring purposes.

Parameters (namely Kurtosis, crest factor and total energy) were then applied to filtered BF signals to identify the condition of the machine. The results obtained based on filtered BF signals were compared to ones obtained based on conventional signals.

The comparison between the results obtained from the acceleration signals and BF signals shows that (a) the blocked force can be used to remove or eliminate the effect of the housing; (b) the trends of kurtosis and crest factor and total energy are more consistent with the severity of the fault. Additionally, the parameters applied to the blocked force signals can offer more effective way of all those tested to detect faults than conventional acceleration signal at least for this case study.

Contents

List of Figures

List of tables

List of symbols

Table 1: Abbreviations

Degree of freedom	DoF
Condition monitoring	CM
Condition Monitoring System	CMS
Hilbert-Huang transform	HHT
Teager-Huang transform	THT
Teager-Kaiser Energy Operator	TKEO
Empirical mode decomposition	EMD
Principle component	PC
Principle component analysis	PCA
Hilbert transform	HT
Crest Factor	CF
Kurtosis	K
Root mean square	RMS
skewness	Sk
kernel principal component analysis	KPCA
Fast Fourier Transform	FFT
Digital Fourier Transform	DFT
Time synchronous averaging	TSA
Time domain averaging	TDA
Kernel principle component analysis	KPCA
Short-Time Fourier Transform	STFT
Fourier transform	FT
Ensemble empirical mode decomposition	EEMD
Intrinsic mode function	IMF

Multi-resolution Fourier Transform	MFT
Differential diagnostic	DD
Structural health monitoring	SHM
Smoothed Pseudo Wigner-Ville Distribution	SPWVD
Blocked force	BF
Finite element analysis	FEA
Singular value rejection	SVR
Frequency response function	FRF
Transfer Path Analysis	TPA

Table 2: Main symbols

Symbol	Meaning	Units
f_m	Mesh frequency	Hz
f_{sg}, f_{sp}	Sidebands around the fundamental gear mesh frequency	Hz
ω_p, ω_g	Rotational speed	rpm
f_s	Sampling frequency	Hz
f	Frequency	Hz
Y	Mobility	mixed
A	Accelerance	mixed
FRF	Frequency response function	mixed
$\boldsymbol{f}$	Force	N or N_m
v	Velocity	ms^{-1} or s^{-1}

a	Acceleration	ms^{-2}
$\bar{\boldsymbol{f}}$	Blocked force	N or $\mathrm{N_m}$
v_f	Free velocity vector	$\mathrm{m/s}$
a_{r}	Receiver acceleration vector	ms^{-2}

Table 3: Subscripts

Symbol	Meaning
S	Denotes source structure
R	Denotes receiver structure
C	Denotes coupled source and receiver structure
C	Denotes coupling source-receiver interface
B	Remote position on receiver
R	Reference position on receiver
i and j	Excitation and response DoFs
N	Number of terminals
M	Degree of freedom
M	Moment
−	The bar notation on $(\bar{\boldsymbol{f}})$ is used to denote a blocked condition

Table 4: Matrices and vectors

Symbol	Meaning
[ ]	Matrix
| |	Matrix determinant
m	Row number
n	Column number
N_p, N_g	number of teeth on pinion and gear

Declaration

No portion of the work referred in this thesis has been submitted in support of an application for another degree or qualification at this, or any other university, or institute of learning.

Date: ……

Signed: ……

Acknowledgements

The printed pages of this dissertation hold far more than the culmination of years of study. These pages also reflect the relationship with many generous and inspiring people I have met since the beginning of my postgraduate work. The list is long, but I cherish each contribution to my development as a scholar and teacher. It is to them that I owe my deepest gratitude.

I would like to thank my director of studies Pro. Andy Moorhouse for his understanding, support and guidance throughout the years I have spent at Salford University.

I would also like to thank my lovely wife and family, who have always supported, encouraged and believed in me.

Finally, I would like to thank my invaluable network of supportive, forgiving, generous and lovely friends without whom I could not survived the process, Meggitt Joshua, Duraid Y. Mohammed.

Thank you for everything

Chapter 1

Introduction

This chapter provides an overview of various strategies for the condition monitoring (CM) of engineering machinery and equipment. It introduces the idea of blocked force before providing information on a variety of existing CM systems and techniques available. It then introduces the aims and objectives of this research followed by a description of the structure and flow of this thesis.

1.1 Introduction

It is a common fact that machines contain combinations of various kinematic linkages mechanically assembled together. When these machines are in operating mode, these linkages produce characteristic sounds and vibrations, often termed as vibration signatures, which are specific to the individual machine depending on their structural design. Identification of these vibration signatures is of prime importance in determining, at an early stage, faults that could otherwise cause structural damage.

These days, run-to-failure is considered an expensive and inefficient approach to CM for most processes and manufacturing operations. Alternative CM systems that depend on the continuous collection and analysis of machine data have proved more acceptable and desirable because of their capability to offer early stage detection of machinery faults [1]. Selecting a suitable CM system is a significant part of guaranteeing increased machine availability, performance and life span, in addition to a reduction of spare parts stocks and breakdown maintenance.

CM methods have proved their worth in terms of efficiency, economics and convenience, with a variety of techniques used successfully to provide an efficient, reliable, and accurate CM method which can also be easily implemented [2, 3].

Research into, and implementation of continuous CM methods, has delivered the above-mentioned benefits, but the majority of implementations has been either on a specific type of machine or to cure a particular class of problem [4].

For example, internally the teeth on gears are often exposed to various sources of errors such as wear, backlash, play etc. These errors can result in geometrical misalignments, which can cause the entire mechanical assembly to vibrate. It is often impractical to monitor the vibrations

generated from the core elements such as bearing and gears during the operation of the gearbox due to reasons such as limited access to the assembly [5].

CM is often employed so as to provide advance warning of mechanical failure of e.g. gears and bearings. The benefits are that maintenance can be planned and down time avoided. CM conventionally applies signal-processing techniques to vibration signals, typically measured on housing. Other techniques, such as oil analysis, will not be considered in this thesis. However, condition-based maintenance (CBM) is a maintenance program that recommends maintenance decisions based on the information collected through condition monitoring [4, 5]. Diagnostics and prognostics are two important aspects in a CBM program. CBM plays an important role in reducing unscheduled machine downtime and avoiding catastrophic accidents in industrial enterprises. The following section presents current maintenance strategies.

1.2 Maintenance strategies

Selecting the most appropriate CM system is important to maximise machine availability, performance and life span, and minimise spare parts inventories and break down maintenance [6]. Companies search continuously to find the best methods to reduce the cost of maintenance; mitigate possible injuries to personnel or damage to the local environment. However, the main objective of maintenance is to prevent machine and/or production failure and production losses. Maintenance strategies can be divided into three different categories:

- **Breakdown maintenance:** Machines are run until they fail, and are then repaired; a crude method of operation that can be very expensive in terms of lost output and machine damage, it may also lead to dangerous occurrences [7].
- **Preventive maintenance**: Also called time-based maintenance, machines are thoroughly inspected and tested at set intervals and any necessary maintenance carried out to remedy faults present found within the system [8].

- **Predictive maintenance**: This strategy requires continuous monitoring of equipment to detect and diagnose defects. Only when a defect is detected, is maintenance work planned and executed [2].

The main objectives for maintenance can be summarised as follows [2]:

- To improve/maintain productivity.
- To minimize the number of repairs and replacement routines.
- To extend the life of the machine.
- To ensure a high quality of products.

For maintenance, the plant equipment can be classified into three categories [2].

1. **Critical equipment:** expensive to repair, or takes a long time to repair.
2. **Essential equipment:** affects the next stage of the process.
3. **General equipment:** is not critical to the process and does not affect plant operations when it is broken.

1.3 Condition Monitoring

CM of machinery is defined as the process of detecting and diagnosing faults within machines enabling prevention of failure of critical and essential machinery [3, 9].

The fundamental purpose of CM is to ascertain reliability/unreliability of a machines' mechanical condition through measurement of pertinent properties of the system such as temperature, oil pressure, electrical current, vibration level and performance level [3].

For a successful CM system the following four stages may be carefully considered; sensor selection, feature extraction, feature comparison and decision process determination, see Figure (1.1).

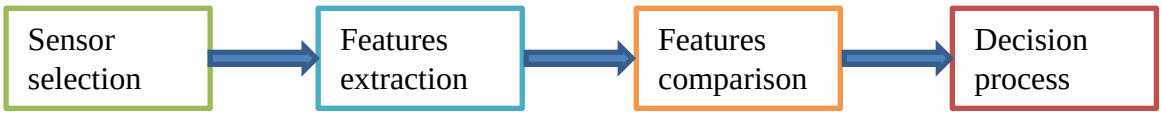

Figure 1-1 Condition monitoring system implementation

The demand for CM has increased as companies have tried to minimise the consequences of machine failures, use existing maintenance resources more effectively, and increase profitability. Some of the technical factors which have increased this demand include [10]

- The increased cost of maintenance due to increased labour and material costs.
- Increased automation of production to maintain competitiveness.
- The expectation of increasing quality of products by customers.
- Increased quality required to meet new product liability legislation.
- Increased safety and reliability expectations reinforced by current legislation.

1.4 Types of Condition Monitoring Systems

These days, run-to-failure is an unwanted approach for most processes and manufacturing operations. The present strategy is to implement methods, which may be more complex and expensive at the implementation stage but can be cost effective in the long run. These include strategies such as real-time detection systems which can provide real-time information for the engineer to allow detection and diagnosis of a fault in its very early stages [3]. Selection of a suitable and appropriate advanced CM system can significantly improve cost effectiveness in terms of efficient performance of the machine which can promise a longer lifespan while minimising unnecessary downtime [6].

There are two types of such CM systems: periodic and permanent. Periodic monitoring (also called off-line CM) is a system in which the machine data is recorded periodically and saved for analysis at a later stage. The analysis may be done in an office environment where there would be techniques available for advanced data analyses [9].

In contrast, the permanent monitoring system comprises a permanently mounted set of sensors or transducers, which can provide data continuously. Although the permanent mounting of sensors may be relatively expensive, this has advantages in scenarios such as:

- unavailability of suitable personnel to perform maintenance tasks, such as is often the case in remote sites, e.g. offshore pumping systems
- continuous monitoring is required to detect the fault at as early a stage as possible to avoid failures
- an immediate response is required to shut down the whole system; and
- in hazardous environments where, for example, the presence of high temperatures, toxic or poisonous gases, exclude the possibility of a human carrying out the necessary maintenance measurements [9].

Conventionally, signal-processing techniques are applied by CM systems on various types of signals. These signals may be vibration or sound pressure levels, thermal variations and dangerous emissions. The determination of all or any of, these signals can lead to efficient fault detection within the associated mechanical parts such as gears, bearings, shafts etc. Figure (1.2) is presented the generalized theory of condition monitoring [9].

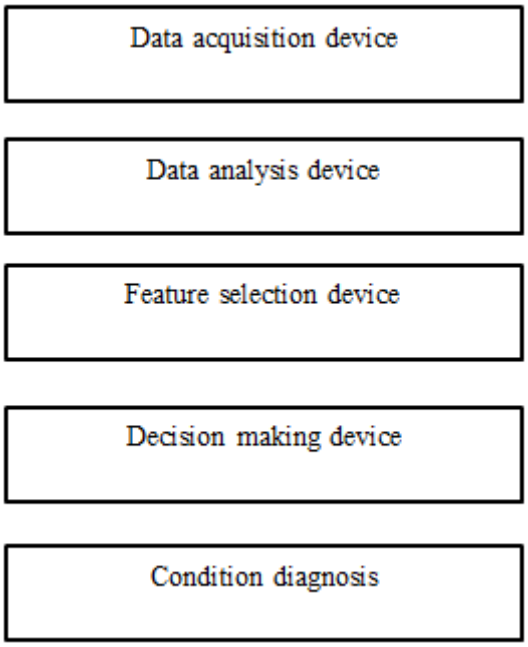

Figure 1-2 Condition Monitoring framework [11]

As can be seen from the figure (1.2) the first box shows that there is a data acquisition device, whose primary function is to acquired data from the system. Examples of these would include measurement devices such as thermometers, accelerometers, or strain gauges. The second box comprises the data analysis device, whose function is to analyse the acquired data. Many methods, some of which will be described in the next chapter have been proposed in this regard. The methods include using wavelets, the Fourier transform, and the Wagner-Ville distribution. Feature selection is a process where specific aspects of the data, which are good indicators of faults in the structure, are identified and quantified.

The decision making device is an infrastructure whose primary function is to take the features and interpret these features. The outcome of the decision making device is the identification of faults [11].

1.5 Condition Monitoring Techniques

Specific CM techniques are often associated with specific measurement types [12]. Although the following section provides details of the above measurement types, vibration analysis

technique is emphasised in this thesis and therefore the trend of this report will gradually focus on it. For completeness sake the following sections presents all the above measurement methods, even though the techniques will not be used in this research. CM techniques in common use today;

1.5.1 Vibration Monitoring

Vibrations are a repetitive response of a system caused by the non-uniform movement of components. Vibrations in healthy machinery arise due to unbalance, transmission error in gears, rolling contact of bearings and impact of other parts. However, as faults develop then additional sources of vibration arise due to such factors as wear causing loosening of parts, bearing faults, gear tooth breakage, cracks in components, corrosion, etc. In addition, all components in the assembly generate their own unique frequencies depending on the nature of their geometries and operation, and the type of fault that occurs [13].

Vibration analysis is one of the most important condition monitoring techniques that is applied in real life. Most of the defects encountered in the rotating machinery give rise to a distinct vibration pattern (vibration signature) and hence most faults can be identified using vibration signature analysis techniques. Vibration Monitoring is the ability to record and identify vibration “Signatures” which makes the technique so powerful for monitoring rotating machinery.

Vibration measurement has been widely used to detect and monitor at least the following conditions on rotating machines [13]:

- Misalignment and/or damage of gear teeth,
- Unbalance parts in rotating machinery,
- Pits and cracks in the component parts of rolling element bearings,

- Misalignment and cracks in shafts,
- Loose parts including excessive wear in e.g. sleeve bearings,
- Deterioration due to a wide range of causes: broken parts, corrosion, erosion, etc.
- Component resonance.

As mentioned above, vibration analysis is one of the most widely applied technologies for CM of rotating equipment, including gears and bearings because features extracted from the vibration signals can accurately reflect the condition of the machine. Also, it has been chosen for this work because it is easy to implement comparing to others such as airborne acoustics. This research focuses on the use of vibration analysis. However, we are trying to achieve more information about the source and for that the vibration is more useful to obtain the detailed information about the source.

1.5.2 Acoustic Monitoring

This technique measures the acoustic or airborne noise signals radiated from machines, because machines in which a fault causes vibration will invariably also produce noise. Microphones, which are relative easy to install, are used to pick up these sound signals. Microphones are remote and non-intrusive, have a higher frequency range than accelerometers and thus are capable of providing more information. This makes acoustic monitoring an attractive option for on-line CM. The biggest single problem with acoustic monitoring is usually the contamination of the signals by background noise [14].

1.5.3 Oil Analysis

This technique is based on analysing the machine's lubrication oil [2]. Oil analysis is performed during routine predictive maintenance to provide meaningful and accurate information on lubricant and machine condition. It is mostly used on equipment for which it is difficult to carry out a vibration or airborne sound analysis, such as when many moving components are close

together, or when the transducer cannot be physically mounted at a suitable location. Oil analysis is typically used in compressors, gas turbines, reciprocating engines and gearboxes [10].

1.5.4 Thermal, Visual and Aural Monitoring

These are other monitoring methods, which use the senses of relevant personnel. These include touch to feel the temperature, visual to generally monitor the system, hearing to detect uneven sounds and smell for any signs of overheating or burning. The monitoring of temperature is also conveniently carried out by using advanced temperature monitoring systems such as thermal imaging cameras that detect thermal energy using infrared thermography technology. Due to their non-contact nature, these cameras can be used to monitor temperatures of electrical motors and other rotating components where wired thermocouples sensors are difficult to install [3].

1.6 Fault Detection and Diagnosis in Gears

Fault detection and diagnosis of vibration in machines is driven by the measurement of cyclic forces generated by the drive shafts. These are modulated forces and can increase with the rotational speed of the machine. It is often found that these occur in integer multiples. These forces can be representative of the type of fault that generates them, i.e. a broken gear tooth would produce a cyclic vibration at its meshing frequency, which is the product of the number of teeth and the gear's rotational speed.

Fault detection can be defined as: identification of the existence of a fault in machinery without knowing the root cause.

Fault diagnosis is defined as: identifying the fault, so that corrective actions can be taken.

Fault prognostics is defined as: enabling the prediction of failure in machines resulting in benefits to plant operators such as shorter downtimes, higher operation reliability, reduced operations and maintenance cost, and more effective maintenance and logistics planning.

1.7 Characteristics of Gearbox Vibration

At this point, it is very important to understand the characteristics of vibration generation phenomenon prior to using vibration as an effective and efficient monitoring strategy for a gear transmission system.

According to Welbourn, geometric errors are the prominent sources of gearbox vibrations: i.e. the difference between the actual orientation/position of the gear and the ideal orientation/position of the gear [15]. These geometric errors can be divided into imperfections inherent to the gears i.e. errors built-in at the time of the manufacture, and elastic deformations at the time of teeth meshing, all of which contribute to the overall vibration produced in the machine.

As explained earlier, vibrations are produced at the gear meshing frequency and transmitted; however, there may be multiple harmonics present. The important factors for any CM method are the sidebands to these frequencies, which are separate from the gearbox shaft frequency.

Randall [16] classified the main causes of the vibrations generated by the gear meshing, due to:

1) Deviations from the ideal tooth profile producing a vibration signal at f_m, the tooth-meshing frequency,

2) Variations in tooth loading which generate amplitude modulation,

3) Fluctuations in the rotational speed, and/or non-uniform tooth spacing which produce frequency modulation effects, and

4) Local tooth faults, which generate additional impulses.

When meshing of the gears takes place, both the magnitude and direction of the load on the tooth become time-variant which causes the tooth deflection to vary [17]. This results in the production of a dominant vibration at the gear meshing frequency and its harmonics f_m ;

$$f_m = \omega_p N_P = \omega_g N_g \tag{1-1}$$

where N_p, N_g = number of teeth on pinion and gear respectively and ω_p, ω_g are rotational speeds of the pinion and gear respectively (these frequencies can be expected to appear in the vibration signals).

The sidebands around the fundamental gear mesh frequency are given by the sum of the mesh frequency and rotational speeds of the gear or pinion [10].

$$f_{sp} = f_m \pm \omega_p \tag{1-2}$$

$$f_{sg} = f_m \pm \omega_g \tag{1-3}$$

where f_{sp}, f_{sg} are sidebands around the fundamental gear mesh frequencies.

Each gear set generates a unique frequency spectrum, which is highly dependent upon the speed of rotation of the participating gears [18]. The important fundamental gear-mesh frequency is the product of the number of gear teeth and the speed of rotation of the gear. The gear-mesh frequencies can show as transients in the spectrum when the transmission is subjected to angular acceleration and as harmonics is operating at a steady speed [4].

Today, it is common practice to place an accelerometer on, say, a gearbox housing and measure the vibration even though the measurement point is some distance away from the gearbox components, which are the actual source of the vibration. Such an approach separates the source from the measuring sensor, and the vibration signal actually measured may not

completely represent the actual vibration of the source [19]. This research will use an inverse method, which has the ability to propagate the vibration back to its source from signals measured on the surface of housing, thereby potentially removing the effect of the housing.

Generally, the vibration or other signal acquired from machine housing, will be composed of a number of components including background noise and resonances, and will include the effect of the housing on the signal, which can be a major issue for the standard CM techniques. Whilst the effect of the noise can be removed, or at least reduced, in measured data, the effect of the assembly housing remains. However, signals contaminated with noise can be cleaned by being filtered to remove the noise and leave the data associated with the actual fault [20].

In this work it is proposed that in-situ blocked force approach [19] be used to remove the effect of the housing, leaving data more suited to CM techniques. The blocked force is the force required to constrain mechanical interface (such as the gearbox housing) so that its velocity is zero. Pre-determined frequency response functions (FRFs) measured on the coupled assembly can be used to back-propagate the signals to a source location. This method has becoming increasingly popular in vibro-acoustics because of its ability to independently characterise structure-borne [21-23].

This research will assess the applicability of the blocked force method to machine CM, and its possible advantages when testing both healthy and faulty gears. Results will be compared to those obtained by other signal types, such as housing acceleration.

It is hypothesised that the blocked force method (BF) will improve consistency in the measured signals from a given component, even when the sensor is mounted on a variety of different machines and that this will lead to more, robust and repeatable fault detection criteria.

1.8 Aim

The aim of this research is to test the use of the blocked force method to determine if there is a significant advantage in using the blocked force signal as opposed to housing acceleration or radiated sound pressure for CM purposes, specifically the detection and diagnosis of fault signals from a gearbox.

1.9 Objectives

In order to achieve above aim, the following objectives will be adopted:

1. Review the most successful signal processing methods used for identifying common gear failure modes.
2. Introduce existing conventional signal processing and analysis methods such as time-domain and frequency-domain.
3. Review the blocked force method and its applications.
4. Design and construct model gearbox.
5. Carry out preliminary measurements on an existing test rig.
6. Implement to detect the seeded faults and evaluate their severity using simple and more advanced signal processing analysis.
7. Implement the same signal processing analysis to detect faults based on blocked force signals.

1.10 Organisation of the Thesis

This thesis is organised as follows:

Chapter 2: surveys the literature on signal processing techniques used to process CM signals.

Chapter 3: Focusses on illustrating the blocked forces. The basic concepts of blocked forces are explained. Source activity of source parameters is introduced. Also it provides an introduction to the inverse problem, with a review of the mathematical background of inverse

methods. The matrix inversion method for the indirect determination of operational forces is reviewed. A simplified measurement procedure, using a fully defined receiver structure, is proposed for the determination of approximate blocked forces.

Chapter 4: Presents the test rig, accelerometer mounting techniques, the data acquisition system and the test rig components.

Chapter 5: Presents some of preliminary measurements of blocked forces using a simple beam structure and complex gearbox test rig.

Chapter 6: Reports the application of fault detection techniques to identify faults in the model gear.

Chapter 7: Reports the use of blocked force signals to enhance fault detection in the model gear.

Chapter 8: Discussion, conclusion and recommendations for future work.

Chapter 2

Background and context

Many condition monitoring techniques and technologies have been established with the intention of achieving the efficient detection and identification of faults within the mechanical transmission system. This chapter presents a review of relevant literature concerned with the condition monitoring of gearboxes using vibration signals. The time domain, frequency domain and time-frequency domains of the measured signals are discussed, and simple and more complex parameters for their analysis and fault detection are presented.

Usually, the measurement emphasis is on the use of accelerometers sited on the gearbox housing to detect vibrations from the core elements and identify the main sources of vibration. This chapter introduces briefly the in-situ blocked force as a possible alternative to housing vibration for general use in vibration fault detection and diagnosis (or prognosis).

2.1 Introduction

Condition monitoring (CM) is the process whereby a particular system, usually industrial machinery, has certain selected parameters monitored and any significant change in one or more of those parameters is taken to be an indication of a developing fault [11].

Each machine has a specific vibration signature related to the structure and the condition of the machine. The vibration signature will also change with change of state of the machine. A change in the vibration can be used to detect incipient defects. This is the basics of condition monitoring methods [24]. Condition monitoring can help to increase the profit of an organization through increased maintenance efficiency and by reducing the risk of accidents by preventing interruptions. Moreover, approximately 65% of industrial machinery failure is due to failure of gears such as pitting, spalling, cracking, wear [24]. This vibration mainly occurred due to excessive fault.

Generally, damage to a system is any change in the system that adversely affects its current or future performance [25]. Obviously, it follows that damage is meaningful only if a comparison can be made between the healthy condition and the second condition. Thus the concept of damage extends to changes to the geometric and/or material properties of the system which adversely affect system connectivity and boundary conditions, to the detriment of present or future performance [26].

Commonly, damage releases energy, which is converted into vibrations. It is therefore possible to record and describe damage by examining the signal energy and signal power [27]. The damage types have different effects. They cause measurable physical phenomena, the signal characteristics of which permit a classification into damage types [28].

Presently, CM is advancing at a rapid rate due to the development of numerous digital signal-processing techniques that are being applied for fault detection, diagnosis and prediction of

remaining life [25]. Generally, signal processing used for machine health diagnosis can be divided into time-domain analysis, frequency domain analysis, and joint time-frequency analysis [25, 29].

Information contained in the vibration signal, and released on analysis, enables the planning of effective maintenance action [5, 30]. Information gained from the vibration signal allows the assessment of the health of the machine and stage of degradation, which is crucial for making maintenance decisions and predicting time to failure. Predictive methodologies have been developed based on physics-based modelling, system dynamics, data-driven evolutionary trends, statistical reliability, etc., [31].

Diagnosis of a fault, for example, generally involves fault detection, isolation and identification. An abnormal condition is detected, the defective component determined and an estimate of the nature and extent of the fault made [32, 33]. Prognostics is the ability to accurately predict accurately the remaining life (time to failure) of a component, machine or system [31, 33]. Such an approach can improve system reliability, effectiveness of maintenance and logistic planning [34]. Prognostics has attracted considerable interest from both industry and the research community, and prognostic systems are being successfully used for monitoring the health condition of relatively simple rotating machines [35]. However, today, the complexity of machines and their associated systems is increasing rapidly, and there is a pressing need to develop prognostic techniques for real world complex systems [35].

Vibration signal analysis is well-suited for the CM of gearboxes because changes in the vibration signature is highly likely to be the result of a change in the condition of the gearbox. This is because defects such as a damaged tooth on a gear will alter both the magnitude and phase modulation of the gear's vibration. Thus, in theory, changes in the vibration signal can be used to give some indication of the existence of a fault [36, 37].

It has been shown that the amplitude of the vibration signal will depend on both the magnitude and physical properties of the forces involved [38]. In addition, other sources of vibration will be present due to unwanted variations in the geometric and mechanical characteristics of the gears, these include the tooth stiffness, shaft misalignment, errors in gear profile and pitch, gear eccentricity and change in load on each tooth as a function of the angle of rotation [38].

A number of techniques for condition monitoring have been developed during the last decades. These techniques generally include three basic steps; measurement of a physical quantity, determination of suitable condition monitoring parameter with advanced signal processing techniques and comparison of that parameter to standard values. The following section briefly discusses fault detection techniques.

2.2 Techniques of Fault Detection

A number of studies are presented on fault detection of gearboxes using various vibration analysis methods. Here we are going to review some of techniques used to detect and diagnose faults of gearboxes using vibration analysis. These techniques can be categorised into three areas: Time domain approach, Frequency domain approach and Time-Frequency domain approach.

Typically, fault detection begins with the time-domain of the transducer signal (which will often be the output of an accelerometer) and many useful parameters can be extracted using time-domain statistical analysis.

The condition of any rotating machinery can be estimated using techniques, which vary from simple level measurements to advanced signal processing. The main idea is to determine a relevant diagnostic parameter representing the degree, or state of development, of a fault.

To extract relevant parameters, the time domain output signals from any measurement system are required to be interpreted and associated with faults in that machine. Industry, based on a

mix of trial and error, and engineering analysis, uses a number of parameters that have been assessed as suitable for the purpose of detecting the presence and level of a defect [39, 40]. Statistical analysis is used to define the time-domain signal.

In CM the most commonly used statistical parameters for signal assessment are the peak value, Root Mean Square (RMS) a measure of the energy contained within the signal, Crest Factor (CF) the ratio of peak value to the RMS value, and Kurtosis (K). These measures are well established for assessing the condition of gears [36]. Stevens et al., claim that such measures are most suitable for detection and diagnosis of faults when the faults add periodic pulses of short time duration onto the base vibration signal [41]. CF has been shown to be a sensitive indicator of the presence of incipient faults but as the damage progresses and becomes well advanced the CF value falls to the level of the undamaged components because the vibration signal becomes more random in character. Thus, statistical analyses based on CF and kurtosis are generally not suitable to detect the later stages of motor defects [42].

These measures require the implementation of some form of averaging to help eliminate random noise. The simplest form of averaging is time domain averaging (TDA) [43, 44] which is the simple sum of equal length samples of the time domain signal and is a well-known method used with time-series analysis. Time synchronous averaging (TSA) is a more advanced noise reduction technique. If the system is undamaged, these methods of averaging produce useful time-series features. However, if there is a high variance in the residual error signal, i.e. as in the case of a damaged system, they may fail to produce usable predictions [45].

To acquire frequency domain information from the time domain, transformation is necessary and this can be done using the Fourier Transform (including the Fast Fourier Transform (FFT) and Digital Fourier Transform (DFT)) and time-frequency techniques [5], which may be complex and costly to implement, especially when dealing with a non-stationary signal. The

Fast Fourier Transform (FFT) is a historically important and commonly used transformation method, which converts a signal from the time domain into the frequency domain. The product of this conversion is a power spectrum that shows the energy contained in the specific frequencies of the time domain signal. This is very useful for analysing stationary signals whose frequency components do not change over time.

Domain transform is a well-known classical signal processing technique and utilizes both Fourier and Inverse-Fourier analyses that estimate the spectrum (Fourier) and cepstrum (Inverse-Fourier) of the signals. The measured spectrum/cepstrum of a damaged gearbox is compared with the spectrum/cepstrum for the normal (undamaged) condition. This is often followed by the application of appropriate filtering to isolate frequency bands believed to be associated with specific kinds of faults. In a similar context, transformed domain analysis, envelope analysis, can also be performed to enhance the features obtained [46, 47].

It is possible to view both time and frequency information simultaneously in a three or two dimensional time frequency plot. The changes in particular frequency components may be related to particular instances in time, allowing the possibility of improved fault location [48]. Each method of time-frequency analysis has its own advantages/disadvantages, but they all require the setting of a number of parameters such as window type (e.g. Hanning), length and overlap and lead to very similar time frequency results. The Short Time Fourier Transform (STFT) was developed to overcome such problems and can be considered as a compromise between time-frequency based analyses of a signal. The STFT exploits a time window to divide the main signal into smaller parts, each part is then assumed to be a stationary signal allowing application of the FT [49]. The process is referred to as the STFT because the main signal is separated into small time intervals. Therefore, it can generate varying spectrum distribution for distinct time windows [48].

Empirical mode decomposition (EMD) decomposes the signal waveform into multiple intrinsic mode functions (IMFs) without leaving the time domain; these tend to be non-linear and non-stationary. Each of these IMFs is considered to be produced by a separate source with its own temporal characteristics. The functions into which a signal is decomposed are not only all in the time-domain, but they are of the same duration as the original signal, which allows for variations of frequency with time to be retained.

A variety of methods have been developed in combination with EMD such as time-frequency analysis with AM-FM demodulation (the Hilbert-Huang transform - HHT) [50, 51]. The Teager-Kaiser Energy Operator (TKEO) that measures the instantaneous energy of signals composed of a single time-varying frequency, and the Teager-Huang transform (THT) with improved signal-noise ratio to investigate faults in gears which, however, has the disadvantage of being unable to estimate frequencies higher than 1/4 of the sampling frequency [52-54]. The parameter which called Total Energy is based on the calculation of energy and uses curve fitting for the meshing frequency and its sideband zones, which is combined as well with EMD for fault detection in wind turbine blades and three phase induction motors [48, 49].

He et al., [64] presented principal component (PC) representations of the measured signals to monitor machine conditions. The principal component analysis (PCA) technique was applied to extract the PC representations for the vibration signals using statistical features for the time- and frequency-domains. They found that the PCA method was effective for machine CM when applied to vibration signals collected from an automobile gearbox.

Another technique known as Kernel Principal Component Analysis (KPCA) has been used to extract nonlinear features from both time and frequency domains of vibration signals [55]. The KPCA was a development of Principle Component Analysis (PCA), with an improvement in

clustering capability [56]. KPCA has been further improved by using two different subspace structures that can usefully be applied during the CM monitoring of gearboxes [55].

A combination of the strengths of KPCA with Ensemble Empirical Mode Decomposition (EEMD) was presented in [57]. The proposed method was named the EEMD-based multi-scale KPCA, and it provides a capable tool for treatment of non-linear multi-scale data and was shown to be sensitive to gearbox faults.

Although the techniques and methods described can detect and diagnose faults, and provide an estimation of time to failure in rotating machines, there are still limitations to their applications. However, a large number of the vibration analysis techniques reviewed here do not comprehensively take into account the vibration characteristics. In addition, not all have been tested for detection of incipient faults, or for all machine components, and not all of them have been used for predicting remaining useful life.

2.3 Gears and type of faults

This section presents the gears, and gear faults with an emphasis on the spur gear and tooth breakage, which are considered in this thesis. The gear is one of the most an important and widely-used mechanical elements in rotating machines [58]. Industrial gearboxes are employed to transmit torque and rotary motion from an input shaft to an output shaft. In industry, breakdown of such crucial components can cause heavy financial losses. Gearboxes have limits on vibration and temperature levels which should be adhered to as exceeding these limits will directly and adversely affect the whole system [5].

As the gear teeth start meshing, they will generate vibration, which travels via the gears to the mounting shafts, to the bearings and to the gear housing where it is detected, usually by an accelerometer. As the vibration travels outwards from its point of origin towards the sensor it will be adulterated by vibrations from a variety of other sources, so that sensor signals will usually need processing and, possibly, filtering [59].

There are various types of gears; spur, helical, bevel and worm gears are the most common types used in industry [60]. All have a driven wheel and a driving wheel, but differ in the arrangement and shape of the wheels. Spur gears were selected from the various types of gears available for the experimental work, on consideration of its proneness to failure due to tooth breakage.

2.3.1 Spur gears

The spur gear, see Figure (2.1), the simplest type of gear which is a toothed cylindrical wheel, is used to convert one drive speed to another, and transmit rotary motion and torque between parallel shafts [60, 61]. It is known that the operational efficiency of spur gears is much higher than for any other gear type and so involute gearing has found many applications in industry. Advantages of spur gears with involute profile can be listed as:

- Simplicity of design, relatively cheap to manufacture and easy to maintain,
- It is simple to change tooth thickness and centre distance (distance between the axes of the two gears in mesh),
- Spur gears are usually high precision products,
- Standard tools can be used to produce nonstandard involute gears,
- For spur gears a change in the centre distance does not result in transmission error,
- Spur gears impose only radial loads on the bearings so there is no end thrust.

However, spur gears are considered slow speed gears, but if noise is not a severe problem, spur gears can be used at almost any speed. Another disadvantage is that spur gears cannot be used where a change of direction between two shafts is required. This is because they have teeth that are parallel to the shaft (normal to the face of the gear).

Figure 2-1 Spur Gear[62]

Table 2-1 Types and Functions of Spur gear

Gear type	Subtype	remarks
Spur gear	Normal spur gears	• Generates less noise with optimum design • Lubrication required for steel pinion but not for plastic • High efficiency • Used for parallel shafts • Easy to design and produce • Single ratio of up to 1:10
	Internal spur gear	• Has compact geometry profile • Used in planetary gear production • Has the same function as normal gears

The gear with the fewer teeth is called the pinion. The speed of rotation is increased when the gear drives the pinion, and reduced when the pinion drive the gear. For this thesis, the spur gears have been chosen with the same number of teeth for ease of calculation of drive shaft speeds and likely vibration frequencies.

2.3.2 Helical gears

Figure (2.2) shows helical gears, which have inclined teeth (teeth cut at an angle to the face of the gear) on the surface of the wheel. Its operation is smoother and quitter as compared with the spur gear. It is mostly commonly used in transmission gearboxes.

Figure 2-2 Helical Gear[63]

2.3.3 Worm Gears

Worm gears resemble screws and thus can drive bevel, helical or spur gears, see Figure (2.3). Worm gears have the advantage that they can be used to translate rotational motion into translational movement. Another advantage is that they can be used to mesh non-intersecting, mutually perpendicular, shafts.

A valuable characteristic of the way in which worm gears mesh is that, when a worm gear turns, the meshing worm wheel also turns, see Figure (2.3), but turning the worm wheel will not turn the worm gear [61].

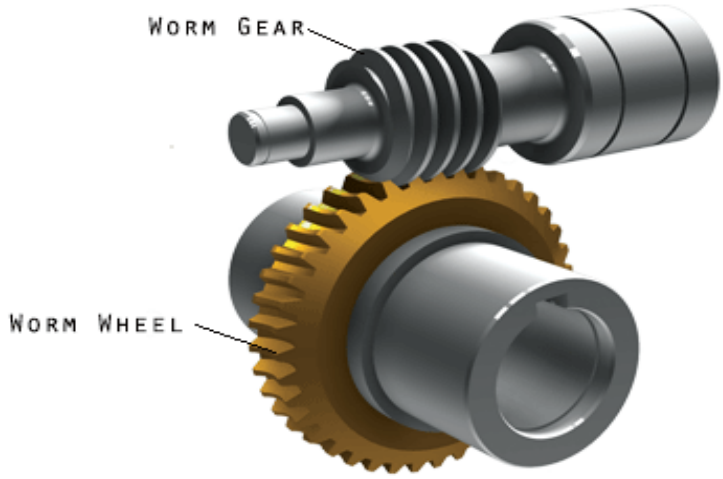

Figure 2-3 Worm Gear[64]

2.3.4 Bevel Gears

These are the gears, which transfer power between two non-parallel or intersecting shafts. These types of gears are most commonly used in the differential drives of automobiles. Bevel gears shown in Figure (2.4) are often used for power transmission between mutually perpendicular shafts. The gear teeth are straight cut to form base of a right circular cone and all point to its apex. The lines of the two shafts "intersect" at the apex of their respective cones. Disadvantage of bevel hears is that they generate considerable noise when run at high speeds and they cannot be used with parallel shafts [61].

Figure 2-4 Bevel Gear[63]

2.4 Type of gear faults (gear failures)

Gears are considered to have failed when they can no longer efficiently do the job for which they were designed. The cause of failure may range from excessive wear to catastrophic breakage. Many modes of gear failure have been identified, for example, tooth breakage, fatigue, wear, impact or plastic deformation.

The force transferred between the pinion and gear has an effect on the teeth, and will sometimes increase the stress on the tooth - thus tooth deformation can occur and tooth breakage is one of the most common causes of gear failure [5]. Such a failure is referred to as a gear failure mode. Following are short descriptions of several faults, starting with the most common; tooth breakage:

Tooth breakage:

Tooth breakage invariably starts with a small crack which begins at the weakest point on the tooth; see Figure (2.5), at the root of the tooth where high stress concentration combines with high tensile stress. The crack will then progress across the whole tooth. The precise direction of propagation of the crack is usually unpredictable, but in the majority of the cases it propagates downwards towards the rim of the gear [61].

This is the gear fault most likely to cause additional serious problems to other components such as bearings and shafts. Lin and Zuo [65] have described how this fault can lead to complete failure of the gearbox and the power transmission system.

Figure 2-5 Fatigue Crack in gear tooth root [66]

Breakage can occur in gears as shown in Figure (2.6), because of a sudden shock load, overload, or impact in excess of the ultimate tensile strength of the material of construction, or a break may be the result of numerous repetitions of stress, below the ultimate tensile strength, which weakens the metal and finally results in failure by fatigue [86]. Gears can fail due to excessive tooth breakage, due to bending stresses or wear.

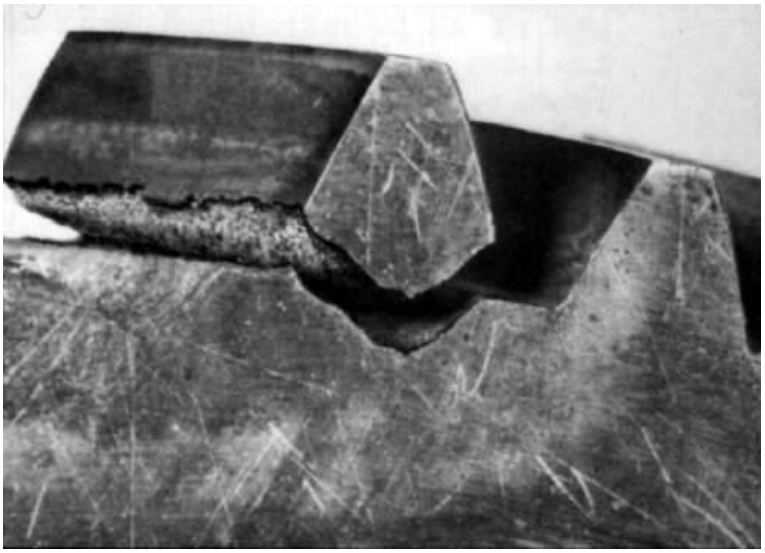

Figure 2-6 Gear tooth breakage[67]

***Pitting*:** is a form of surface fatigue as shown in Figure (2.7) and is due to the contact stress being greater than the surface fatigue strength of the gear material. Over time with repeated application (possibly millions of times) of the load, minute amounts of material are removed and a pit is formed. Once a pit is present it spreads at an accelerating rate because an additional impact load is imposed on the surrounding the un-pitted areas, causing fracture in a tooth already weakened [68].

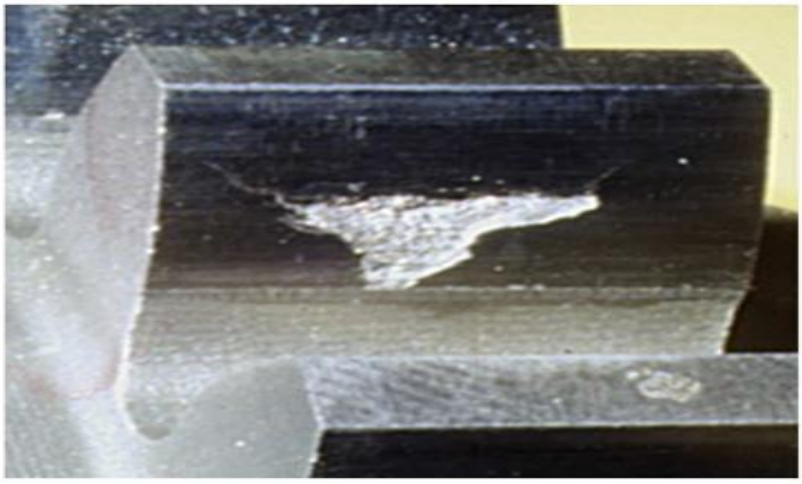

Figure 2-7 Pitting in a gear tooth [69]

***Wear failure*:** Wear is the removal of material at the point of contact between pairs of teeth. Figures (2.8) and (2.9) show typical gear tooth wear faults. As the teeth move in and out of contact, they experience local deformation in the region of the contact due to the mechanical forces in action [70]. If this deformation is excessive wear, (removal of a layer of material from the surface) can be rapid and the teeth will wear rapidly.

Wear usually takes one of two forms [66]: Adhesive wear - metal particles are transferred from one tooth to its mating tooth by a form of welding action; and abrasive wear - caused by abrasive particles being present in the meshing area.

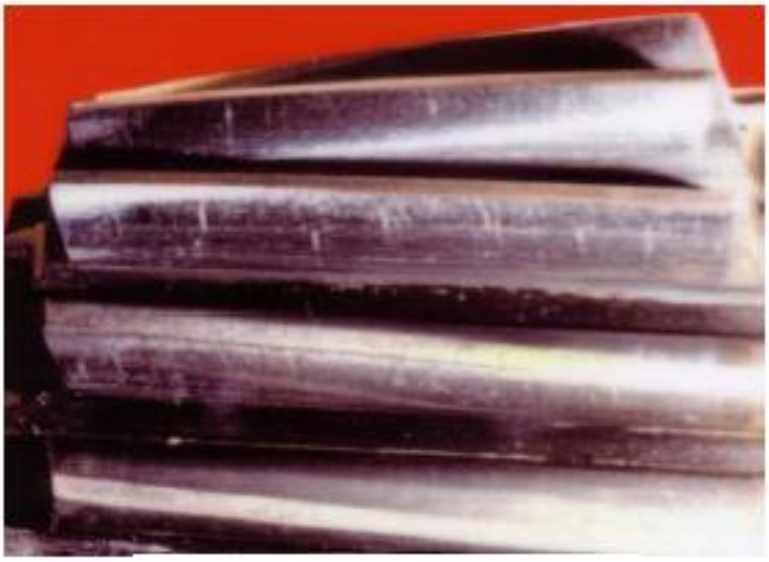

Figure 2-8 Photo of Gear Adhesive Wear [71]

Figure 2-9 Photo of Gear Abrasive Wear[71]

Crack: Fatigue is one of the most common forms of failure in gears. A fatigue crack in a gear tooth root usually begins in the root fillet and while the precise direction of propagation of the crack is usually unpredictable, in the majority of the cases it propagates downwards towards the rim of the gear, [66].

Additionally, distributed defects include misalignment and surface inaccuracies. Both distributed and local gear faults increase vibration levels. From the CM viewpoint, localized

defects are more important, especially tooth breakage because this can occur with little warning and its effect has been catastrophic in machines such as helicopters [72, 73].

Vibration is caused even in healthy gearbox by tooth meshing, gear shaft rotation, imbalance as well as by additional mechanisms due to the existence of a fault. The vibration measured as a result of the above mechanisms is further affected by the properties of the housing. To overcome the additional effect of the housing, an inverse method is proposed.

2.5 The proposed approach

In the previous chapter, proposed method called in-situ blocked force has been briefly discussed. It is an inverse method, which the acquired vibration signals are propagated back towards the excitation source to provide a more direct measurement of the actual source mechanisms. This method could be useful for CM because it might offer the possibility of (a) better fault location, and (b) establishing criteria for fault conditions [19].

Generally, the gearbox housing is considered to be passive and is excited by a number of embedded active mechanical components, such as bearings etc. To understand the vibration of the machine housing, the classical approach was to apply signal processing to the measured transducer signals to extract information about possible faults in the active components. Of course, the overall vibration signal is a composite signal which, when discretized, will reveal combinations of excitations coming from a variety of active components and resonances of the housing [19]. If the exciting forces can be determined and interpreted that could reveal more precise information about the nature of the active sources of vibration and which are potential faults.

Excitation forces can be determined by a number of existing inverse methods [74-77]. However, most of these would not be practical in the context of CM since they require the machine to be dismantled for certain measurements (such as frequency response function

measurements), which is not practicable because of the time required, the impossibility of separating the individual components in a gearbox, and the associated costs.

To overcome these and other similar problems, the in-situ blocked force method has been developed and offered the advantage that all measurements are conducted in-situ on the assembled machine [78], and thus offers the clear advantage that all measurements can be made at one place and with the gearbox in assembled form. So far, no published report has been found on using the in-situ blocked force method in the field of condition monitoring, specifically for detecting faults in rotating machines. To test this approach in the CM field for fault detection a gearbox test rig has been designed and built, and is fully described in Chapter 4. This test rig will be used for acceleration and blocked force measurements.

A variety of inverse methods exist by which the excitation forces can be determined [79-82], but most of these would not be practicable in a CM context because they require the machine to be dismantled for certain of the measurements.

This method has been recently used for the diagnosis and prediction of structure-borne sound and vibration inside vehicles [83, 84] and dwellings [85, 86]. The blocked force has since found applications within the fields of Transfer Path Analysis (TPA) [83, 87], dynamic sub-structuring (DS) [88, 89] and virtual acoustic prototyping (VAP) [90].

The aim of this research is to employ the same approach for the indirect measurement of blocked forces at the gear mesh point in a gearbox and to use the acquired blocked force signals for detecting the presence of seeded faults.

2.6 Summary

Much of the above-mentioned research work has been carried out to develop reliable methods and techniques for the purpose of fault detection in gears, but have not been fully successful. Proven techniques include vibration analysis but no single technique has shown itself to be a

universal method that can detect all machine faults. This research project focuses on detecting and diagnosing faults to determine if there is an advantage in using the blocked force signal as opposed to housing acceleration for condition monitoring purposes. The aim is to apply this new method to gearboxes to test its performance, to apply to a real machine some of the techniques that have been successfully applied in the laboratory.

Although the vibration measurement is the most widely used CM technique in industry due to its proven ability to detect the presence of faults, nevertheless, it is still limited when it comes to identifying total faults present and, currently, can identify only 60% to 70% of all machine faults [91, 92].

There remains a need to develop a universal technique to detect and diagnose faults at an early stage and predict remaining useful life for all rotating machinery components. Surveys report that these components (gears, bearings and shafts) that are the most likely causes of major machine breakdowns if the fault is not detected at early stages [49]. Despite signal processing-based fault diagnosis being widely used and found to be a powerful and effective tool, analysing, interpreting and diagnosing the complex signals faults produce requires considerable experience and expertise [93-95]. Thus, more consideration should be given to components and their types of faults to improve and develop the way of measuring them. Blocked forces may have the potential to do this because they have an inherent capability for noise reduction and signal enhancement. The use of blocked force signals will be investigated in this research as a means of developing enhanced CM techniques. In the following chapter, discussion with more details about the proposed approach: the in-situ blocked force will be given

Chapter 3

The in situ measurement of the blocked force of vibration sources

In the previous chapters, the background of condition monitoring, fault detection techniques, types of gears and their defects has been presented. A brief discussion has been given about the proposed blocked force method as well. This chapter introduces the blocked force concept and explores measurement methods to obtain the blocked force.

3.1 Introduction

In the previous chapter, a brief description was given about fault detection techniques, types of gear and faults, and a new approach, the blocked force method. In this chapter, more details are given about the blocked force method and its applications.

Vibration response of open assembly is caused by the internal forces and the transfer function is related to source and receiver. These internal forces are not easy to model or measure so, as an alternative, equivalent operational interface forces are typically used [84]. Also, in many situations, it is not easy to determine the direct load using, e.g., force transducers located at the connecting interfaces.

Blocked forces have an inherent capability for noise reduction and signal enhancement. They have been known and used for some time in such areas as prediction of structure-borne sounds in order to eliminate the noise source. Elliot and Moorhouse [78, 86, 96, 97],[83] have demonstrated how beneficial the blocked force method could be for the intrinsic characterization of the source. This research explores utilizing the blocked force method in the field of condition monitoring of machines. The method is proposed to be used in situ to perform all the measurement tasks at one place and with the gearbox in assembled form [78], which could offer significant advantages over other, more conventional methods.

This thesis will focus on exploring the use of the blocked force method in-situ and will also discuss all the potential benefits that this method could offer in the context of condition monitoring. Conventionally, the CM of machines has been performed by acquiring the vibration data from the machine housing and using these vibration signals to detect the underlying source of the fault signal. It is recognised that inverse methods require extensive measurements and management effort to be successful in the field. However, on the other hand,

these methods, have already provided established platforms for criteria for fault conditions and locations [19].

The inverse method procedure to successfully locate a fault is to discretize the housing structure into active areas, where the potential fault sources could be, and passive areas. The confidence with which the sections are obtained is heavily dependent up on selecting the correct boundaries when discretizing the housing, as there may be sources of faults that could be shared across boundaries. Generally, the source regions consist of components, which could generate vibrations; these include gears, etc. It has been noted that the frequency domain can be used to express the vibration fields in two parts 1) as the product of an excitation function acting at source boundaries and 2) as a matrix of frequency response functions between the boundaries and receiver locations [19].

It has also been the case that passive structures have been excited by the active components located in the active sections of the housing. During the condition monitoring, the signals obtained from the housing in this case are a mixture of the vibrations from active components and the resonance of the housing due to those vibrations. This causes extreme difficulties in identifying the actual source of the fault and offers a substantial challenge; to study the signals obtained and filter out the actual source of the fault and identify the condition of the components residing inside the housing. In situ measurements, when performed using the inverse method require the measurement of the frequency response function (FRF) prior to the analysis. The FRF is a passive property that describes the linear relation between an applied force and a resultant response. Thus, the passive measurement can be conducted by exciting the points with a known force (accelerometer positions at the interface or where it is easy to apply the force) which will be described later in chapter 5.

The accelerance A_{ij} of the structure (between DoFs i and j) is defined as the complex ratio of the acceleration response to the input force,

$$A_{ij} = \frac{a_i}{f_j} \tag{3-1}$$

where f_j is the force and a_i is the acceleration, i and j indicate the excitation and response DoFs, respectively.

An assumption here is that this ratio does not vary due to any of the factors such as the level, spectral shape or time characteristics of the input force. In addition, another assumption is that the source, as a system, is linear and does not vary with time. In other words, the machine housing is considered a linear, time invariant system.

It is possible to describe the passive properties of an assembly in any of the kinematic variables typically encountered, i.e. displacement, velocity or acceleration. It is possible to interchange between any of the above through integration or differentiation with respect to time. In this work we will deal exclusively with acceleration, since this is the quantity we measure directly. Mobility based methods in cited works are readily converted into accelerance form through the relations,

$$a = i\omega v \tag{3-2}$$

$$A = i\omega Y \tag{3-3}$$

Where a and v are the acceleration and velocity, respectively, and A and Y are the accelerance and mobility, respectively.

The examination of the advantages of the inverse methods must be considered in order to maximise them when condition monitoring [19]. One way to measure the forces is by inserting force transducers between the source and a structure. In this way the movement of the source may be prevented, which may also restrict the measurement of the true blocked force. However, force transducers need to be compressible (i.e. move) to function and so are not ideal for these types of measurements. Nevertheless, it is possible for the blocked force to be measured in this way over limited frequency ranges, though making measurement on any sort of complex structure poses extreme difficulties and uncertainties [19].

3.2 Source parameters

Sources of structure-borne sound have been, typically, categorized in terms that included both the dynamic properties of the structure and source activity. It is assumed that a "black-box" approach may be used in which an internal source induces an excitation which is transmitted by means of a linear, passive structure to the source interface [98]. With these assumptions it follows that the internal workings of the source may be assumed to be unknowable and need not be considered. It follows that the sources of observations may be adequately explained in terms the terminal outputs only. Either the blocked force and/or the free velocity at the terminals are sufficient to describe the active properties (i. e. internal excitation) of the source.

3.2.1 Source activity

The source strength (or source activity) depends on level and nature of the internal excitation. The internal excitation may be due to impacts, pressure fluctuations, frictional or rotating forces, though most often is a combination of such mechanisms. It is because direct measurement of the internal excitation mechanism is often practically impossibly, and always difficult, that the source activity is described in terms of measurements made at the source terminals [23].

When this method is useful for source characterization, it is necessary to define the passive and active properties of the source. In this thesis, the emphasis is different, which is not the source characterization, but simply we are looking for the signal represents the source mechanisms. We then can focus on active properties and neglect the passive properties.

3.2.2 Source, receiver and interface

Any structure can be divided into a source and receiver, coupled along an interface. The figure (3.1) illustrates the schematically source, receiver and the interface. The source is an arbitrary region of the assembly that contains all of operational components while the receiver is the remaining portion of this assembly. Where we placed the interface is a crucial decision but, to some extent, arbitrary provided the source mechanisms are all contain within the source.

Experimentally, it is a very important decision to choose where to put the accelerometers. For defining the interface, we are going to start with simple beam structure where the interface is the two-coupled points of the source and receiver beams, see chapter 5. Moreover, for more complex structure (gearbox test rig), two choices of interface will be investigated. In one, the 'source' includes the shaft and in the second it just includes the narrow region containing the mesh points. For the gearbox test rig, it is begun with the interface considered as the two supporting bearings and the shaft to define the blocked force on that region. The aim was to calculate the blocked force at the interface close to gear meshing points.

The point (c) at degree of freedom is used to separate the source and receiver. While (b) points are set of DoF on receiver that will be used later to characterise blocked forces and (r) is the remote reference point on receiver that is not in (b) will be used for validation purposes.

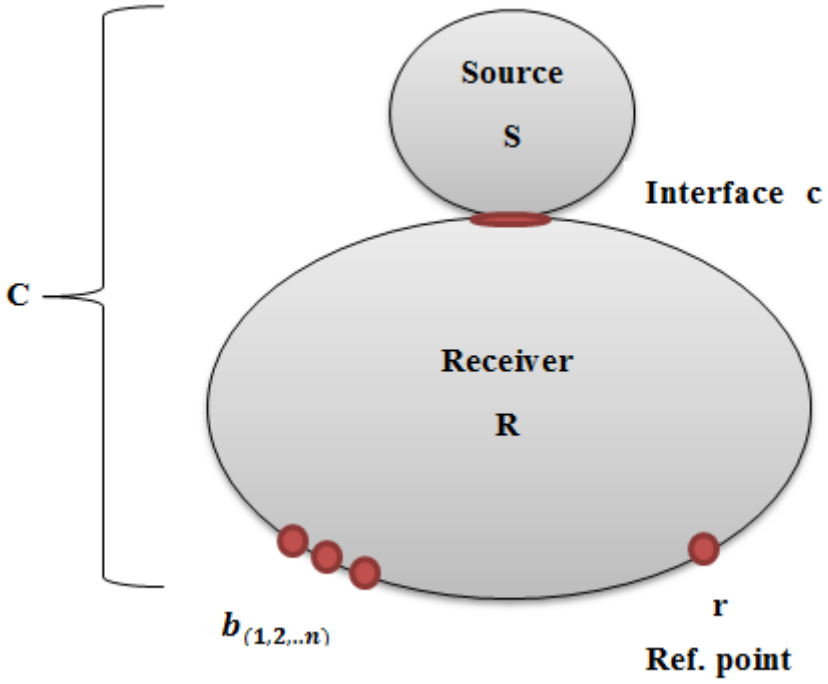

Figure 3-1 General schematic of source, receiver and interface

Free Velocity

Elliott and Moorhouse have defined the free velocity, $\mathbf{v}_{S_c}^{\mathbf{f}}$ (or equivalently, the free acceleration $\boldsymbol{a}_{S_c}^{\mathbf{f}}$ **,** where superscript **f** denotes a free quantity), as "the operational velocity, of the unconstrained source [96] it is measured at the terminals of the source when the generalized forces at those terminals are zero.

$$\mathbf{v}_{S_c}^{\mathbf{f}} = \left(\mathbf{v}_{S_c}\right)_{f_{S_c}=\mathbf{0}} \tag{3-4}$$

A necessary condition is that no other structure in any way limits the movement of the source. It is possible to approximate this condition for small sources by suspending the source elastically by, for example, springs of low stiffness, but there must be no connection at the coupling points. Larger sources could be placed on a resilient layer of such low stiffness that it has no effect on the measurement in the frequency range of interest. The measurement of free velocity is considered a relatively easy measurement for the characterisation of a structure-borne signal [23].

In other words, the free velocity of a machine (at a connection point) is the velocity manifested at that point when the machine is run under normal operating conditions but is freely suspended such that it is not connected to any external structure [99]. As the free velocity may be generated by various complex mechanisms acting at any point internal to the machine, no general model can be formed [100].

The disadvantage of the free velocity is that, it cannot be measured because the source is designed to operate whilst attached to a receiver structure. Simply, the source cannot be operated properly unless it is coupled to a receiver and hence the dismantling of the source-receiver assembly and free suspension of a source is problematic. Thus, measurements of free velocity are usually compromised and time consuming. An alternative to the free velocity is the blocked force [101].

Blocked force

With reference to figure (3.1), the blocked forces $\bar{\boldsymbol{f}}_{\mathbf{S_c}}$ (in this work the over bar will be used to distinguish the blocked force from the standard operational force) are defined as the forces required to counter an operational source's activity so that the velocity on the source-receiver interface is suppressed to zero.

$$\bar{\boldsymbol{f}}_{\mathbf{S_c}} = (\boldsymbol{f}_{\mathbf{C_c}})_{\mathbf{v}_{S_c}=\mathbf{0}} \tag{3-5}$$

where $\boldsymbol{f}_{\mathbf{C_c}}$ is the force exerted by the 'source' on the receiver structure and the subscript $\mathbf{v}_{S_c} = \mathbf{0}$ indicates that it is blocked at its boundary.

Which means the movement of the source is completely restricted. In practice, this can only be approximated as it requires an infinitely rigid receiver. Force transducers need to be inserted between source and receiver to measure the force. For several sources this modifies the mounting situation, yielding blocked force data which is not truly representative. The

measurement of blocked force is generally considered one of the more difficult measurements in structure borne source characterization [97].

Source activity for multiple degrees of freedom (DoF)

The dynamic characteristics of structure-borne vibration are usually expressed in terms of accelerance, and its reciprocal, impedance [88]. However, accelerance is the more practical to measure because while impedance measurements require the source terminals to be blocked for every degree of freedom (DoF), accelerance measurements have a more achievable constraint, requiring only the source terminals be free [102]. The latter is much easier to achieve practically. Thus, in what follows only the accelerances are described in any detail.

Blocked force and free velocity are both complex functions of frequency. They are linked by the mobility $\mathbf{Y}_{\mathbf{S_{cc}}}$ of the source, defined as follows:

$$\mathbf{v}^{\mathbf{f}}_{S_c} = \mathbf{Y}_{\mathbf{S_{cc}}}\bar{\boldsymbol{f}}_{\mathbf{S_c}} \tag{3-6}$$

The equation (3.5) uses vectors and matrices to show both multiple terminals and multiple DoF at each terminal. An overview of the matrix notation used in this thesis is provided in Appendix (A). For sources with M DoF at each terminal and N terminals, the blocked force and the free velocity terms extend to vectors with size $(\mathrm{NM}) \times 1$:

$$\mathbf{v}^{\mathbf{f}}_{S_c} = \begin{pmatrix} \mathrm{v}^{\mathrm{f}}_{S\,n=1,m=1} \\ \mathrm{v}^{\mathrm{f}}_{S\,n=1,m=2} \\ \cdot \\ \cdot \\ \cdot \\ \cdot \\ \mathrm{v}^{\mathrm{f}}_{S\,n=N,m=M} \end{pmatrix} \qquad \bar{\boldsymbol{f}}_{\mathbf{S_c}} = \begin{pmatrix} \bar{f}_{\mathrm{Sn}=1,m=1} \\ \bar{f}_{\mathrm{Sn}=1,m=2} \\ \cdot \\ \cdot \\ \cdot \\ \cdot \\ \bar{f}_{\mathrm{Sn}=N,m=M} \end{pmatrix}$$

Each entry in the vector a_{f} represents accelerations (either angular or linear) at one of the source terminals. Correspondingly, each of the vector entry in $\bar{\boldsymbol{f}}_{\mathbf{S_c}}$ may be considered a generalised force, describing either translationary or moment forces.

For sources with N terminals and M DoF at each terminal, the accelerance term extends to a square matrix of size $(NM) \times (NM)$. Figure (3.2) depicts the general case, $N = 1$, which represents a single point of excitation. 6 DoFs are involved in the excitation of the receiver structure; the $6x6$ accelerance matrix which represents the orthogonal forces $\boldsymbol{f}_x, \boldsymbol{f}_y$ and $\boldsymbol{f}_z$ and moments M_x, M_y and M_z. With the corresponding response quantities $a_x, a_y, a_z, \theta_x, \theta_y$ and θ_z; has the following form as in Eq. (3.6):

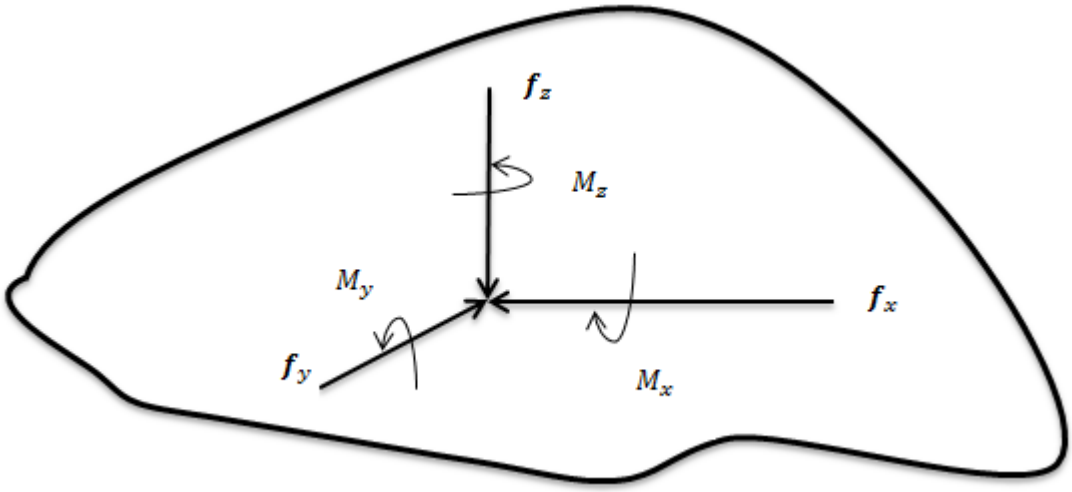

Figure 3-2 Point excitation, general case (after [103]). Six degrees of freedom are involved: three translational and three rotational components

$$\mathbf{A} = \begin{pmatrix} A_{a_x f_x} & A_{a_x f_y} & A_{a_x f_z} & A_{a_x M_x} & A_{a M_y} & A_{a_x M_z} \\ A_{a_y f_x} & A_{a_y f_y} & A_{a_y f_z} & A_{a_y M_x} & A_{a_y M_y} & A_{a_y M_z} \\ A_{a_z f_x} & A_{a_z f_y} & A_{a_z f_z} & A_{a_z M_x} & A_{a_z M_y} & A_{a_z M_z} \\ A_{\theta_x f_x} & A_{\theta_x f_y} & A_{\theta_x f_z} & A_{\theta_x M_x} & A_{\theta_x M_y} & A_{\theta_x M_z} \\ A_{\theta_y f_x} & A_{\theta_y f_y} & A_{\theta_y f_z} & A_{\theta_y M_x} & A_{\theta_y M_y} & A_{\theta_y M_z} \\ A_{\theta_z f_x} & A_{\theta_z f_y} & A_{\theta_z f_z} & A_{\theta_z M_x} & A_{\theta_z M_y} & A_{\theta_z M_z} \end{pmatrix} \quad (3\text{-}7)$$

For more than one source terminal, interaction between the terminals must be included. If there are N terminals, the source accelerance matrix will increase in size to $6N \times 6N$. Obviously, it would be very time-consuming to attempt to determine every matrix element experimentally. This is doubly true if it is required to obtain accelerances containing rotational DoF. Petersson

and Gibbs have suggested that three quarters of accelerance matrix involve translations or moments, while only one quarter consists of purely of translation motion [103].

In a practical situation, often only three DoF are taken into consideration; the force/acceleration normal to the surface f_z, and the two moments/angular accelerations about the in-plane axes (M_x and M_y) [23].

Source invariance

When characterising source strength using free velocity or blocked force, the activity of the source is assumed invariant of the constraints exerted on it by the receiver, it is assumed that whether in the Free State, or the blocked state, or any intermediate state, the internal source is assumed to act in identically the same way. It is accepted that this assumption has limits for some classes of sources of structure-borne sound [101, 104]. Such feedback will affect source activity and so "in-situ measurements", where the source is mounted in a manner that models the conditions of the actual installation, would appear better suited to obtain representative source characteristics.

Reciprocity

Reciprocity plays an important role for accelerance as shown in Equation (3.8). The theorem of reciprocity communicates the transfer function between positions 1 and 2 to the transfer function between positions 2 and 1. The accelerance matrix is symmetric, and the off-diagonal elements are related through the principle of reciprocity:

$$A_{ij} = A_{ji} \tag{3-8}$$

The accelerance function possesses a reciprocity property, which can be used to verify the measurement data. A simple comparison between the off-diagonal matrix elements can expose the problems with the measured data and provide an indication of the quality of the measured

accelerances. If the off-diagonal elements are of high quality, it is likely that the point accelerances on the diagonal are also of good quality.

3.3 Direct measurement (source characterization)

Free velocity can be measured directly quite easily by freely suspending the source. In theory, the blocked force can also be measured directly, but only approximately, using a large blocking mass.

The direct measurement of forces and moments offers greater challenges than the measurement of linear or angular velocity because the transducers used for the measurements must be inserted between the source and the receiver [101]. At present, both the transducers and methodologies exist for the direct measurement of the moments. Thus, it has been assumed that it is not possible to directly measure the operational moments [23].

There are two general strategies for characterising sources based on forces; (i) direct methods in which force sensors are used to measure the forces directly, and (ii) indirect methods, which do not use force sensors in the line of the force flux [23].

Unlike operational forces, the direct measurement of blocked force may only be approximated as it requires an infinitely rigid receiver. Like the operational force however, it has been shown that the blocked force may be acquired indirectly through an inverse procedure [105]. In this research, the indirect measurement will be adopted to obtain the blocked force. It is practically impossible to insert force transduces in gearbox to get direct measurement of the forces.

3.4 The inverse problem

The inverse problem is a popular researched topic [22, 23, 106] in which the general idea is to back-calculate the inputs to a system from knowledge of the outputs. When an inversion method is applied to matrices, principal challenges must be addressed. In general, the main challenge is concerned with inverse methods is ill-conditioning. If the conditioning is poor, the

answer is very sensitive to errors. So, in that case, the answer can be improved by over-determined.

Further to ill conditioning, careful manipulations of the FRF matrices may be required to successfully solve the inverse problem. Compared to the conventional CM methods available, the blocked force requires an additional stage in which the FRFs, which are used to characterize the machine's structure, are measured. This is the additional step, over and above standard CM measurements, that is required to solve the inversion problem [19]. More details with regards to the inverse problem are described in the following sections.

3.4.1 Fundamentals of matrix inversion

Before considering the inverse problem, we briefly discussed some fundamentals related to inversion matrix for completeness. A system of n linear equations can be written in matrix form [107-109],

$$\mathrm{z} = \mathbf{H}\,\mathrm{x} \tag{3-9}$$

Here, z and x are $n \times 1$ column vectors, and **H** is a $n \times n$ square matrix. (For an overview of matrix notations and definitions, see Appendix). To solve Equation (3.9) for x it requires an inversion of the matrix **H**:

$$\mathrm{x} = \mathbf{H^{-1}}\mathrm{z} \tag{3-10}$$

The inverse $\mathbf{H^{-1}}$of a $n \times n$ matrix **H** is defined as:

$$\mathbf{H^{-1}H} = \mathbf{HH^{-1}} = \mathbf{I} \tag{3-11}$$

where **I** is the $n \times n$ identity matrix. If $\mathbf{H^{-1}}$ exists, **H** is said to be non-singular. Otherwise, **H** is said to be singular. If **H** is singular, Equation (3.10) has no solution or infinitely many solutions.

For a non-singular matrix **H**, a perturbation in x leads to a perturbation in z:

$$z + \Delta z = \mathbf{H}(x + \Delta x) \tag{3-12}$$

Similarly, a perturbation in z will lead to a perturbation in x:

$$x + \Delta x = \mathbf{H^{-1}}(z + \Delta z) \tag{3-13}$$

Simplifying Equation (3.13) as following:

$$\Delta x = \mathbf{H^{-1}}\, \Delta z \tag{3-14}$$

Equations (3.13) and (3.14) present one of the central problems of the matrix inversion; the propagation and in some cases amplification of input errors to the output (the errors in z are propagating into x via the inverse matrix). The stability of x with respects to errors in z depends on the condition of **H**. If small changes in Δz result in small changes in Δx, the matrix **H** is said to be well-conditioned. Additionally, if small changes in Δz result in large changes in Δx, the matrix **H** is said to be ill-conditioned. The condition of matrix therefore describes the sensitivity of the output x to changes in the input z. A measure for the stability of the solution is the condition number of **H**. It is very normal to use regularisation but it will not be used in this thesis.

Matrix condition

For a perturbation in **B**, an upper bound of the relative error in **x** is given [104, 109, 110]:

$$\frac{\|\Delta \mathbf{x}\|}{\|\mathbf{x}\|} \leq \|\mathbf{H}\|\left\|\mathbf{H^{-1}}\right\| \frac{\|\Delta \mathbf{B}\|}{\|\mathbf{B}\|} \tag{3-15}$$

Here, $\|.\|$indicates a matrix norm, see Appendix. The term is called the condition number of the matrix **H** [109].

$$\kappa(\mathbf{H}) = \|\mathbf{H}\|\left\|\mathbf{H}^{-1}\right\| \tag{3-16}$$

From Equation (3.15):

- For small κ, the error $\|\Delta\mathbf{x}\|/\|\mathbf{x}\|$ will be small when $\|\Delta\mathbf{z}\|/\|\mathbf{z}\|$ is small.
- For large κ, the error $\|\Delta\mathbf{x}\|/\|\mathbf{x}\|$ can be large, even when $\|\Delta\mathbf{z}\|/\|\mathbf{z}\|$ is small.

Values for the condition number lie between 1 and infinity: $1 \leq \kappa < \infty$. A high condition number($\kappa \gg 1$) indicates an ill-conditioned matrix. The condition of a matrix is an intrinsic property of the matrix, and independent of the algorithm used for inversion.

When using the 2-norm in Equation (3.16), the condition number can be expressed as the ratio of the smallest and the largest singular value of **H**:

$$\kappa(\mathbf{H}) = \|\mathbf{H}\|_2\left\|\mathbf{H}^{-1}\right\|_2 = \frac{\sigma_{\max}(\mathbf{H})}{\sigma_{\min}(\mathbf{H})} \tag{3-17}$$

Briefly, when the condition number is large the solution is sensitive to errors. The implications for the determination of the blocked force are discussed later.

Singular value decomposition

Singular value decomposition (SVD) is required to obtain the singular values of a matrix. The SVD factorizes an $m \times n$ matrix **H** into the three matrices **U**, **S**, and **V** [108].

$$\mathbf{H} = \mathbf{USV^h} \tag{3-18}$$

U is an $m \times m$ real or complex unitary matrix; **S** is an $m \times n$ rectangular diagonal matrix with non-negative real elements; $\mathbf{V^h}$ is an $n \times n$ real or complex unitary matrix.

The diagonal entries of **S** are the singular values σ_i of **H:**

$$\mathbf{S} = \text{diag}(\sigma_1, \ldots\ldots, \sigma_p), p = \min[m, n] \tag{3-19}$$

The *m* columns of **U** and the n columns of **V** are called the left-singular vectors and right-singular vectors of **H**, respectively [108].

The generalized inverse

For a rectangular matrix **H** of size $m\ x\ n$, where $m \neq n$, the inverse is not defined. Instead, a generalized inverse or pseudo-inverse can be calculated:

$$\mathbf{H^{-1}} = (\mathbf{H^H H})^{-1}\mathbf{H^H} \tag{3-20}$$

The inverse matrix $\mathbf{H^{-1}}$ has size $m\ x\ n$. The generalized inverse was first proposed by Moore[111], and later by Penrose [112], which is often called the *Moore-Penrose pseudo-inverse.*

For the generalized inverse, a least square method is used to solve Equation (3.10). The SVD is employed for the calculation of $\mathbf{H^{-1}}$. From Equation (3.18), the inverse of **H** is readily available:

$$\mathbf{H^{-1}} = \mathbf{V S^{-1} U^h} \tag{3-21}$$

Equation (3.21) still requires the inversion of **S**. However, **S** is a diagonal matrix that can be easily inverted by replacing the singular values on the diagonal by their reciprocal values;

$\mathbf{S}^{-1} = \text{diag}\left({}^{1}/_{\sigma_1}, \ldots\ldots, {}^{1}/_{\sigma_p}\right)$. The SVD therefore is a convenient tool to calculate the generalized inverse.

3.4.2 Methods to mitigate matrix inversion problems

The above sections have discussed the problems that are associated with matrix inversions such as ill-conditioned matrices and the subsequent amplification of errors in the input data. In order to mitigate these problems, there exist varieties of methods, which can improve the processes involved within matrix inversions.

Over-determination

In over-determination, a larger amount of input data is supplied to a problem than is required to solve it. For example, for a system as in Equation (3.8) with n unknown variables (x has size $n \times 1$), m known variables (z has size $m \times 1$) are supplied to solve the problem, where $m > n$. The matrix **H** therefore has size $m \times n$, and Equation (3.10) has the following form:

$$\mathbf{x_{nx1}} = (\mathbf{H_{mxn}})^{-1}\mathbf{z_{mx1}} \tag{3-22}$$

As mentioned above, the matrix $(\mathbf{H_{mxn}})^{-1}$ has size $n \times m$. The use of the generalized inverse to obtain **H** leads to a best-fit approximation for the solution [23], that is it gives a least squares solution.

3.5 Review of inverse force determination

Indirect measurement and quantification of operational forces has been a popular subject among engineers especially within the automotive industry where a significant amount of research literature exists, dating back to the 1980's on indirect identification of structural loads [113-115]. This area of research gained in popularity and a continuous flow of publications is now being witnessed [116-118]. In this section, the main developments and findings in the field of inverse force determination are reviewed. Topics discussed include associated errors, over-determination and regularization methods and optimization of response measurement locations.

For a single DoF, a vibrating source, connected to a receiver structure, exerts a varying force at the interface that in turn excites the receiver as in figure (3.1). The force $\boldsymbol{f}_{C_c}$ and the acceleration $\mathbf{a}_{C_b}$ are linked by the receiver transfer accelerance through, $\mathbf{a}_{C_b} = \mathbf{A}_{R_{bc}}\boldsymbol{f}_{C_c}$. If there is more than one contact or component of motion, $\boldsymbol{f}_{C_c}$ and $\mathbf{a}_{C_b}$ are vectors and $\mathbf{A}_{R_{bc}}$ is a matrix:

$$\boldsymbol{a}_{C_b} = \mathbf{A}_{\mathbf{R_{bc}}}\boldsymbol{f}_{\mathbf{C_c}} \tag{3-23}$$

Thus if the receiver structure acceleration $\boldsymbol{a_{C_b}}$ is remote from the contact interface, $\mathbf{A_{R_{bc}}}$ is considered as a transfer accelerance matrix. The following discussion will classify the transfer accelerance matrix as FRF matrix. The operational forces at the source-receiver interface can be obtained using the Equation (3.24) where the $\boldsymbol{f_{C_c}}$ can be solved as:

$$\boldsymbol{f_{C_c}} = \mathbf{A_{R_{bc}}^{-1}} \boldsymbol{a_{C_b}} \qquad (3\text{-}24)$$

Equation (3.24) allows a procedure, which consists of three steps for obtaining the contact forces between source and receiver indirectly:

1. The forces are applied at each of the contact positions one at a time in order to obtain the FRF matrix $\mathbf{A_{R_{cb}}}$ of the uncoupled receiver structure (housing). The responses at all response positions are recorded during this procedure.
2. The source is connected to the structure, and the acceleration $\boldsymbol{a_{C_b}}$ at the same response positions are recorded during the operation of the source.
3. The FRF matrix is inverted and multiplied with the velocity response vector frequency by frequency. Then, the operational contact forces are calculated from Equation (3.24).

3.5.1 In-situ Blocked Force

When using Equation (3.24) the operational forces obtained are constrained to the given source-receiver combination. If there are any changes to the source-receiver arrangement, the source is moved or the structure is changed in some way, then the force must be re-calculated via a new set of measurements of the frequency response functions.

To overcome this constraint Moorhouse et al., [105] developed a modification of Equation (3.24). These authors suggested inverting the frequency response function matrix of the coupled accelernaces, $\mathbf{A_{C_{bc}}}$ instead of the uncoupled receiver accelernaces $\mathbf{A_{R_{bc}}}$ see Equation (3.25) which gives the blocked forces, independently of receiver structure.

$$\bar{\boldsymbol{f}}_{\mathbf{S_c}} = \mathbf{A_{C_{bc}}^{-1}} \boldsymbol{a_{C_b}} \qquad (3\text{-}25)$$

Again, the above bar notation is used to denote a blocked condition. The attractiveness of Equation (3.25) is that it yields blocked forces of the source when coupled to a receiver structure. The direct measurement of blocked forces poses practical challenges. Furthermore, *in-situ* determination of blocked forces circumvents the problem of source invariance. Since the source activity is obtained in a representative mounting condition, results can be assumed to be similar to those in other similar mounting conditions.

Equation (3.25) requires the determination of the coupled (transfer) accelerance matrix. Provided there is access to the source-receiver interface to attach accelerometers, this is similar to the determination of the uncoupled accelerance matrix. Equation (3.25) was successfully used in several studies such as [119, 120] but it does not solve problems associated with matrix inversion, or the challenge of obtaining all necessary accelerance terms.

Moreover, a relatively new approach, known as the in-situ blocked force method, has the advantage that blocked forces can be obtained from a two-stage measurement conducted in-situ, i.e. when the source is connected to a receiver, thus facilitating independent source characterization, while the source is operated under realistic conditions [105].

The forces in Equation (3.24) are specific to the receiver structure, so that the same source on a different receiver will produce different contact forces. Therefore, even a slight modification in the receiver or source position would require new set of calculations of the operation forces to obtain a new set of measurements for the modified FRF matrix.

As with Equation (3.23) so with Equation (3.24), the operational forces obtained are constrained to the given source-receiver combination. Again, if there are any changes to the source-receiver arrangement, the source is moved or the structure is changed in some way, then the force must be re-calculated via a new set of measurements of the frequency response functions.

Again using Equation (3.25), blocked forces independent of the receiver structure can be obtained. Equation (3.25) can also provide information of the blocked forces when the source and structure of the receiver are coupled.

Several studies [119-121] have applied Equation (3.25) with success; however, the problems associated with matrix inversions and the challenges of obtaining all necessary accelerance terms remain. The in-situ approach allows for blocked force to be estimate from active and passive measurements made on the assembly in its natural state, unlike the direct measurement which requires the interface to be constrained, which is typically not possible in practical scenarios.

It is important to understand the differences between the operational and blocked forces where the operational force describes the force applied to receiver by source whilst the blocked force describes the force applied by source to infinitely rigid receiver. The blocked force is transferable when the receiver is changing (it theoretically should be the same when the source is changing form housing to another). However, if the source is moved or the receiver structure is changed, a new calculation of the operational forces is required, which entails a new set of measurements of the altered FRF matrix.

Having measured the 'acceleration', it is multiplied by the inverse accelerance matrix to calculate the blocked force at the interface as in Eq. (3.25).

On-board validation-predicting operational response using the acquired blocked forces.

$$\boldsymbol{a}_{\mathbf{C_r}} = \mathbf{A}_{\mathbf{C_{rc}}} \bar{\boldsymbol{f}}_{\boldsymbol{S_c}} \tag{3-26}$$

where $\boldsymbol{r}$ is a new set of reference DoF and $\mathbf{A}_{\mathbf{C_{rc}}}$ is the transfer accelerance between the source contact points and the remote response position. The predicted acceleration is then used to validate the obtained blocked force signal by comparing it with the directly measured acceleration.

3.5.2 Errors associated with inverse force determination

There are two types of errors, which play an important role in the process of inverse force determination, they are: 1) statistical or random errors 2) deterministic or systematic errors.

Statistical errors

Statistical errors that are associated with the inverse force determination include [122]:

- Random noise in the FRF estimates;
- Random noise in the operational response signals.

A general introduction to the inverse problem in Section 3.4 also addressed the problem of random errors. This can be further explained as, for example, if FRF matrix is inverted, then depending on its condition, small errors in vector b can result in large errors in the vector x, see Equation (3.14). This means that random errors are almost inevitable in the response vector which is obtained during the force determination, because the response vector is contaminated with background noise and the resonant behaviour of the receiver structure.

As a result, the condition of the FRF matrix assumes importance. Noisy measurement data in combination with an ill conditioned FRF matrix can give rise to large errors in the force estimates. If the errors in the response velocity vector are large, but the condition numbers of the FRF matrix are small, the errors in the measured velocities are simply propagated to the force estimates without much amplification.

An investigation was conducted by Blau [123] on errors introduced by a typical FFT of FRFs and response spectra on the excitation forces which had been inversely determined. Blau developed an error model in which individual force estimate is statistically calculated using the statistical errors found in the FRFs and responses. The results of Blau's investigations can be found in [124]. One of his findings was to show a tendency for random errors to distribute

uniformly across the force spectrum. Another highlight was to show relative errors to be larger for weak forces.

Deterministic errors

Deterministic errors in inverse force determination include [122]:

1. neglected degrees of freedom in the FRF matrix, e. g. rotational motion,
2. non-linear behaviour of the receiver structure,
3. sensor mass loading,
4. excitation misalignment during FRF measurements,
5. Inconsistencies between elements of the FRF matrix, due to changing conditions during multi-run measurements.

In comparison, random errors are easier to deal with than the deterministic errors and there are very few publications that deal with the effect of deterministic errors.

In order to achieve reliability in results obtained from inverse force determination, Fabunmi [125] has suggested that the number of structural modes that contributes to the response at a certain frequency must be equal to the number of unknown forces. Using a greater number of response signals compared to the number of forces does not provide reliable force estimates. This is one of the examples of over-determination of the system. Although the conclusions from Fabunmi were based on work conducted with beams only, the recommendations can be applied to a wide variety of structures.

Gajdatsy [122] estimated errors in the determined forces by using a simplified Finite Element (FE) model of an aeroplane. In this case, the errors originated due to inconsistencies in the FRFs. The conclusion was that even small systematic errors may result in significant errors in the estimated forces.

3.5.3 Over-determination and regularization methods

In order to reduce the errors observed during the inversion of the matrix, a several mathematical methods exist and can be employed. The most important methods are over-determination, singular value rejection, and regularization techniques [23].

Thite and Thompson, conducted a systematic investigation to investigate the use of inverse methods for the quantification of structure-borne transmission paths [82]. The most important conclusion from Thite and Thompson and others [77, 126, 127] include:

1. In terms of where the modal overlap was larger, over-determination caused the reduction of condition numbers, which improved considerably the force estimates at higher frequencies. Over-determination was not effective however, where the frequencies were lower. An increase in the over-determination although reducing the occurrences of high condition numbers, did not significantly reduce minimum conditions numbers.
2. Use of the singular value rejection technique has been shown to be a promising tool to reduce amplifications of errors.
3. The effect of error estimates in FRFs and operational responses on the threshold criteria found that neither method can be applied universally, nor it remains a challenge to select a threshold suitable for the Singular Value Rejection (SVR).
4. Two methods, the Tikhonov (using ordinary cross-validation regularization) and iterative inversion were investigated for the selection of regularization parameter. In comparison to over-determination and SVR, both methods performed well in terms of producing better results. However, both methods require higher concentrations during modelling due to the complexities and both require longer computational times. Further studies by Choi et al., on the Tikhonov regularization parameter can be found in [128, 129].

5. The noise level in the FRFs was found to affect the condition numbers. It was found that when higher levels of noise caused a reduction in condition numbers at lower frequencies, but caused an increase in condition numbers at higher frequencies. At lower frequencies it is often the case that the modal densities are very low. The performance of the system was worse when the noise levels in the FRFs were low and produced larger condition numbers which, in turn, produced a higher level of noise in the responses [23].

In the context of automotive engineering, the determination of the inverse force was also studied by Gajdatsy [122]. He found that using a simple engineering judgement and experience, the SVR can generally be applied with a relative threshold of 1% of the largest rejection value. He also found that an over-determination factor of 2 is generally recommended.

3.5.4 Optimization of response measurement locations

A further reduction in the errors that are produced during the matrix inversions is possible by careful selection of the measurement points used to obtain the response. It should be noted that two parameters are generally affected when accelerometers are placed in position; 1) measurement noise in the response signal 2) condition number of the FRF matrix [130].

Therefore, it is recommended that accelerometers should not be placed near a nodal line as that causes the output signal to drop at the resonance frequencies which reduces the signal to noise ratio [122]. In terms of the bending wavelength of the structure, if the location of the two response points (two accelerometers) is very close, identical FRFs are obtained. If these FRFs are used in the inversion process, it creates two linearly dependent rows in the FRF matrix which results in a higher condition number [122]. Therefore, a potentially effective method is to optimize the location of the sensor in order to obtain meaningful information to solve problems associated with the inversion methods. However, to locate these optimal positions where the response can be measured is a significant challenge. In this regard, Thite and Thompson [126, 128] have reviewed various methods which can be used to optimize the locations to measure

the response. These include the Guyan reduction approach, methods of maximum/average modal kinetic energy or average driving point residue, the effective independence method and Gram-Schmidt orthogonalization. They also considered a sensor placement criterion proposed by Blau in order to determine the inverse force. Thite and Thompson also suggest a procedure to find the best combination of response positions which is based on the "composite condition number" method. Another method to calculate the best possible combination of response positions was proposed by Zheng et al., based on a 'coherence factor' of the transfer function matrix [131].

3.6 Summary

This chapter has explained source activity and accelerance as two basic source parameters. It has demonstrated that the blocked force methods may be used to measure source activity if the source is independent of any sort of constraints imposed by the receiver. Moreover, source, receiver and interface brief discussed.

One of the drawbacks of using the blocked force method has been identified as the requirement of additional measurements to characterize the machine, using the frequency response function. In addition, there are the solutions required for ill-posed inverse problems. Moreover, further investigations on the application of the blocked force method are required to investigate its potential adaptation for use with condition monitoring.

For condition monitoring, it has also been noted that most commonly used methods are applicable only in the frequency domain, which potentially conceals some features of the time-domain signals which could be useful for the fault detection. It is worth noting that the blocked force represents a property which is associated with the source region only and it doesn't depend on those boundary conditions which are outside the source region. This establishes a

platform for this thesis in which the blocked force method will be tested to determine its applicability to condition monitoring and its advantages and disadvantages will be investigated.

The blocked force signal will be used in this research as an alternative to housing acceleration. Thus, the following chapter presents the test rig, which will be used to obtain the blocked force signal using the inverse process.

Chapter 4

Experimental test rig

This chapter describes the test rig used for the experimental investigation and the data acquisition system. It also presents the accelerometers and accelerometer mounting techniques. The experimental procedure and steps used to collect and analyse the vibration signals from the gearbox, for healthy and faulty gear conditions are described.

4.1 Introduction

Vibrations originate from many and various sources on any rotating machine. Components such as shafts, generator, gears and bearings generate different vibrations and noise. Aspects of the new approach, the blocked force, introduced in Chapter 3 will be tested further in Chapter 5 using test rig, described in this Chapter. However, the test rig will be used for both conventional acceleration and inverse measurements.

Before starting any measurement, the test rig was divided into source (the active part) and receiver (the passive part). The blocked force will be defined at the interface between them. Once the source, receiver and interface are known, the two stages of measurement begin.

The test rig will be used in this research for sets of two measurements:

1) Inverse (blocked force) measurements: these will be conducted using several accelerometers mounted on the housing or on the interfaces as described in chapter 5. To obtain the blocked force signals, the measurements are divided into two sets;
   A) Accelerance measurement: for this test, a hammer is used to excite each point at the interface or on the housing in order to measure the accelerance presented in the previous chapter. However, each FRF was calculated from averages 3 excitations.

It should be noted that, in theory, a shaker could also be used to measure the accelerance as well as a hammer but in practice it is impossible to use because of the mounting is difficult.

B) Acceleration measurement: in these tests, the measurements are divided into two stages;

i. Simulated acceleration where the hammer is used to excite one remote point (this point is used as reference point to validate the obtained blocked force) and responses are recorded, and

ii. Actual acceleration generated by the motor. These acceleration measurements are the same as those used in conventional CM but the data will be processed differently.

Calculation of the blocked force is always carried out in the frequency domain, which means the measured acceleration will be transformed into the frequency domain. Once the blocked force signal has been calculated and validated, it is then transformed back into the time domain. Subsequently, signal processing will be used to investigate whether the results could be useful for fault detection.

2) The acceleration measurements: these will be conducted using the same test rig for measuring the acceleration so one of the accelerometers mounted on the housing will be considered as accelerometer which has been used to collect the vibration signals for the healthy and faulty condition of the gear to illustrate more traditional methods for fault detection and identification as described in chapter 6.

The flow chart, Figure (4.1), shows the process of the experimental tests for both acceleration and blocked force measurements.

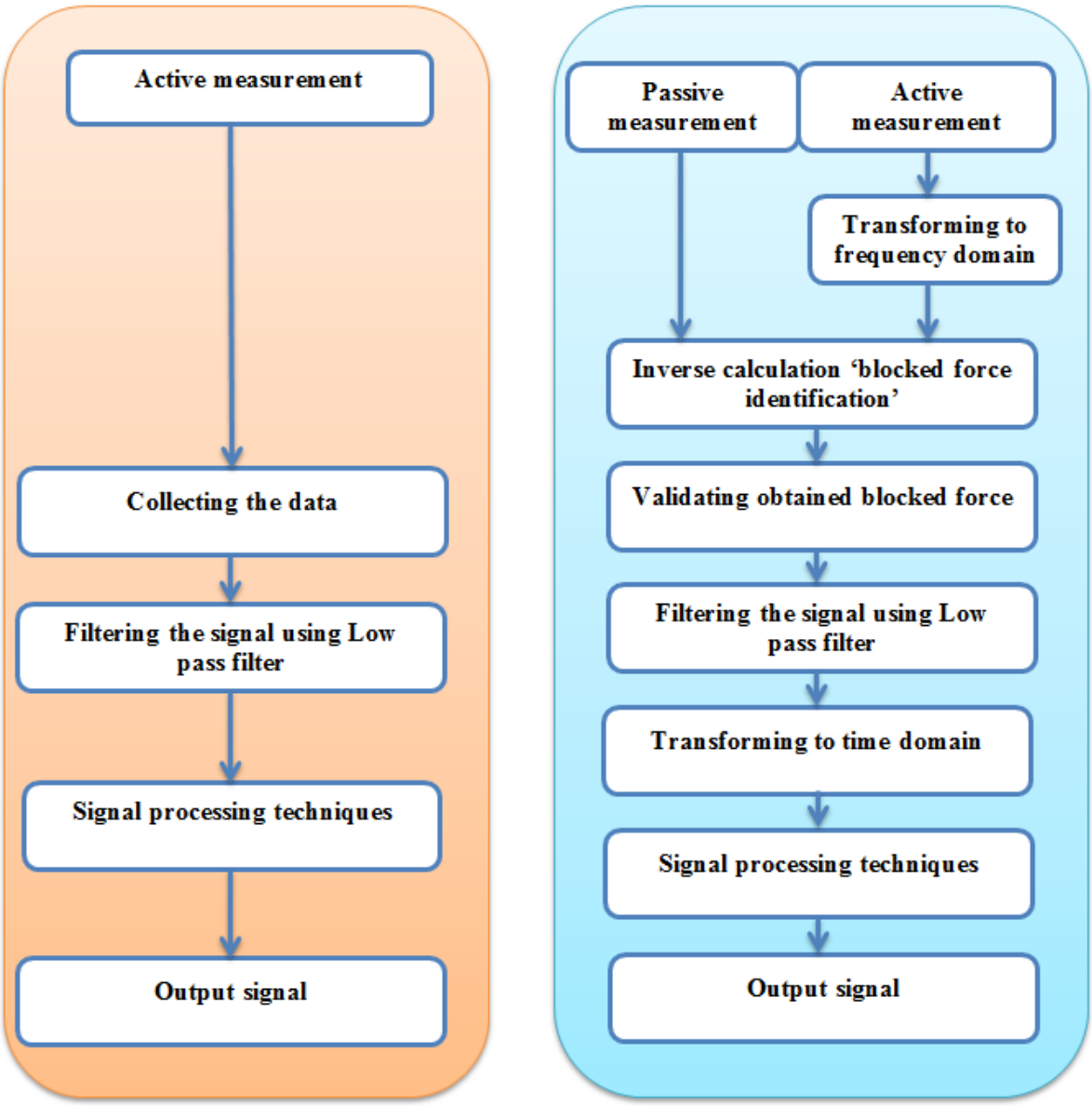

Figure 4-1 Scheme flowchart for the two different measurements: the left column shows the conventional route to CM using acceleration signal and the right column corresponds to the blocked force process. The same signal processing is applied to both signals

4.2 Test rig experiments

The test rig chosen for this research is not only because it is widely used in industry, but also because it allows faults to be easily simulated and numerous CM techniques to be extensively applied and evaluated.

Figure (4.2) and (4.3) are an illustrative photograph of the realistic test rig and gearbox components used in this study. To begin with, experimental data was collected using the test

rig. Tests were carried out for different shaft speeds using a healthy pair of spur gears and one suffering from two levels of tooth breakage on the pinion: fault 1 - 25% tooth removed, fault 2 - 85% tooth removed. The “% tooth removal” refers to the percentage length removed from a single tooth. A schematic of the gear with 25% and 85% tooth removed is shown in Figure (4.4). However, two different speeds were chosen at random but fairly representative of gearbox speed in typical vibration. There are three sample frequencies: 51.2 kHz, 25.6 kHz, and 12.8 kHz, so, the maximum sample rate in the software has been used in this thesis for flexibility.

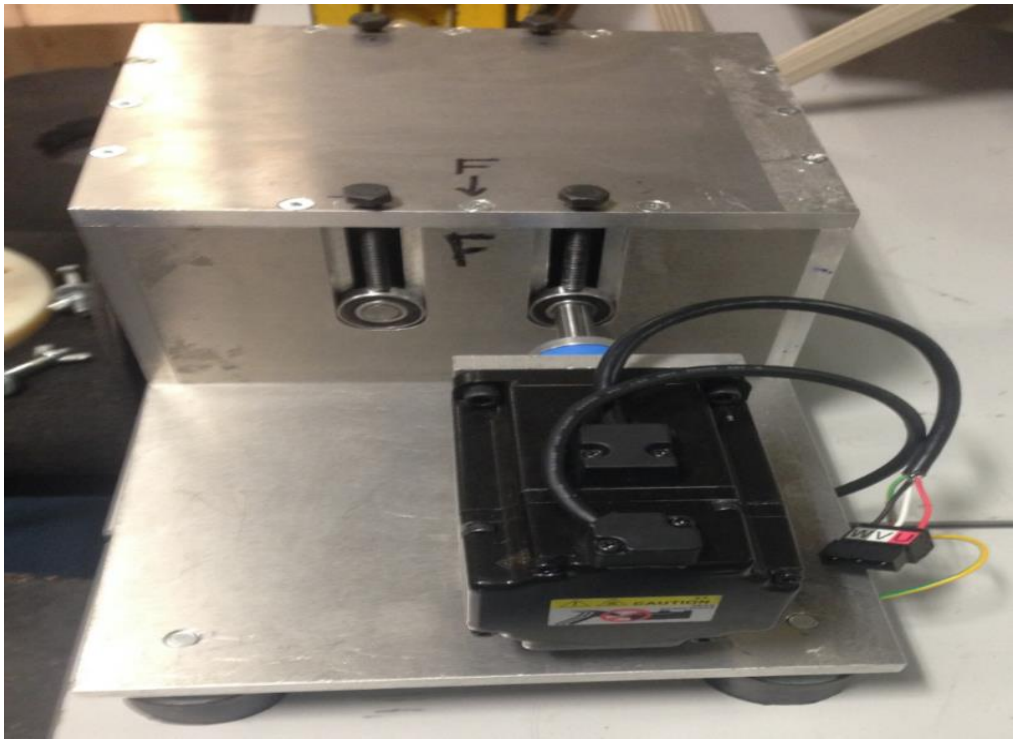

Figure 4-2 Photo of test rig

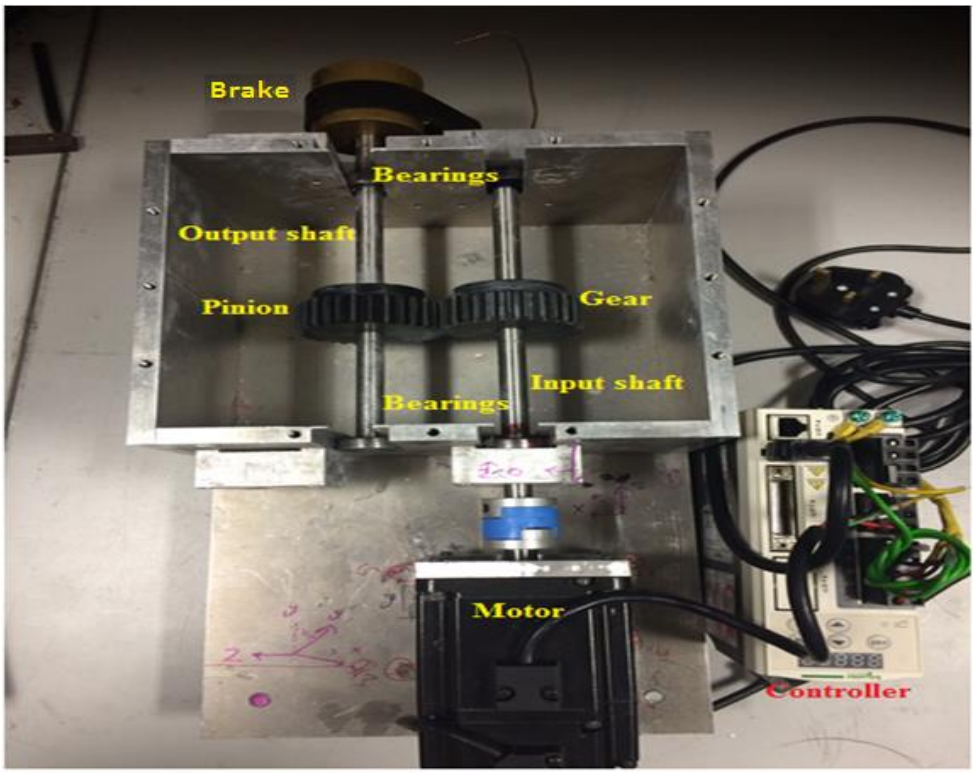

Figure 4-3 Photo of gearbox test rig components

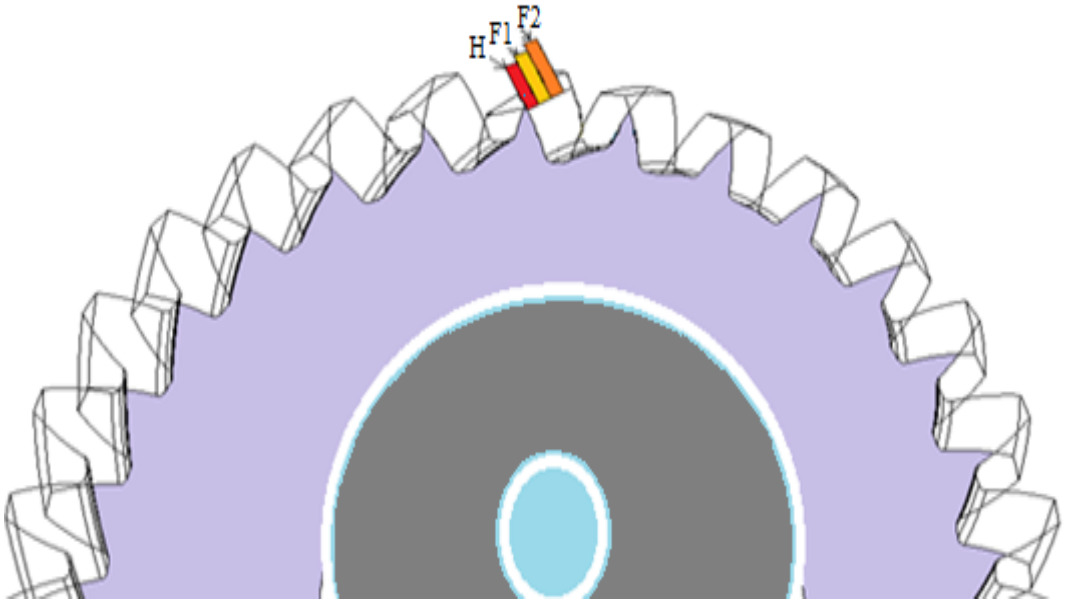

Figure 4-4 Faulty gear condition, the red colour indicates the healthy tooth (zero tooth removed), yellow indicates the first fault (25% of tooth removed), orange indicates the second fault (85% of tooth removed)

4.3 Test rig components

In this section, test rig components for both tests are presented as following:

4.3.1 Spur Gears and Bearings

The spur gear, described in Chapter Two and used in the tests is detailed in Table (4.1) and shown in Figure (4.5). Supporting bearing used in this research (RS Deep Groove Ball Bearing 6190121 RS 6001-2RS, 12mm x 28mm x 8mm).

Figure 4-5 Spur gear used in this project

Table 4-1 test rig specifications of the gear

Parameters	**Value**
Type of test gears	Spur
Material of gear	Steel
No. of teeth, pinion	30
No. of teeth, gear	30
Bore Diameter	12mm
Pitch Diameter, pinion	60mm
Pitch Diameter, gear	60mm
Hub Diameter	50mm
Face width	20mm
Type of fault in gear (Removal teeth %)	25 and 85 %

4.3.2 Gearbox Housing

Figure (4.6) shows two different covers used in this research, one of aluminium and another of steel. As mentioned in Chapter 3, one of the main potential advantages of blocked force method is that the effect of the housing can be removed from the signal and the blocked force should be the same.

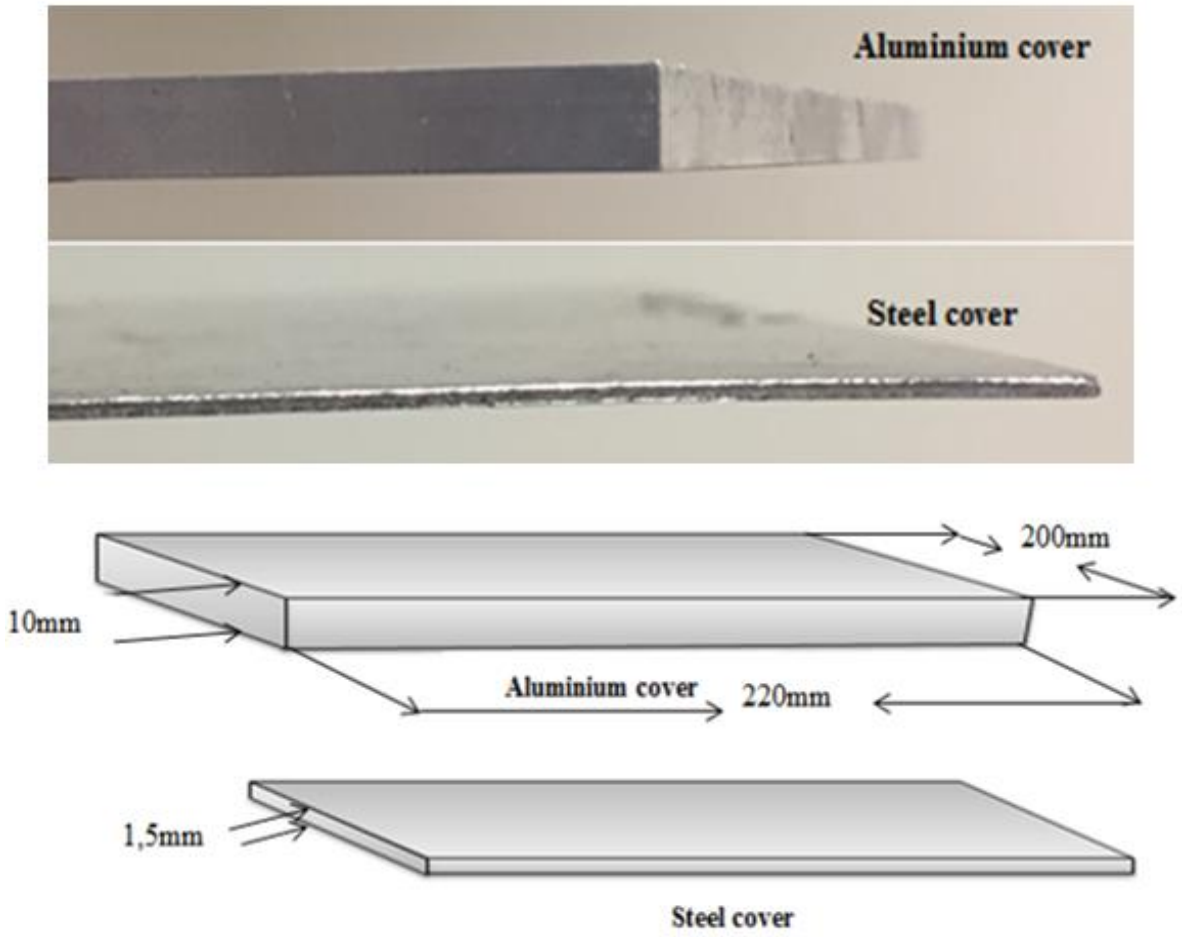

Figure 4-6 Two gearbox covers (one aluminium of thickness 10 mm, the other steel of thickness 1.5 mm)

4.3.3 Shafts

The drive shaft has a pinion or gear attached to it, and is the means by which power and motion are transferred. By virtue of their function, shafts act as the axes of rotation of the gears. Two shafts were used in this case study; input and output.

4.3.4 Motor and Controller

Figure (4.7) shows the drive DC motor used to operate the system to provide operational data (with speeds 0-3000 rpm). It is very important for making comparative measurements to ensure that the speed is exactly repeatable, hence the need for a controller. Figure (4.8) shows the controller which is used to adjust and operate the motor at the required speeds.

Figure 4-7 DC Motor (Schneider Electric 0.4 kW Servo Motor, 220V, 1.27nm, 3000 rpm, BCH0801O12A1C)

Figure 4-8 Controller (Schneider Electric 0.4 kW Encoder Feedback Servo Drive, 2.6 A, 220 V, 0 +55 °C, LXM23DU04M3X)

4.3.5 Impact Hammer

The hammer used to measure the Frequency Response Function (FRF) physically excites each excitation point (where each accelerometer has been mounted on chosen visible interface) on the housing with an impact of known frequency content and, here, with sensitivity 10.41 mV/N and frequency range 5000 Hz. Hammers such as this are standard items of equipment in the field of structural dynamics testing, however, it is not widely known in CM. It serves the purpose of providing artificial or simulated excitation of the machine in a controlled way, which can be helpful in the preliminary test phase, as described later. The impact tip material used in this thesis Plastic. However, the number of impacts is 3 times.

Figure 4-9Artificial hammer, types 8206-001

4.3.6 Accelerometers

Accelerometers are electromechanical devices, widely used in research and industry to measure the movement of mechanical surfaces and provide an electrical output (voltage) which is directly proportional to the acceleration of the surface. Piezoelectric accelerometers, the most commonly used accelerometers today are inertial devices and comprise two main elements; a seismic mass which generates the inertial force and a wafer thin piezoelectric crystal on which the force acts and which produces an electrical charge [132].

Piezoelectric accelerometers are robust, accurate and sensitive as well as being light, small and relatively easy to mount on the vibrating surface [133]. For frequencies in the range of a few Hz to about 20 kHz, piezoelectric accelerometers are probably the most suitable of all

accelerometers [132]. Accelerometers are used for both measurements with a sensitivity of 10 mV/g. Vibration range is up to 6 kHz; bandwidth from 0.3 Hz to 6 kHz.

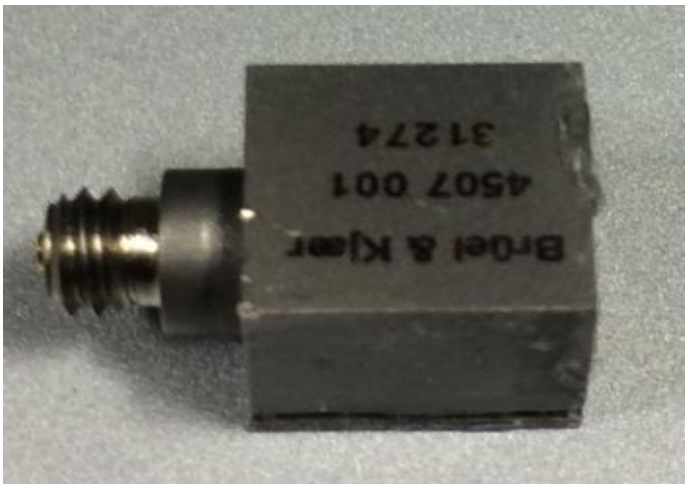

Figure 4-10 Photo of piezoelectric accelerometer

Accelerometer mounting techniques

It is necessary for any accelerometer to be mounted correctly [2]. There are recommended mounting techniques, such as those in BS ISO 5348-1998 *Mechanical vibration and shock - Mechanical mounting of accelerometers*, for attaching accelerometers to accurately measure the vibration of surfaces. For an accurate measure of the acceleration, the accelerometer must be mounted so there is close mechanical contact between the accelerometer and the surface whose acceleration is to be measured. Bad (loose) mounting can adversely affect vibration measurements by seriously reducing the usable frequency range.

4.3.7 NetdB data acquisition unit

NetdB is a commercially available 12-channel acquisition front-end from 01dB-Metravib dedicated to vibro-acoustic applications (signal recording, frequency analysis, acoustic power, modal analysis, sound quality, and acoustical imaging), see Figure (4.11). NetdB is Ethernet technology based, allowing synchronization between a computer and several NetdB systems. The data synchronization process enables data from several sources to be recorded simultaneously in real time without any loss synchronisation.

- Sample rate is 51.2 kHz,
- Data resolution: 0.39625
- Dynamic range dB (24 bits)
- FFT window (3276)

Figure 4-11 NetdB data acquisition device (Data resolution: 0.39625. Dynamic range dB (24 bits))

4.4 Processing and Analysing Software

After the measured signal from the accelerometer is received, the accuracy of the fault detection and diagnosis will depend on the software used to process the data. The NetdB acquisition card used in this research has 12 channels on which to record and save the measured data. MatLab software was used to analyse this data. The results obtained using these codes can be seen in Chapters 5, 6 and 7.

4.5 Experimental procedure

The NetdB is designed to interface any test rig to a computer in order to measure, monitor and record variables such as acceleration.

- The NetdB, accelerometers, and cables were correctly connected together and checked.
- The mounting locations for the transducers were cleaned of dust, dirt, oil and paint and the accelerometers were glued using appropriate super glue (Everbuild Stick2 industrial

superglue GP). The interfaces were chosen random where it is possible to connection between receiver and source. Care was taken to avoid unnecessary crossing of cables to avoid introducing unnecessary electromagnetic noise and minimise power supply frequency pickup.

- The positions of accelerometers have been chosen at random (in CM they can be mounted on the cap of the bearing or on the housing). In our case study, we choose to mount them on the housing firstly for ease of mounting and removal, secondly, for easy excitation and thirdly to provide illustration of removing the effect of the housing.
- The mesh frequencies for both speeds are at 275 and 425 Hz respectively. Therefore, the signal above 1000 Hz will be filtered using low pass filter for both measurements (conventional and blocked force measurement in frequency domain) to be consistent, after which the filtered signals will be transformed into time domain and then subjected to signal processing techniques.
- For inverse measurement to obtain the blocked force, the two-stage measurement procedure was conducted as mentioned in a previous chapter. The assembly is divided into source, receiver and interface, see section (3.2.2). Measurement of FRFs and operational acceleration has been introduced above, and examples are given in the following chapter to illustrate the location of sensors and the details of the measurement procedure.
- For acceleration measurement, as mentioned above one accelerometer has been chosen and used for analysis, after which it has been transformed and filtered. After that the filtered signal has been transformed to time domain and subjected to signal processing techniques to identify the condition of the machine, as described in Chapter 6.
- Housing covers of two different materials were used to provide two different sets of test data which could be used to validate the obtained blocked force. The obtained

blocked force signals for two housings will be filtered using low pass filter in frequency domain and then transformed to time domain. After that some signal processing techniques will be applied, as described in chapter 7.

- The computer saved the measured data for the acceleration and blocked force tests and then used MATLAB for analysis.

4.6 Summary procedure

A standard test procedure was developed to ensure good measurement practice. Each accelerometer was clearly labelled by colour coding to help ensure it was always used in the same orientation. Data was collected from all transducers for all tests, whether the data was of immediate interest or not, as this did not alter the acquisition time.

Measurements were often taken on separate days to ensure confidence in the repeatability of data collected. The first file in any data acquisition period was analysed, using the Matlab software, before further data was collected to ensure that sensible data had been recorded.

The test rig, described above, will be used for the blocked force measurement as described in the next chapter. Chapter 6 will describe the use of signal processing techniques for fault detection. In Chapter 7 the same signal processing techniques will be applied for fault detection using the obtained blocked force signals.

Chapter 5

Preliminary measurements of blocked forces

This chapter is focused on the preliminary measurement of the blocked force. In order to refine the blocked force technique and its application, several experiments have been carried out

using a coupled beam system and the test rig. Later in the thesis, the test rig will be used to acquire the blocked forces arising from a gear fault.

5.1 Introduction

As mentioned in the chapter three, the measurement of blocked forces requires a two-stage measurement procedure; the accelerance and acceleration measurements. The test rig, presented in the previous chapter, is here used to illustrate the blocked force technique. Refining the technique began with a simple test using beam structure before moving on to the gearbox test rig itself.

The benefit of the inverse method is that it allows one to avoid directly measuring the desired quantity, which in our case is the force, by measuring instead a more accessible quantity (acceleration) from which the desired quantity can be derived [134].

However, despite the strong research record and many publications on the topic, inverse force determination remains a topic for experts. Obtaining the accelerance matrices requires technical expertise in the measurement of accelerance, and handling the subsequent data processing requires judgement on how to set parameters for over-determination and regularization [110].

The internal forces are usually difficult to measure or model so, typically, equivalent operational interface forces are used instead. In most practical situations it is extremely difficult to mount force transducers at the connection interface for a direct determination of the blocked force [84]. Elliott and Moorhouse have demonstrated [21, 96] that the acceleration at the interface and the accelerance of the combined source-receiver structure can be used to calculate the blocked force. Both acceleration and accelerance can be obtained from the measurements made.

It is likely that accelerometers can be placed close to the connection between source and receiver. However, the accelerance measurement is likely to be difficult. To overcome this difficulty and to obtain more accurate results, the principle of reciprocity is applied to enable the use of remote measurement positions [96]. The experimental validation using two parallel beams coupled at two points is presented in [105] and the technique developed is used here.

Previous studies have used the blocked force as tool for prediction purposes whilst in this work we will investigate its use for condition monitoring using the test rig described in the previous chapter.

In the following sections, preliminary measurements of blocked forces are made on a simple beam structure. Following this a more complex assembly is considered; the gearbox test rig, shown in Figure (4.2).

5.2 Blocked Force Experiments using beams

Before taking blocked force measurements on the test rig, it was necessary to refine the techniques on a simpler, more controlled system.

In practice, multiple contacts will be used to support a real vibration source. Figure (5.1) shows the experimental beam coupling setup for this test. The source and receiver were coupled rigidly at two points through two 3 cm^2feet. The source and receiver were coupled rigidly by screws forcing the structures to couple in-plane.

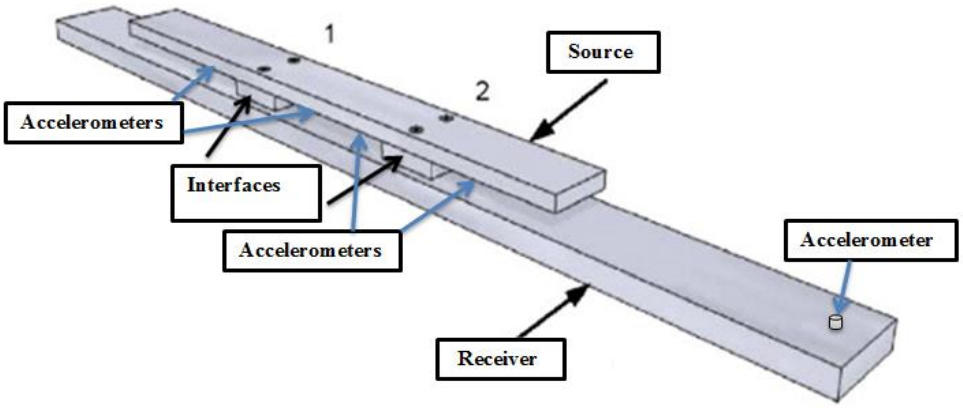

Figure 5-1 Schematic of two beams coupled at two points: it shows illustration of source beam (with two feet footings) coupled to a receiver beam rigidly, 1 and 2 indicate interfaces, Four accelerometers are mounted underneath the upper beam and one accelerometer as remote point (reference point) on lower beam

Using the beam structure shown in the figure above, the remote measurement of blocked forces was investigated. It was shown by Elliott [101], that the blocked force, measured in-situ using the special case of equation (3.23), could be used to predict the behavior of the source whilst installed in a different environment (housing). It was further shown that the more degrees of freedom included in the characterisation, the better prediction was obtained [101].

5.3 Measurement setup

The upper beam was considered as a source while the lower one was considered to be the receiver. Accelerometers were mounted underneath of upper beam and a force hammer used

to excite above each point in turn (the “excited points” were immediately above the accelerometers). In-plane accelerance was not measured and therefore not accounted for.

A reference accelerometer mounted on the lower beam was used for blocked force validation by comparing the measured and predicted acceleration (composed using the acquired blocked forces). The following sections illustrate the measurement of accelerance and acceleration based on the beam experiment.

5.3.1 Accelerance measurement

Shown in Figure (5.2) is an illustration of accelerance matrix measurements. Here, four positions were chosen to describe the source-receiver interface, these positions were immediately above the accelerometers. A force hammer was used to excite each point on the upper source beam (each point of these positions), and resultant accelerances were arranged into the matrix,

$$\mathbf{A} = \begin{pmatrix} \mathrm{A}_{11} & \mathrm{A}_{12} & \mathrm{A}_{13} & \mathrm{A}_{14} \\ \mathrm{A}_{21} & \mathrm{A}_{22} & \mathrm{A}_{23} & \mathrm{A}_{24} \\ \mathrm{A}_{31} & \mathrm{A}_{31} & \mathrm{A}_{33} & \mathrm{A}_{34} \\ \mathrm{A}_{41} & \mathrm{A}_{41} & \mathrm{A}_{43} & \mathrm{A}_{44} \end{pmatrix} \tag{5-1}$$

where 4x4 are the number of forces and responses. (A_{11} Represents a transfer function between the impact force at point $\boldsymbol{f}_{c1}$ and response at point a_{b1}. A_{12} a transfer function between the impact force at point $\boldsymbol{f}_{c1}$ and response at point $a_{b2}2$, and so on, in Eq. (5.1)).

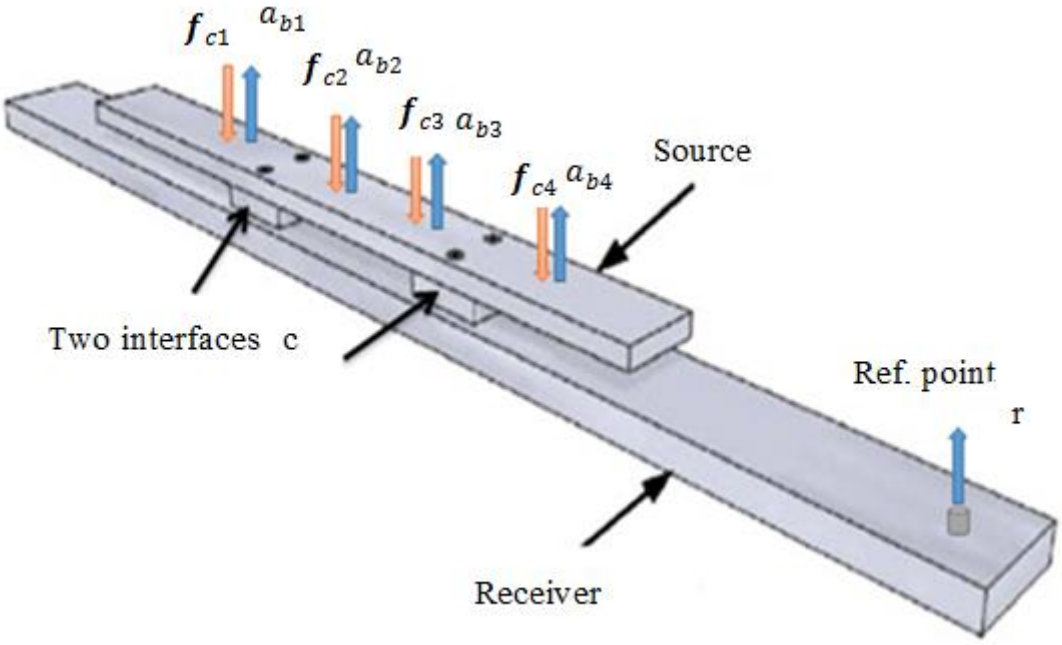

Figure 5-2 Schematic of an ideal source and receiver system to illustrate the measurement of the accelerance of a coupled system. The orange arrows are the applied forces (hammer blows) and the blue arrows are the response points for FRF measurement

It is worth to mention that the coherences for all measurements were checked while measurements were conducted but not reported in this thesis. However, the checked of accelerance using the reciprocity check has been reported in this thesis.

5.3.2 'Acceleration' measurement

Figure (5.3) is an illustration of the measurement of the 'acceleration'. The hammer is used to simulate internal forces and that is why they are not true operational accelerations. An excitation was applied at one point on the upper source beam and response measurements made using the interface and remote reference accelerometer. The acceleration, denoted ($\boldsymbol{a}$), is arranged into a vector as shown in Eq. (5.2).

$$\boldsymbol{a} = \begin{pmatrix} a_1 \\ a_2 \\ a_3 \\ a_4 \end{pmatrix} \tag{5-2}$$

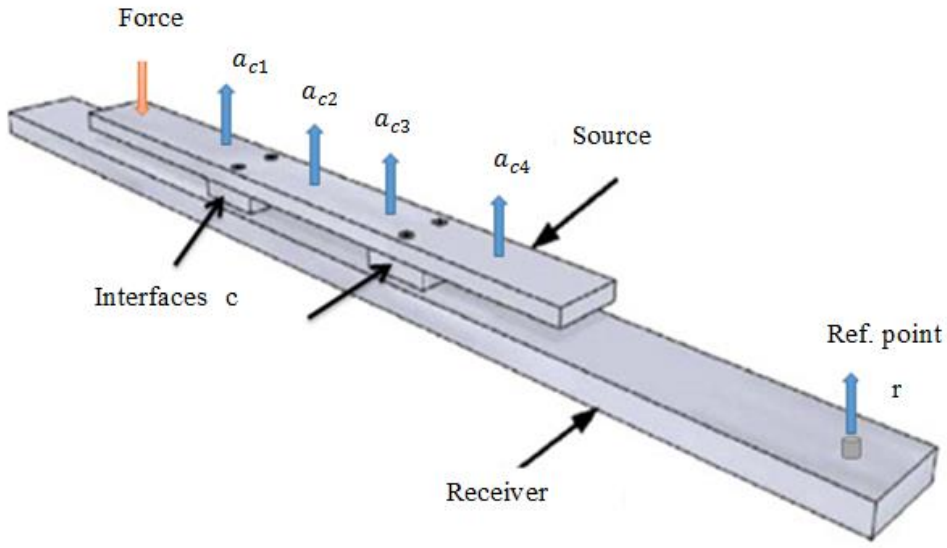

Figure 5-3 Schematic of source and receiver assembly is illustrating the measurement of 'acceleration' of a coupled beam at each point. The orange arrow is the applied force and the blue arrows are the responses points for 'accelerations' measurement

Referring again to Figure (5.3) it can be seen that the points where the accelerations are measured correspond to those included in the accelerance matrix, as in Figure (5.2). The only required measurements at the contact points are the acceleration responses (linear and angular) to a remote exciting force (linear only). If additional measurements are included, i.e. more remote points than the product of the number of contact points and degrees of freedom, the problem can be overdetermined [101, 110]. The combination of these two measurements (accelerance and 'acceleration') allows for the blocked force of the source to be calculated.

5.3.3 Pre-processing data check

In the previous section, the procedure of inverse measurement was explained. In this section, the importance of carrying out preliminary checks to obtain the correct data, amplitude and phase of the accelerance is described. Reciprocity, which was presented in Section (3.2), is one of several ways of checking the data and it plays an important role with the accelerance matrix.

The measured interface accelerance matrix should be reciprocal, i.e. the matrix should be complex symmetric. However, if it is not reciprocal, it can lead to problems in determining the blocked force. Thus, it is very important to check the data before attempting the inverse

procedures and one way to do that is by comparing reciprocal values. For that, various experiments have to be done in order to measure and check the data.

Figures (5.4) and (5.5) show examples of reciprocity of accelerances. All show good agreement across the entire frequency range. Other reciprocities show similar levels of agreement but even though these reciprocity checks give confidence in the results they do not guarantee the quality of the measurements because these are random examples from the full set of reciprocal curves.

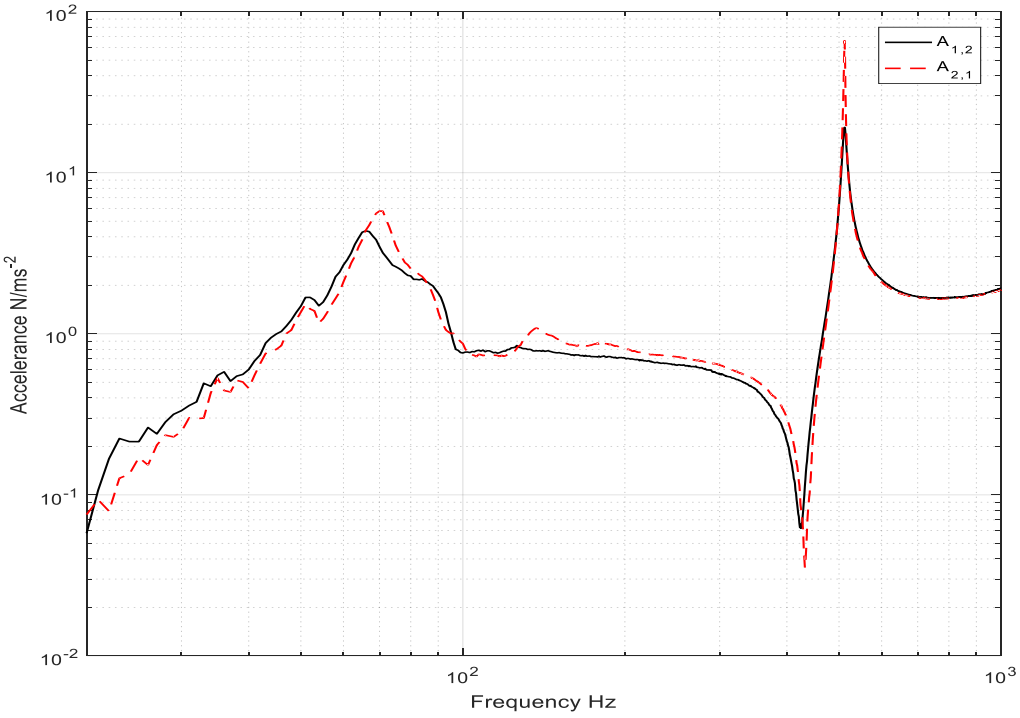

Figure 5-4 Reciprocity of the two accelerances $A_{1,2}$, $A_{2,1}$

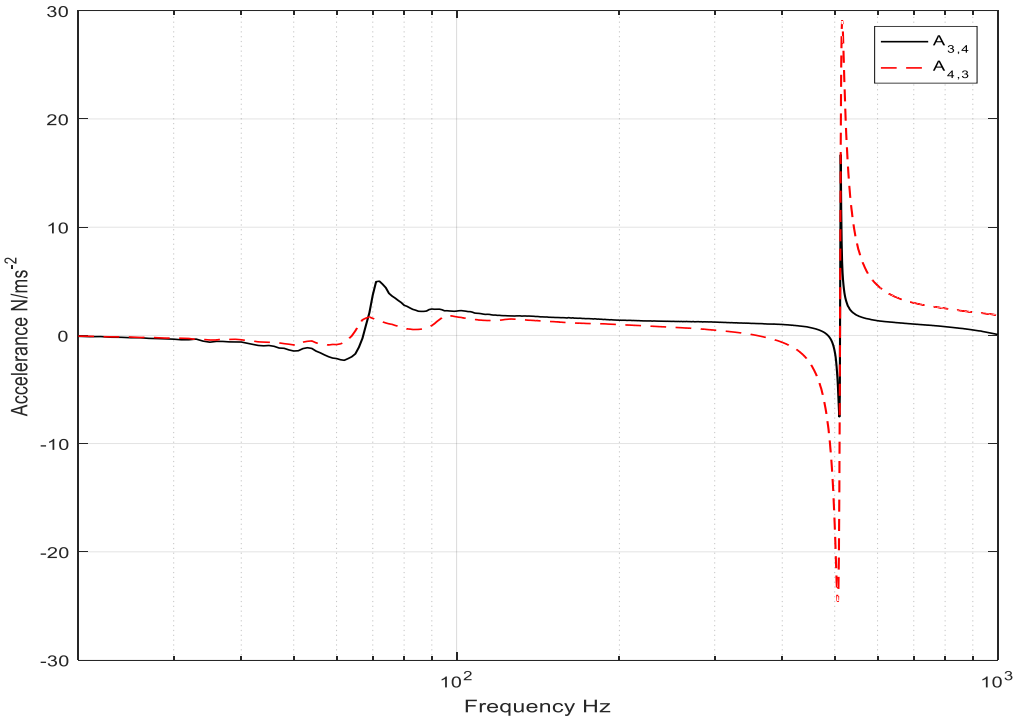

Figure 5-5 Reciprocity of the two accelerances $A_{3,4}$, $A_{4,3}$

Having measured the 'operational acceleration', it is then multiplied by inverted accelerance to calculate the blocked force, as in Eq. (3.25). In the following, the term 'On-board validation' is used to mean validation of the obtained blocked force signals, see Figure (5.6).

5.3.4 On-board validation

On-board validation using artificial excitation has become popular as tool to ensure the quality of measured blocked forces and cross-check the obtained results [85]. It is difficult to determine which degrees of freedom are of most importance when describing the structural couplings between a source and receiver.

As mentioned previously, having measured the accelerance, it is then checked and combined with the measured 'acceleration' to obtain blocked force signal using Eq. (3.25). Once obtained blocked force signal at the interfaces, it is then used to predict the acceleration using Eq. (3.26), (Two blocked forces which have been at the interface were used to predict this acceleration), which will be compared with measured acceleration for validation of that blocked forces.

Figure (5.6) represents the result obtained from the on-board validation of the coupled system of the beam. The obtained result is good especially considering that the calculations in this work were carried through without regularization. It would be expected that the results would be improved by the inclusion of additional DoF, but these results are considered sufficient to demonstrate the procedure.

In general, the frequency spectra show good matching between predicted and measured results, especially below 557Hz, even though the differences increase with the increase in frequency.

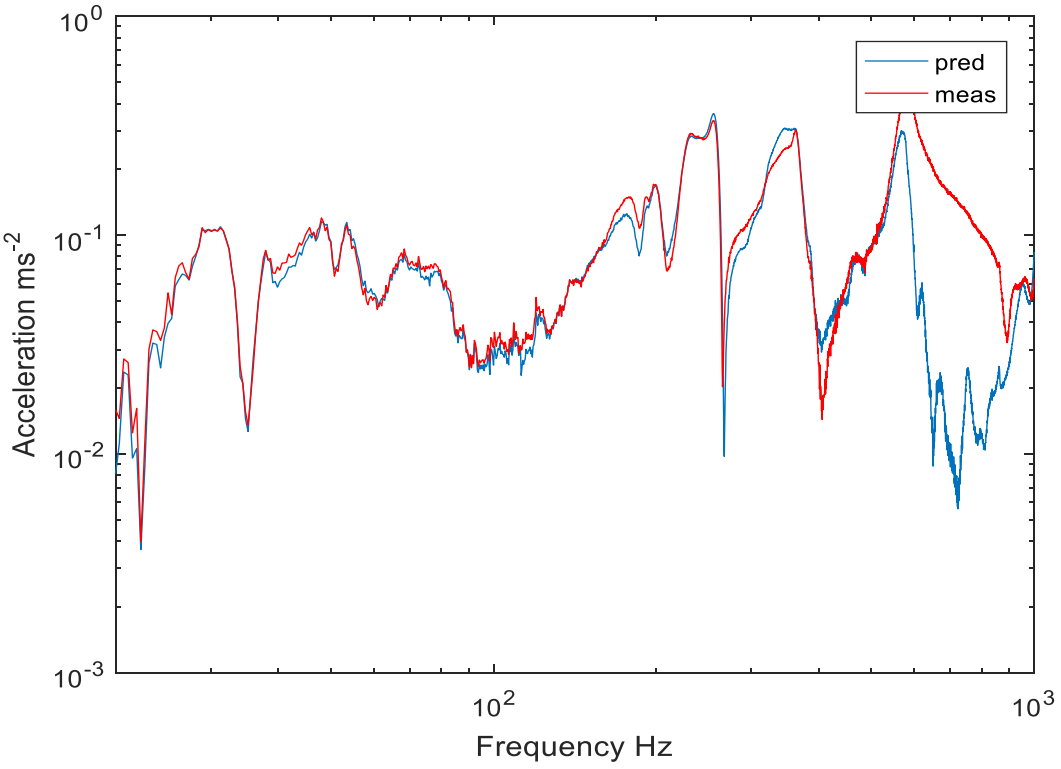

Figure 5-6 On-board validation for artificial excitation of beam experiment. The red line is the measured response. Blue line is the response predicted using blocked force

It was shown above that the blocked forces of a vibration source might be obtained without having to dismantle or modify the source-receiver assembly. In the following section, tests on a structure with greater complexity (the gearbox test rig) are described.

5.4 Blocked force experiments using realistic test rig

Having demonstrated the measurement of blocked force in the previous section using a simple beam structure, the measurement of blocked force with the same procedures was conducted using the test rig presented in Chapter 4. For the purposes of this experiment, the accelerance and acceleration have been measured as described above.

In this case, two different operational measurements are considered:

(a) Artificial 'operational' measurement: a force hammer is used to excite the drive shaft with a controlled and repeatable excitation.

(b) Real operational measurement: in this case, the motor is running and the accelerometers on the interface are removed (otherwise the gears cannot be run).

In real operation, the signal possesses a number of harmonics which makes inspection of the results challenging. The artificial excitation, however, yields a smooth response in the frequency domain, from which it is easier to observe trends.

Obviously, with the test rig, the source, receiver and interface are different from those of the beams shown in Figure (5.1). Here there is not a single source; it is a combination of gear, shaft and supporting bearings. The interfaces are junctions between the gear shafts and housing.

5.5 Blocked forces based on an artificial excitation

In this section, the hammer used for artificial excitation, so, the motor has been disassembled and removed. Two interfaces have been chosen on which to mount the accelerometers. One further remote (reference) point is used for validation purposes (on-board validation) as described above.

5.5.1 Measurement setup

The major difference between this case study and the previously described experiment is the more complex gearbox structure. In this test rig, the components were assembled in the housing, which was disconnected from the motor. Here, the source was assumed to be one shaft with its gear and two supporting bearings, while the housing was the receiver. Two interfaces were defined as the junctions between the source and receiver (as shown in figure (5.7) with two red squares). Ten accelerometers were required on the interface which made the arrangement even more complicated and one accelerometer used as reference point for validation.

Figure (5.7) shows a schematic of the test rig, the impact points (these are marked as excitation points), and relevant accelerometers mounted on the supporting bearings and housing. In this test, the force hammer impacted on the input gear shaft on the top of the shaft head, as shown by the black arrows and red crosses. Accelerance and 'acceleration' measurements were measured using the hammer as mentioned above. Thus, to begin with, the hammer was used to excite each point on the interface to measure the accelerance matrix. The accelerance matrix was arranged as following:

$$\mathbf{A} = \begin{bmatrix} A_{1,1} & A_{1,2} & A_{1,3} & A_{1,4} & A_{1,5} & A_{1,6} & A_{1,7} & A_{1,8} & A_{1,9} & A_{1,10} \\ A_{2,1} & A_{2,2} & A_{2,3} & A_{2,4} & A_{2,5} & A_{2,6} & A_{2,7} & A_{2,8} & A_{2,9} & A_{2,10} \\ A_{3,1} & A_{3,2} & A_{3,3} & A_{3,4} & A_{3,5} & A_{3,6} & A_{3,7} & A_{3,8} & A_{3,9} & A_{3,10} \\ A_{4,1} & A_{4,2} & A_{4,3} & A_{4,4} & A_{4,5} & A_{4,6} & A_{4,7} & A_{4,8} & A_{4,9} & A_{4,10} \\ A_{5,1} & A_{5,2} & A_{5,3} & A_{5,4} & A_{5,5} & A_{5,6} & A_{5,7} & A_{5,8} & A_{5,9} & A_{5,10} \\ A_{6,1} & A_{6,2} & A_{6,3} & A_{6,4} & A_{6,5} & A_{6,6} & A_{6,7} & A_{6,8} & A_{6,9} & A_{6,10} \\ A_{7,1} & A_{7,2} & A_{7,3} & A_{7,4} & A_{7,5} & A_{7,6} & A_{7,7} & A_{7,8} & A_{7,9} & A_{7,10} \\ A_{8,1} & A_{8,2} & A_{8,3} & A_{8,4} & A_{8,5} & A_{8,6} & A_{8,7} & A_{8,8} & A_{8,9} & A_{8,10} \\ A_{9,1} & A_{9,2} & A_{9,3} & A_{9,4} & A_{9,5} & A_{9,6} & A_{9,7} & A_{9,8} & A_{9,9} & A_{9,10} \\ A_{10,1} & A_{10,2} & A_{10,3} & A_{10,4} & A_{10,5} & A_{10,6} & A_{10,7} & A_{10,8} & A_{10,9} & A_{10,10} \end{bmatrix} \quad (5\text{-}3)$$

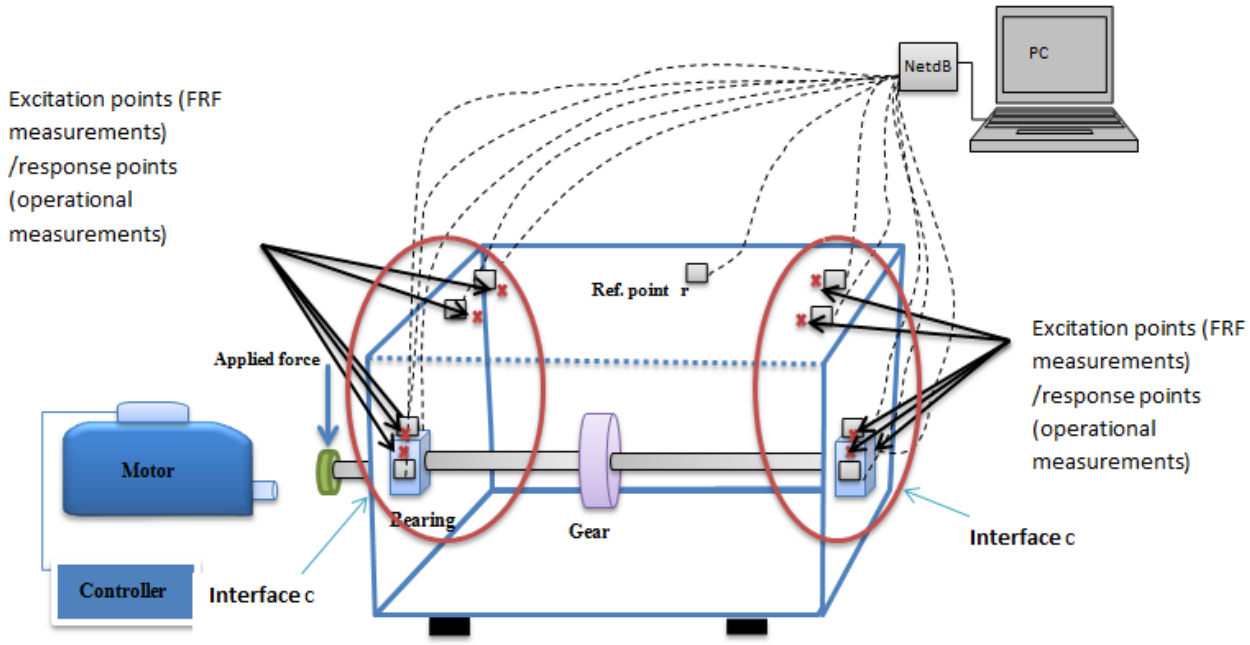

Figure 5-7 Schematic of test rig (gearbox) showing a two-stage measurement procedure for obtaining blocked forces at the interfaces (c) in the red circles. The red crosses indicate the excitation and response points for FRF and 'acceleration' measurement, r is the (remote) reference point using for validation purpose for case study. The blue arrow indicates a measuring excitation point for artificial excitation

5.5.2 Pre-processing data check

Figures (5.8) and (5.9) represent reciprocity checks of different elements using the test rig. These reciprocities show very good agreement across the entire frequency range. These reciprocal accelerances were chosen at random but the same constraint applies here as above, these plots do not guarantee that all the measurements are good, but it does give us confidence.

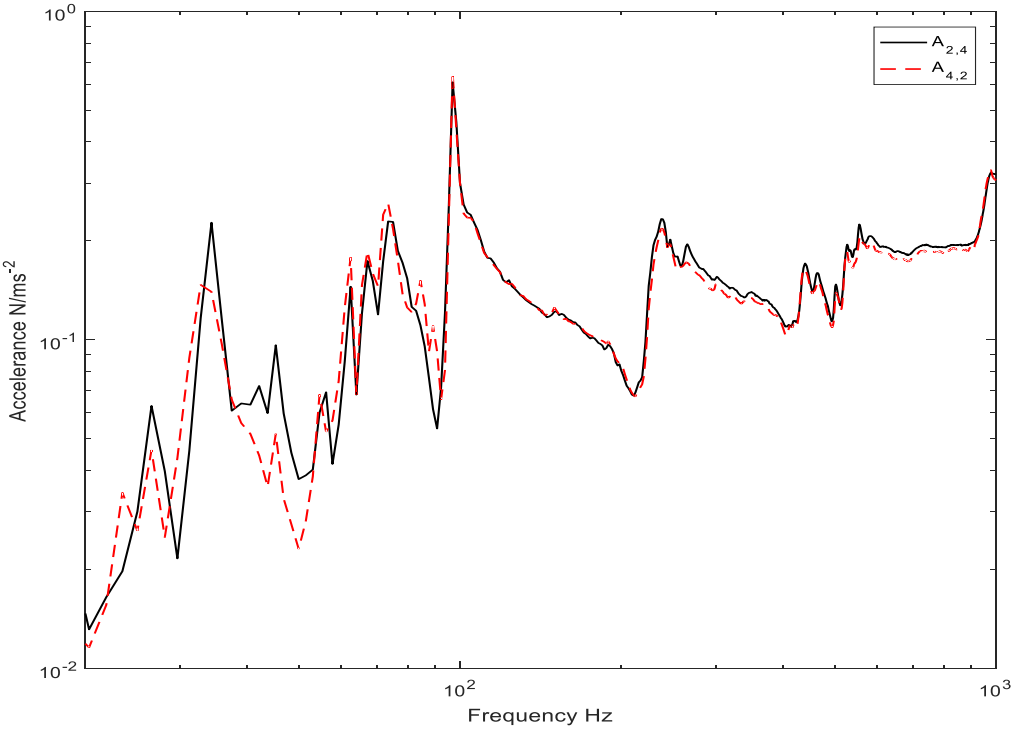

Figure 5-8 Reciprocities of different elements $A_{2,4}$ and $A_{4,2}$

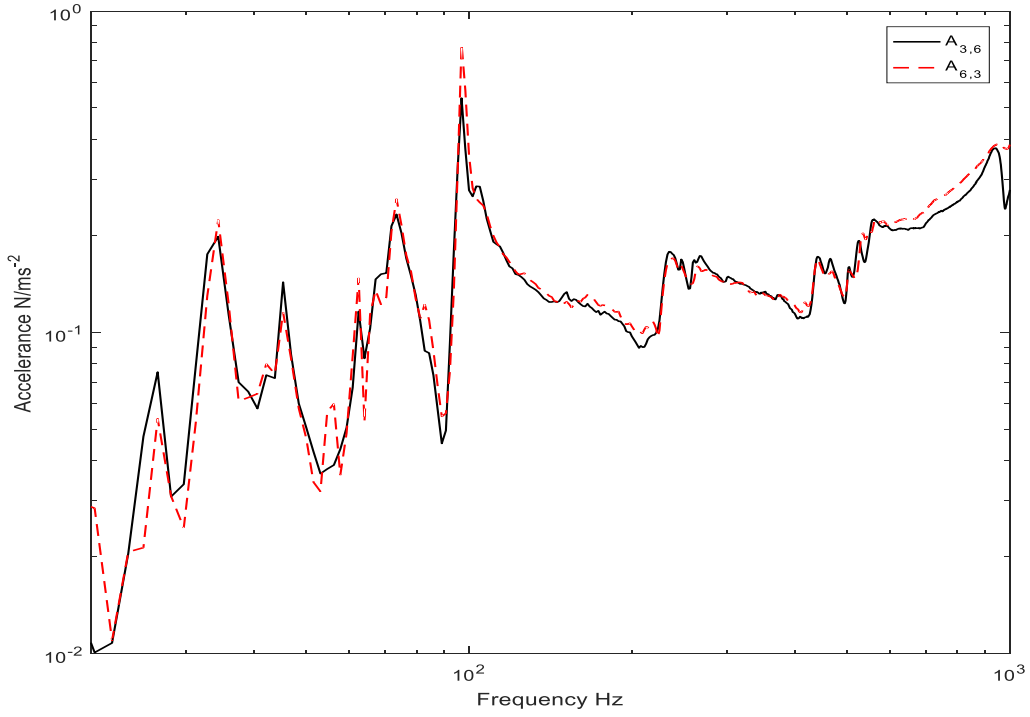

Figure 5-9 Reciprocities of different elements $A_{3,6}$ and $A_{6,3}$,

Other reciprocities had a similar level of agreement see more in Appendix **B**. Having checked the accelerance data, the acceleration was measured by using an artificial excitation of the shaft. Again, Eq. (3.26) was used to predict the acceleration based on the blocked force signal obtained using the test rig. The predicted acceleration was used to validate the blocked force signal by comparing it with the measured acceleration.

5.5.3 On-board validation

As stated in Section (5.3.4) an on-board validation is used to validate the obtained blocked force for the data taken from the test rig. To meet the requirement of testing quality for a rotating machine (gearbox test rig) it is necessary to have confidence in the predicted acceleration based on blocked forces. Therefore, some form of validation for the obtained blocked forces is necessary.

Figure (5.10) shows on-board validation results using ten blocked forces. The obtained result is excellent especially considering that the calculations in this work were carried through without regularization. The predicted response is in excellent agreement with the directly measured response across the majority of the frequency range. However, there is a small under-prediction between about 500 Hz and 900 Hz, which suggests that a source of energy may not have been accounted for, (possibly a neglected DoF).

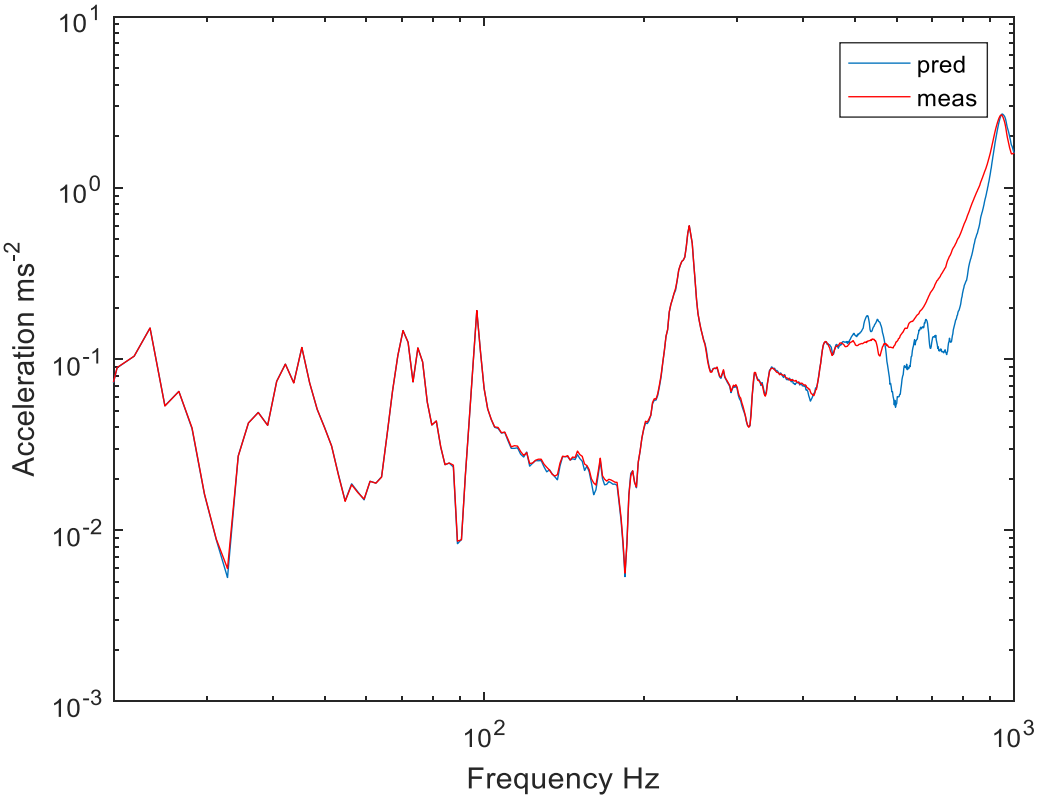

Figure 5-10 On-board validation for artificial excitation using test rig. The red line is the measured response. Blue line is the response predicted using the blocked force

Having obtained the blocked force signal based on artificial excitation of the gearbox test rig, a further test was conducted using same procedure but based on real operational excitation and with more complexity by changing the interface and adding more components.

5.6 Blocked forces based on real operational data

In the previous case, one shaft with two support bearings and gear was assumed to be the source and the force hammer was used to artificially excite the structure to measure accelerance and 'operational acceleration'. In the following, the force hammer is only used for measuring the accelerance, however, the excitation is provided by the operational source itself, by gear meshing driven by the motor. Further, in this test, additional components were added to both structure and interface changed.

5.6.1 Measurement setup

Unlike the previous test, the system considered here is more complicated because of the additional shaft, etc. The interface between the two sets of meshing gear teeth (small region) was assumed to be a source and the rest of the housing was assumed to be the receiver. Here, two accelerometers were required on the interface because the region of the interface is very small to insert more accelerometers. Four accelerometers were mounted on the housing as shown in Figure (5.11). However, three of these accelerometers were excited and one used as remote point for validation purposes. The tests comprise (1) FRF measurement (machine switched off) with accelerometers on the source region boundaries (small region at meching point) and hammer excitation at locations on the housing (2) accelerometers mounting on the interface removed and vibration signals are recorded at the same positions on the housing.

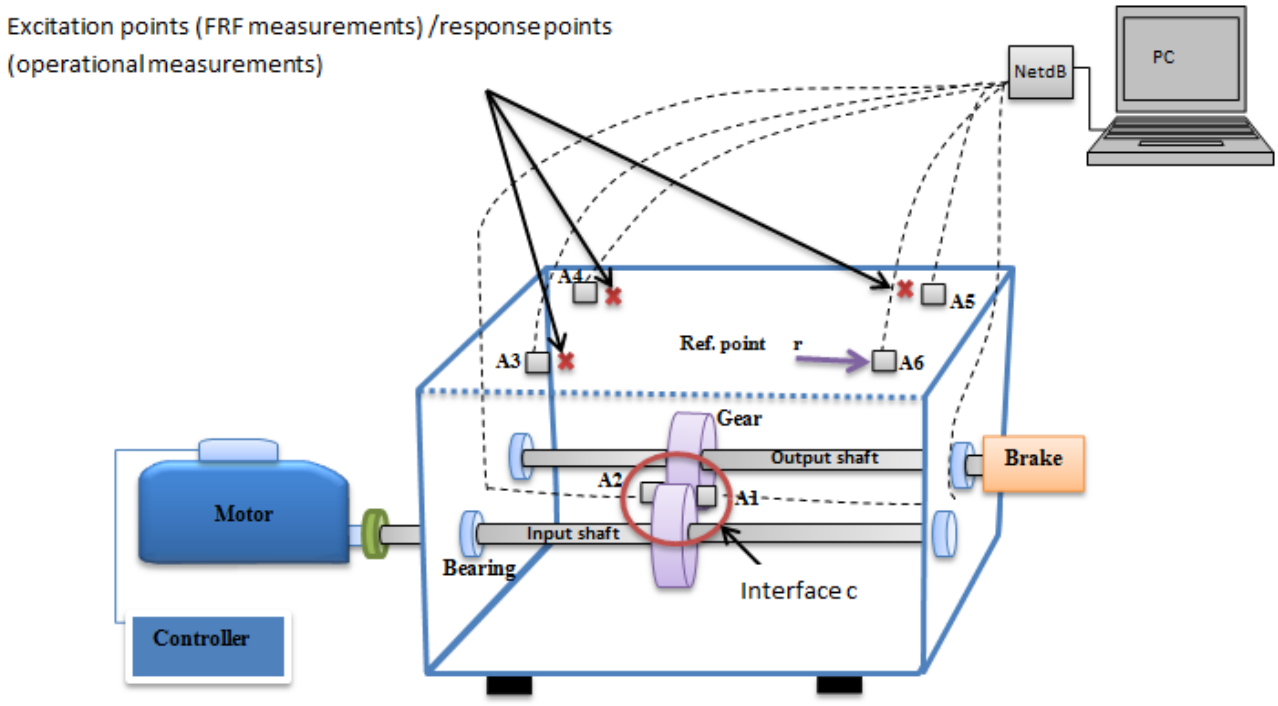

Figure 5-11 Schematic of the test rig showing Source and receiver assembled structure (accelerometer positions on the interface and housing). Two-stage measurement procedure for obtaining blocked forces at the interface (c) in a red square between the meshing teeth. While A_3, A_4 and A_5 are excitation points for FRF measurement but response points for the operational measurement). A_6 is the reference point for validation purpose.

It was difficult or impossible to excite the interface point (source region) because it was inside the machine, see Figure (5.12).

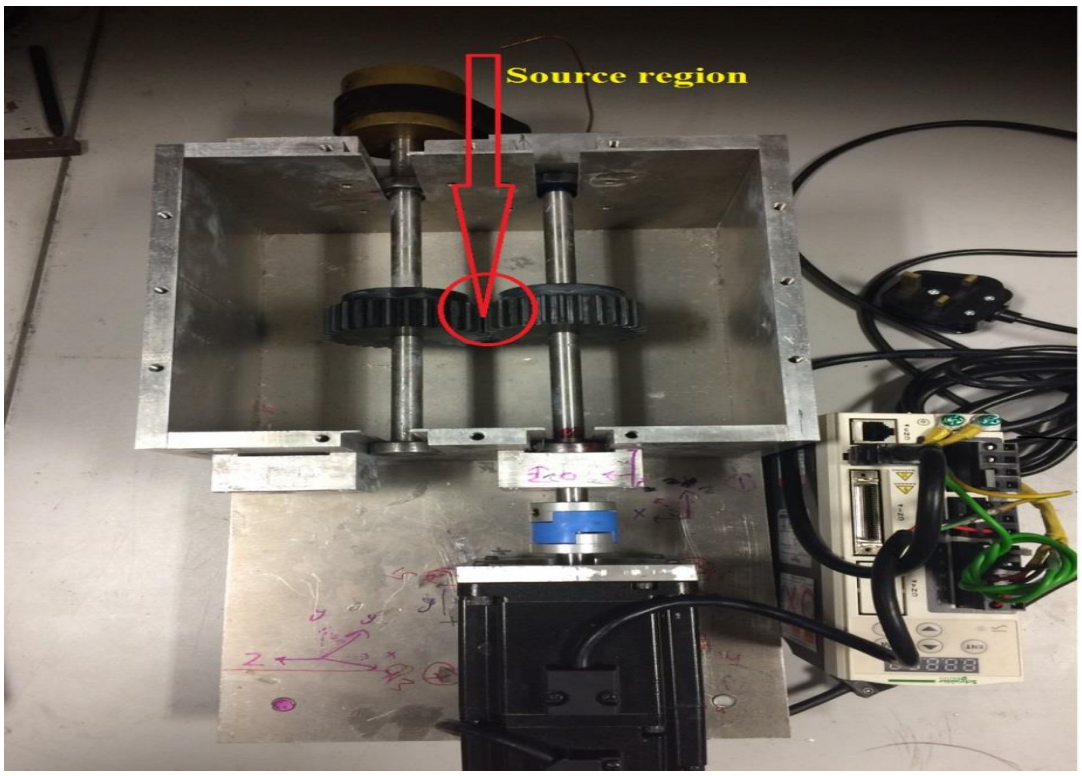

Figure 5-12 Source and interface in test rig

Preliminary measurement has abeen conducted using 2 DoFs. However, a single DoF was considered appropriate in this experiment:

- Because we used spur gear, the load is transformed mainly through vertical direction which why we used single DoF in that direction. It is worth to mention that for other type of gears such as helical gear, additional DoF may be used but this for future work).
- For first time attempt the experiment we start it simple DoF
- It is initially considered 2 DoF using 4 accelerometers and from that we found the result gained of 2 accelerometers using one DoF is similar. We tried to use more DoF (using more accelerometers) and detailed description with 2 DoFs did not perform better.

The accelerance was measured by exciting the chosen positions on the housing with two accelerometers mounted on the interface (gear meshing teeth).

The measured accelerance was arranged into a matrix as shown in Eq. (5.1). It is should be noted that the reference point was not included in the accelerance matrix. Having measured the accelerance, the accelerometers mounted on the interface were removed and the motor turned on to be able to measure the real operational acceleration signal. Here, we invoke the reciprocity principle to avoid direct measurement, which would require excitation inside the housing and the accelerometers on the housing. Using the reciprocity principle, the position of the excitation of response may be interchanged so; we apply the excitation externally on the housing while the accelerometers are mounted inside the housing.

5.6.2 Pre-processing data check

As in the previous case of the tests, Figure shows a reciprocity check. Once again, good agreement is seen through most of the frequency range, with some divergence below 80Hz and above 600 Hz. Again, these results do not guarantee the measurements but do give confidence.

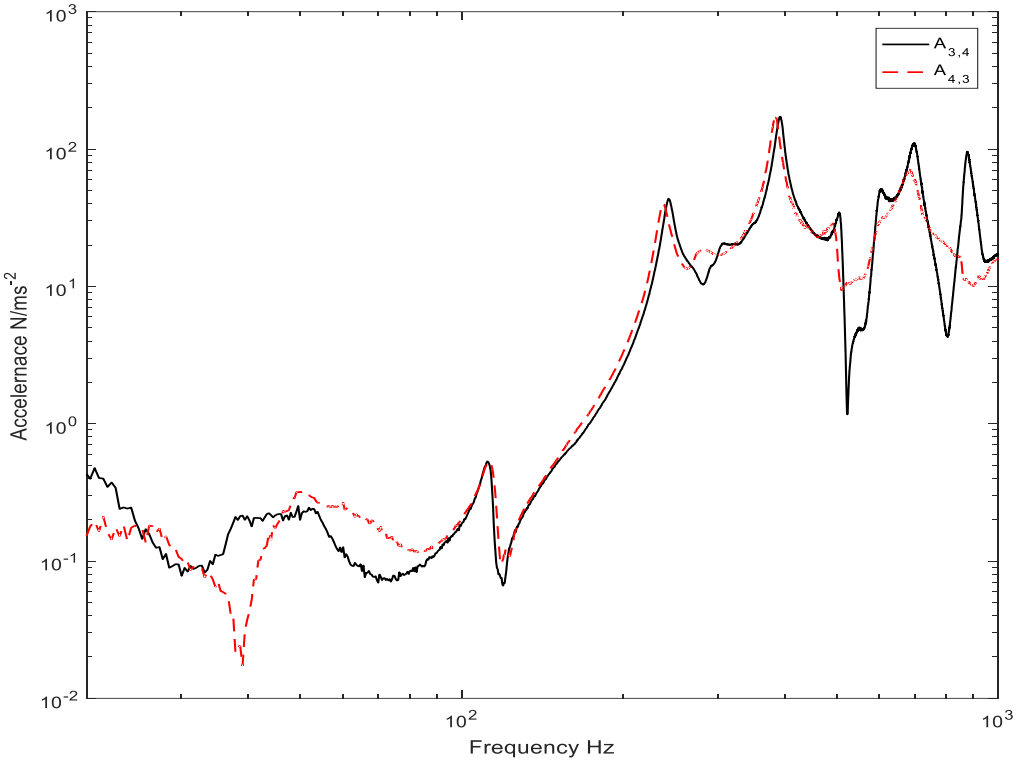

Figure 5-13 Reciprocity of two accelerances $A_{3,4}$ and $A_{4,3}$

Having measured and checked the accelerance as in figure (5.13), the operational acceleration is measured and then transformed to frequency domain. After that, it is combined with the inverse accelerance matrix to calculate the blocked force signal.

5.6.3 On-board Validation

Again an on-board validation is used to validate the blocked force for the data obtained from the test rig. Eq. (3.26) has been used to predict the operational acceleration, which used to compare with the measured acceleration, in order to validate the obtained blocked force signal. By replacing the (artificial) 'operational' excitation with the real acceleration, acquiring the resultant blocked force and performing on-board validation using real acceleration, will allow a demonstrating of the method. The comparison between predicted and measured accelerations provides a validation of the calculated blocked force.

This blocked force describes the source independently and can be used to make predictions. Moreover, the acceleration as driven by the motor was measured and responses determined at the same positions as the accelerometers (except for those on the interface which were removed). As mentioned in section (3.2.2) the remote point which has been used to validate the obtained blocked force signal by comparing it with the measured one was not included in the acceleramce matrix.

For completeness, two sets of blocked forces were considered, one from the original test rig, and the other from the test rig as modified by a top sheet of different material and thickness, as described in Chapter 7.

Figures (5.14) and (5.15) show the results obtained from the on-board validation using two blocked forces at the gear mesh interface at two different speeds. As can be seen, there is good level of agreement which was obtained across the majority of the frequency range, which suggests that most of the contributing DoF were accounted for.

The agreement between predicted and measured operational accelerations is good in the majority of frequency range. Again, this suggests that most of the contributing DoF have been accounted for.

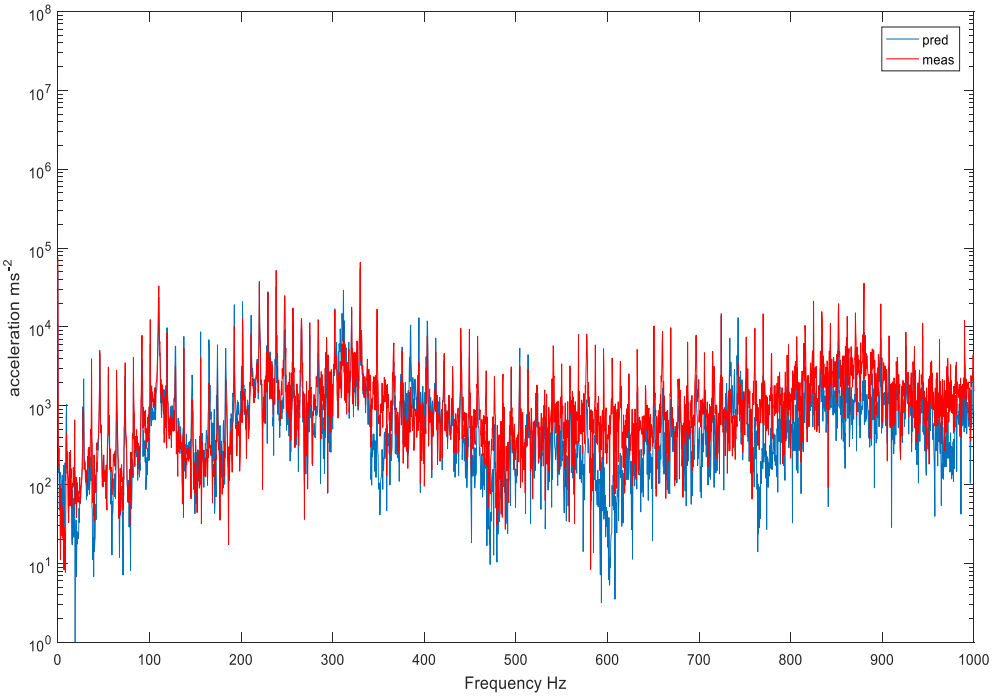

Figure 5-14 On-board validation results of two blocked forces using aluminium cover. The blue line is the predicted acceleration. Red line is the measured acceleration at 550 rpm

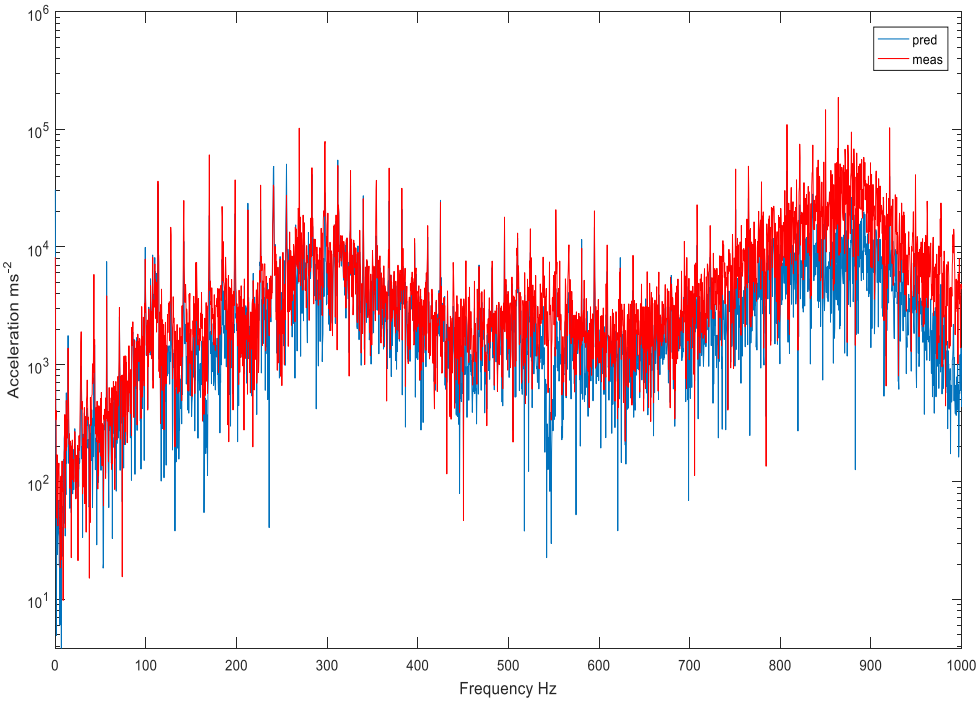

Figure 5-15 On-board validation results of two blocked forces using aluminium cover. The blue line is the predicted acceleration. Red line is the measured acceleration at 850 rpm

There are, however, under-predictions at some frequencies. This again suggests that some energy may not have been accounted for. Therefore, it can be said that the in-situ blocked force can be used as an invariant source descriptor for the test rig.

5.7 Summary

This chapter began by illustrating the preliminary measurement of the in-situ blocked force technique on the simple beam structure before moving onto a more complex structure, the gearbox. In order to test the blocked force and its application in CM, the accelerance and operational acceleration were measured using the purposed built test rig. However, accelerance was measured using the force hammer whilst the acceleration measurement was divided into two parts; using the hammer to simulate the 'acceleration' and secondly operating the motor to obtain the real acceleration. Note that the interface was different for the two tests. It was relocated to be close to the gear mesh point to extract the impulsive signal due to the gears meshing.

For both tests the beam and the test rig, experimental results obtained showed good agreement. Additionally, the blocked forces obtained were validated using on-board validation. Thus, this chapter has shown that the blocked force can be measured for a gearbox.

The following Chapter 6 will present some signal processing techniques and their applications for CM and determine the presence of a fault in the gearbox. Initially they will be applied to the signal after it will be filtered in order to illustrate their use using one accelerometer from which have been used for blocked force measurement as in figure (5.11).

Chapter 6

Fault detection based on acceleration signal

In this chapter, the acceleration signals measured on the housing have been used for identifying a suitable signal characteristic for determining broken tooth faults in gears. The acceleration signal was collected and both conventional and advanced techniques were applied to detect the faults.

6.1 Introduction

There are many conventional techniques which are used to monitor the condition of rotating machinery. Most of these methods are easy to understand and simple to implement. Certain of them will be used here and applied to the measured acceleration signal from a gearbox in order to assess the gearbox condition, and it will be used later to evaluate indirect blocked force signals. Advanced signal processing methods are also used for reasons discussed later.

Some of these techniques extract diagnostic information directly from time domain signals whilst others gather the information from the frequency domain.

Vibration analysis involves the collection of relevant data from a machine which can then be displayed as a time domain plot or transformed using standard techniques into the frequency domain [48]. Fault detection techniques include many statistical parameters based on the time domain, frequency domain and time–frequency domain to detect damage of the gearbox.

The test rig described in Section (4.1) was used to simulate the behaviour of a real rotating gearbox into which faults could be seeded. When the faults were present the gearbox imitated the response of a real machine and could be used to investigate methods for the detection and diagnosis of the seeded faults.

It is worth to mention that each accelerometer position used for the blocked force measurement can also be considered individually in the appraisal of the conventional approach in this chapter. So, two accelerometers have been chosen at random and used for conventional measurement. However, the results of one accelerometer has been shown in this chapter while the other results are similar.

Review of basic signal analysis techniques

The most commonly used signal processing strategies for the CM of machinery are time and frequency domain analysis.

Time domain analysis

The time domain is a plot of signal amplitude versus time and time-domain analysis is appropriate where periodic vibration (which may take the form of impulses) occurs [48] [135]. The most common statistical indicators obtained from time domain signals for machinery are root mean square (RMS), kurtosis (K), crest factor (CF) and skewness (Sk) [136, 137]. A commonly used term for these indicators is "condition indices" and according to their values the condition of a gearbox, for example, would be judged acceptable or not, as the case might be.

If the value of the statistical parameter, e.g. the RMS, increased that would be taken as an indication of the gearbox's deteriorating condition. The assumption is that measured values for a damaged gear would be greater than the corresponding values for a baseline gear, and by comparing like with like, e.g. RMS values of a given vibration signal with a fault present with baseline values for the same gear, the fault and its level of severity could be detected. The RMS is a measure of energy in the signal but K and CF of a signal are measures of its 'spikiness', the presence of peaks in the signal, which can be of great use in detecting the early stages of gear damage. K and CF both increase with increase in vibration generated by the early growth of a fault, but beyond a certain stage, as the damage increases and the defect spreads, the vibration becomes more random in nature and K and CF reduce to more normal levels. Advanced signal processing will also be considered in this research in order to test their effectiveness in detecting and diagnosing faults in the given gearbox system, when the gearbox operates under various speeds and different degrees of tooth breakage.

6.2 Feature extraction

In condition monitoring, signal-processing techniques are used as a tool for successful machine health monitoring and fault diagnostics. An important step is to determine a good diagnostic parameter, e.g. a parameter that changes in a manner that accurately reflects the fault. After

considering a number of statistical parameters that could be suitable for this purpose, it was decided that the most commonly used statistical indicators: root mean square (RMS), kurtosis (K), crest factor (CF) and skewness (Sk) would be the most effective parameters to reflects changes in the level of the fault [39, 40]. These statistical parameters are defined in the next section.

6.3 Statistical measures

These techniques extract statistical parameters from the time-domain signal to indicate damage to a gearbox. The chosen parameters are:

a) Root mean square (RMS)

The RMS is defined for signal x as

$$\mathrm{RMS} = \sqrt{\frac{1}{\mathrm{N}}\sum_{\mathrm{i}=1}^{\mathrm{N}}(\mathrm{x}_\mathrm{i}^2)} \qquad (6\text{-}1)$$

where x is the amplitude of the time domain signal, N is the total number of samples and subscript *i* refers to the i^{th} sample.

RMS is a simple and common approach to the measurement of the overall intensity of a signal, and provides an averaging effect, which reduces the influence of individual impulses in, say, a vibration signal [5]. For gears the RMS of the vibration signal is a good indicator of general health level. However, by its nature the RMS of a signal is not sensitive to isolated peaks in the signal, and this parameter has not been found to be sensitive for diagnosing tooth failure in gearbox systems [39, 138].

b) Kurtosis

Kurtosis examines the shape of the amplitude distribution of the time-domain signal, and is defined in Eq. 6.2 [139]. If the amplitude distribution of a vibration signal is Gaussian then the

corresponding value of the kurtosis is 3. Strictly, kurtosis is the fourth normalized moment of the spectral amplitude. It describes how a signal is grouped around its mean value.

$$K = \frac{\frac{1}{N}\sum_{z=1}^{k}(x_z - \bar{x})^4}{\left[\frac{1}{N}\sum_{z=1}^{k}(x_z - \bar{x})^2\right]^2} \quad (6\text{-}2)$$

where x_z is the z^{th} sample of the time series, $\bar{x}$ is the mean value of the time series, and k is the total number of data points.

The higher the kurtosis value the sharper the peak(s), and the longer their tails in the signal. The lower the kurtosis, the more rounded the peak(s). The value of the kurtosis will increase if the vibration signal contains sharp peaks. Thus, the value of the kurtosis will be higher for faults which impose an impulsive character on the signal.

c) Crest factor

This feature is considered here because it is generally considered useful for the detection of early stage defects in bearings and gears. The CF is the ratio of the peak level of the time-domain signal to its RMS value [25]. Thus, the value of the CF will increase when the signal contains peaks. For gears under normal conditions $2 \leq CF \leq 6$ [48], so if the value of the CF increases above 6 that should be taken to mean the presence of a defect. This parameter is suitable for such cases, which have sources of vibration such as occur with tooth removal from a gear as we are investigated here, or bearing defect.

$$CF = \frac{\text{peak level}}{\text{RMS}} \quad (6\text{-}3)$$

d) Skewness

Skewness is the normalized third central moment;

$$SK = \frac{E[(x_i - \bar{x})^3]}{RMS^3} \quad (6\text{-}4)$$

where E the expected value of the function.

Skewness is used to measure symmetry of the signal and for a symmetrical amplitude distribution SK = 0. Skewness reflects whether an amplitude distribution curve is skewed to the left or right of the Gaussian distribution. When SK is positive the amplitude distribution is asymmetric with its "pointed end" extending towards higher, more positive values. If SK is negative, again the amplitude distribution is asymmetric but the tail extends towards lower values [39].

6.4 Total energy

This parameter is based on the calculation of energy and uses curve fitting for the meshing frequency and its sideband zones. If the signal $\boldsymbol{x(f)}$ represents the fitted curve for a frequency band from $\boldsymbol{f_1}$ *to* $\boldsymbol{f_2}$, the total energy of signal $\boldsymbol{x(f)}$ in that band (TE) can be expressed as:

$$TE = \int_{f_1}^{f_2} x(f)df \quad (6\text{-}5)$$

where $\boldsymbol{f_1}$ and $\boldsymbol{f_2}$ are lower and upper frequencies of the frequency band, respectively.

For Equation (6.5), integration may be done for the whole range of frequencies using a FFT. However, this integration is numerically performed using the trapezoidal rule and calculating the area between adjacent points using an equation for the spectral envelope obtained curve fitting. TE method was also applied to detect in wind turbine blade suffering from different lengths of crack and helical gear tooth breakage faults in the experimental. However, the results show that the values of the TE must be increased once the fault increases [48, 49].

6.5 Empirical mode decomposition method

Recently, EMD has been applied to many different types of time domain signals to decompose them into IMFs, each of which is taken to be generated by a separate physical source with its own time characteristics [140]. Huang et al [141, 142] and Wu et al [143] argued that real signals will often include many different simple intrinsic modes of oscillation and used EMD methods to identify such oscillatory modes in data sets given the following assumptions:

1- ‘‘The data set contains at least one maximum and one minimum (two extrema);

2- The time interval between two consecutive extrema defines the characteristic local time scale; and

3- If the data contained no extrema but did contain inflections, then the signal can be obtained by integration of the components’’.

In this technique, a number of intrinsic mode functions (IMFs) components could be extracted defined as a function that satisfies the following conditions [139].

“(i). in the full data set, the number of extrema and number of zero-crossing must either be equal or differ at most by one.

(ii). at any point, the mean value of the envelope defined by local maxima and the envelope defined by the local minima is zero’’.

The IMFs indicate the simple oscillatory modes in the signal and an EMD process extracts the IMFs subject to the following steps [144]:

(a) “Identify all the extrema of the signal, and connect all the local maxima by a cubic spline line as the upper envelope. Repeat the procedure on the local minima to produce the lower envelope.

(b) Designate the mean of the two envelopes as m_1, and the difference between the signal $x(t)$ and m_1 as the first component, h_1, so that:

$$h_1 = x(t) - m_1 \quad (6\text{-}6)$$

(c) If h_1 is an IMF, take it as the first IMF of $x(t)$. If h_1 is not an IMF, take it as the original signal and repeat the steps above until k_{1k} is an IMF, and designate k_{1k} as $c_1 = h_{1k}$

(d) Separate the first IMF c_1 from $x(t)$ by

$$x(t) - c_1 = r_1 \quad (6\text{-}7)$$

(e) Treat residue r_1 as the original signal and subject it to the same process as above, therefore we can get other IMFs, $c_2, c_3, \ldots . c_n$, which satisfy

$$r_1 - c_2 = r_2$$

:

$$r_{n-1} - c_n = r_2 \quad (6\text{-}8)$$

By summing Equations (6-6) and (6-8) we obtain:

$$x(t) = \sum_{i=1}^{n} c_i(t) + r_n(t)'' \quad (6\text{-}9)$$

The signal $x(t)$ can now be decomposed into n intrinsic modes with residue r_n.

6.6 Experimental studies

The test rig setup was constructed to study fault detection in a gear. The details of the experimental setup and procedure are presented in the following subsections.

6.6.1 Experimental setup description

Figure (6.1) represents a schematic of the test rig showing accelerometer position and components within the gearbox casing. The experiment was carried out at two different speeds. As can be seen as in the figure, the accelerometers A_4 and A_5 have been chosen at random to

use it for fault detection. However, the only results from one accelerometer are shown, the other results are similar. The data was acquired using the NetdB data acquisition card.

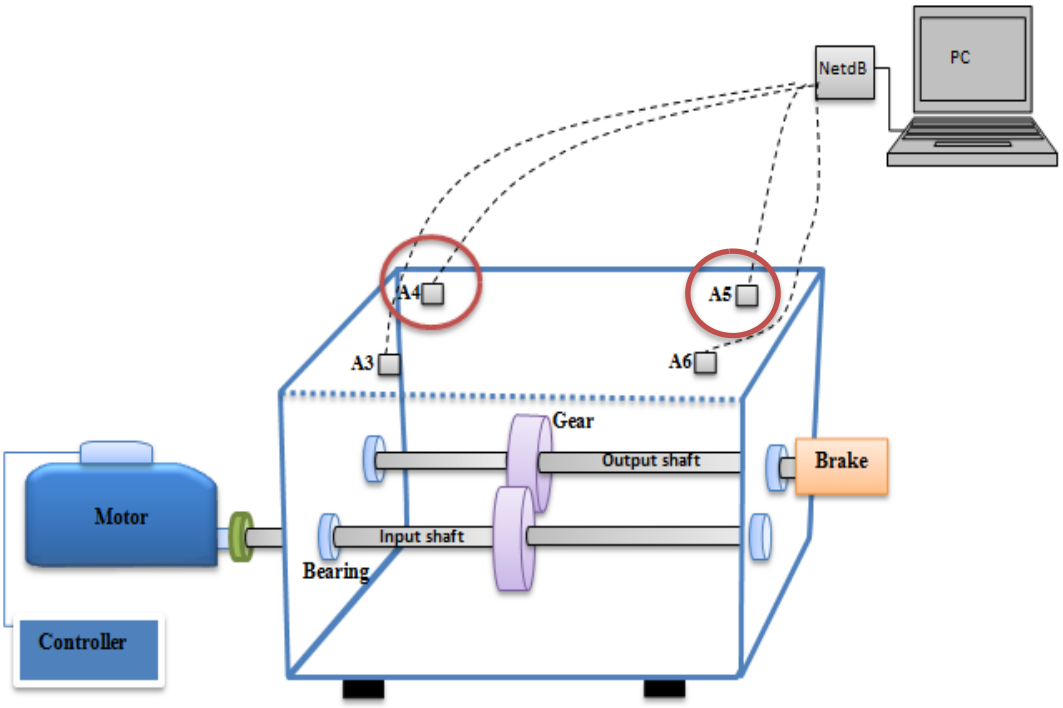

Figure 6-1 Schematic of test rig and the position of the selected accelerometers (selection was at random)

6.6.2 Experimental procedure

In this experiment, the vibration signal was acquired from the baseline gear at shaft speeds of 550 and 850 rpm, this signal is considered as the baseline. In a second test, a fault is induced in the one gear as shown in Figure (4.4) and the corresponding vibration readings were extracted. The sampling frequency of 51 kHz was used for collection of data for flexibility (so, it can be used for any analysis later). The characteristic vibration frequencies of the test rig are listed in table:

Table 6-1Characteristic vibration frequency at 550 and 850 rpm

Parameters	Value (Hz)	
	550 rpm	850 rpm

Gear mesh frequency (GMF)	275	425
Shaft rotating frequency (fs)	9.167	14.167

6.7 Experimental results of vibration investigation

The vibration characteristics of any rotating machine are to some extent unique, due to the various transfer characteristics of the machine. However, the aim here is to find which indicator is the most effective at detecting changes due to the presence of a defect in the gear, based on the measured acceleration signal and can be applied later based on the blocked force signal. Figure (6.2) represents the time domain signals for baseline and faulty conditions at a speed of 550 rpm.

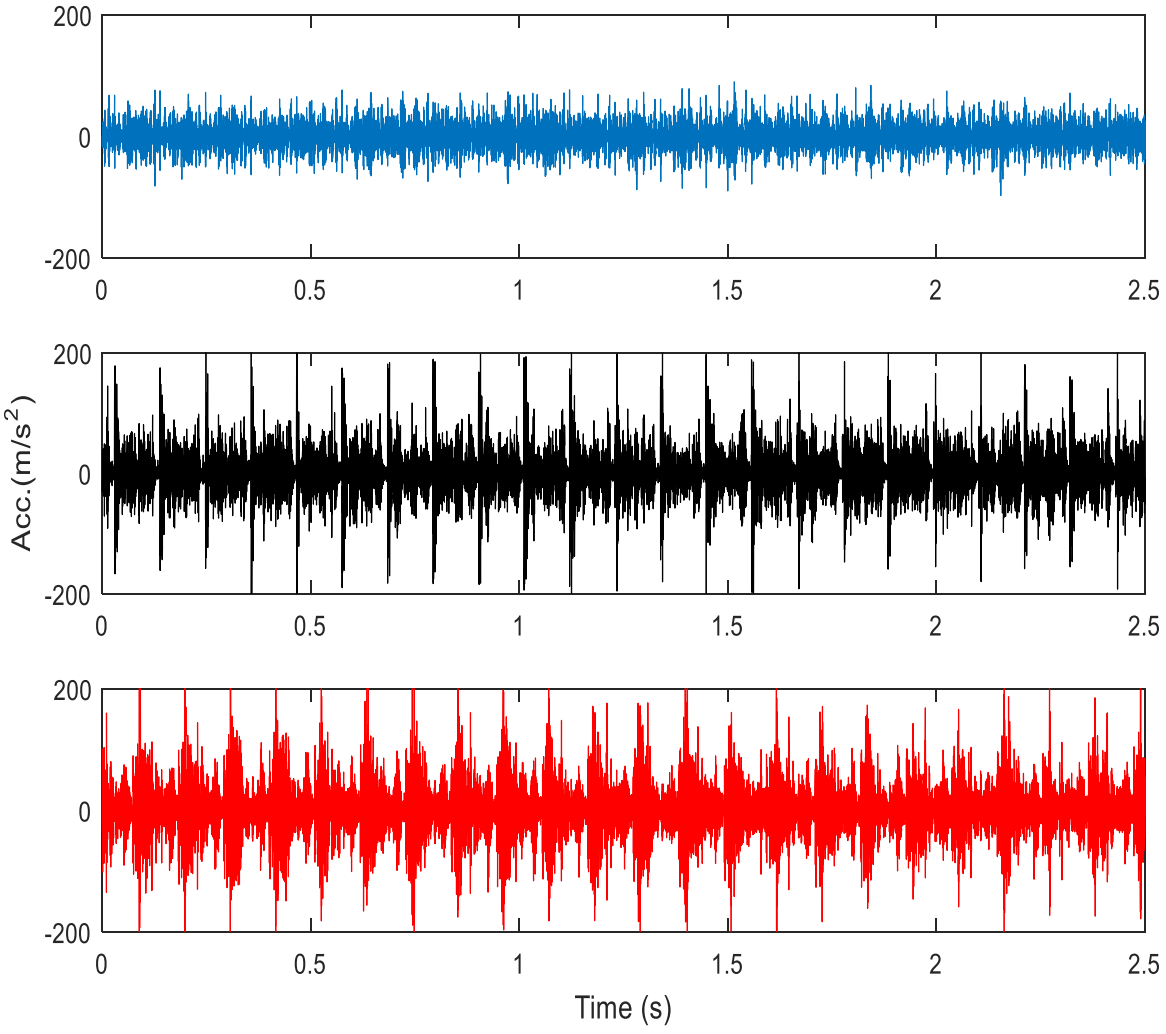

Figure 6-2 Time-domain signals. Blue is the baseline signal and black and red are the fault signals at 25%, 85% tooth breakage respectively, all at speed of 550 rpm

The time domain signals shown in Figure (6.2) are complex and visually nondescript. Such signals are representative of those typically encountered in CM and highlight the need for statistical identification methods. For comparison, the baseline vibration signal was used as a reference by which to assess other cases.

6.8 Experimental result using FFT

Frequency analysis of the experimental vibration signals collected from the baseline machine and under the two tooth breakage fault conditions at different rotational speeds was carried out using the FFT, as shown in Figures (6.3) to (6.6) respectively.

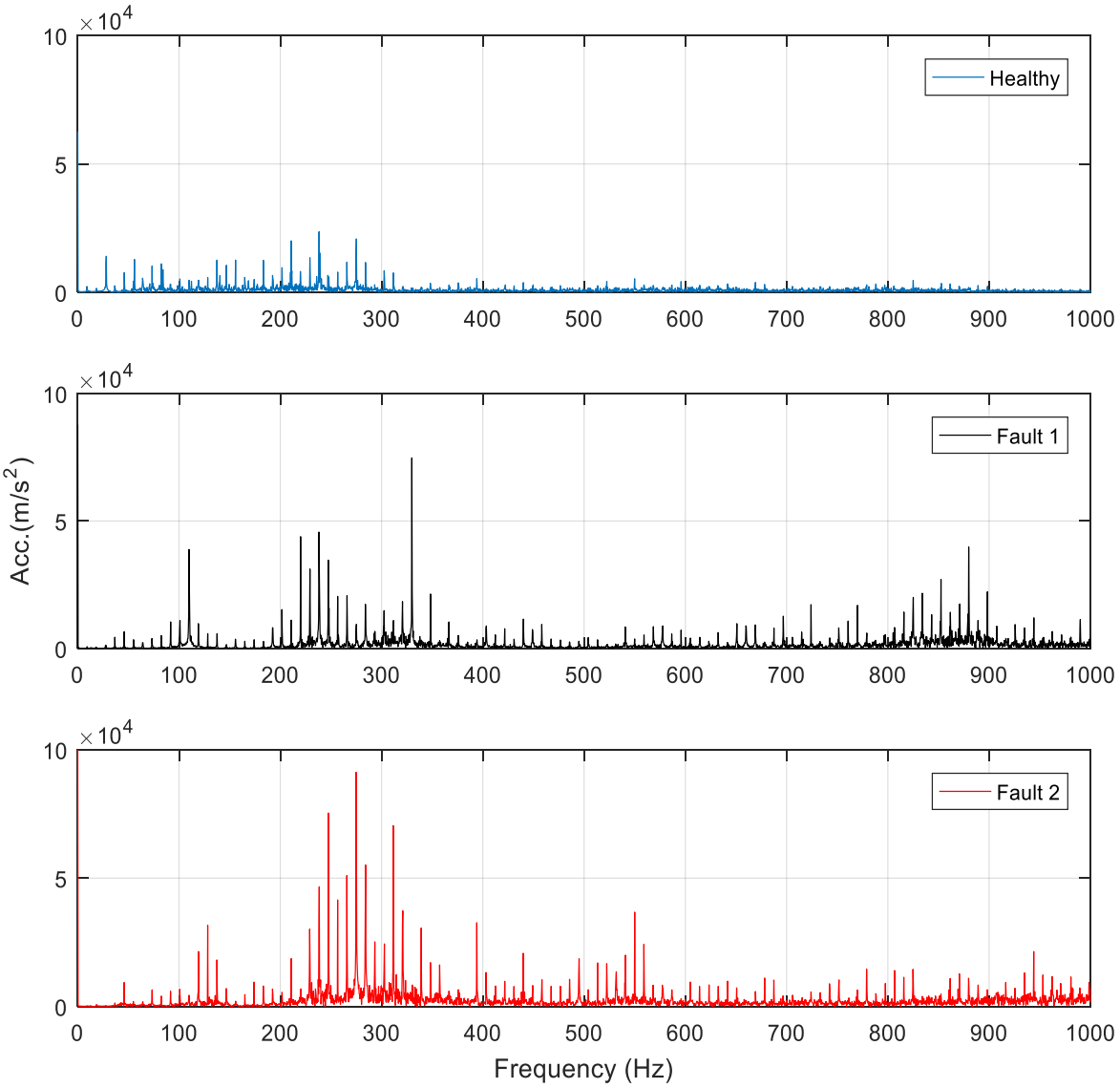

Figure 6-3 FFT for baseline and faulty signals for aluminium cover at 550 rpm, the blue line indicates the baseline condition, the black line is for the 25% tooth breakage and the red signals is for 85%

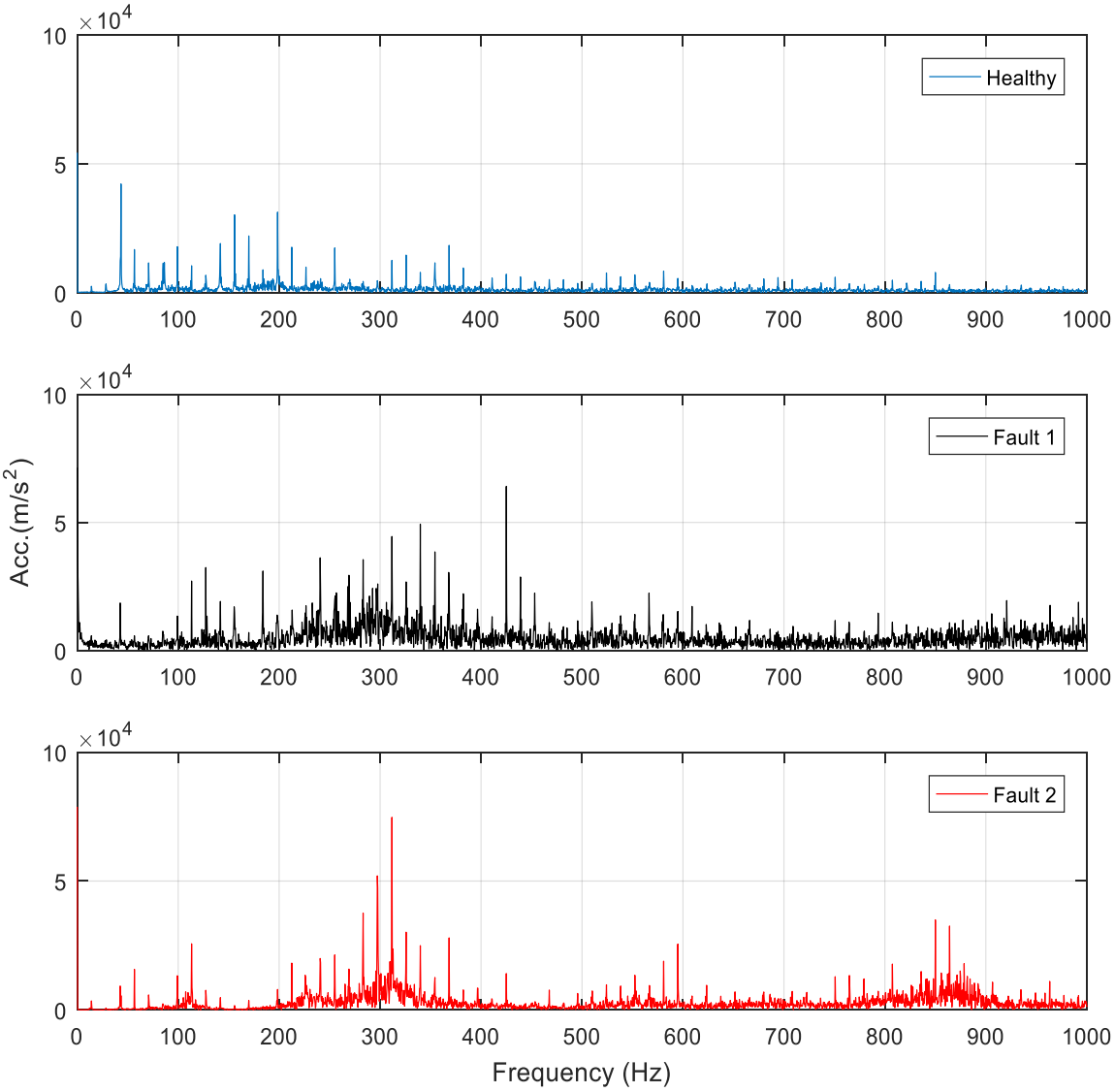

6-4 FFT for baseline and faulty signals for aluminium cover at 850 rpm, the blue line the baseline condition, the black line is for the 25% tooth breakage and the red line is for 85%

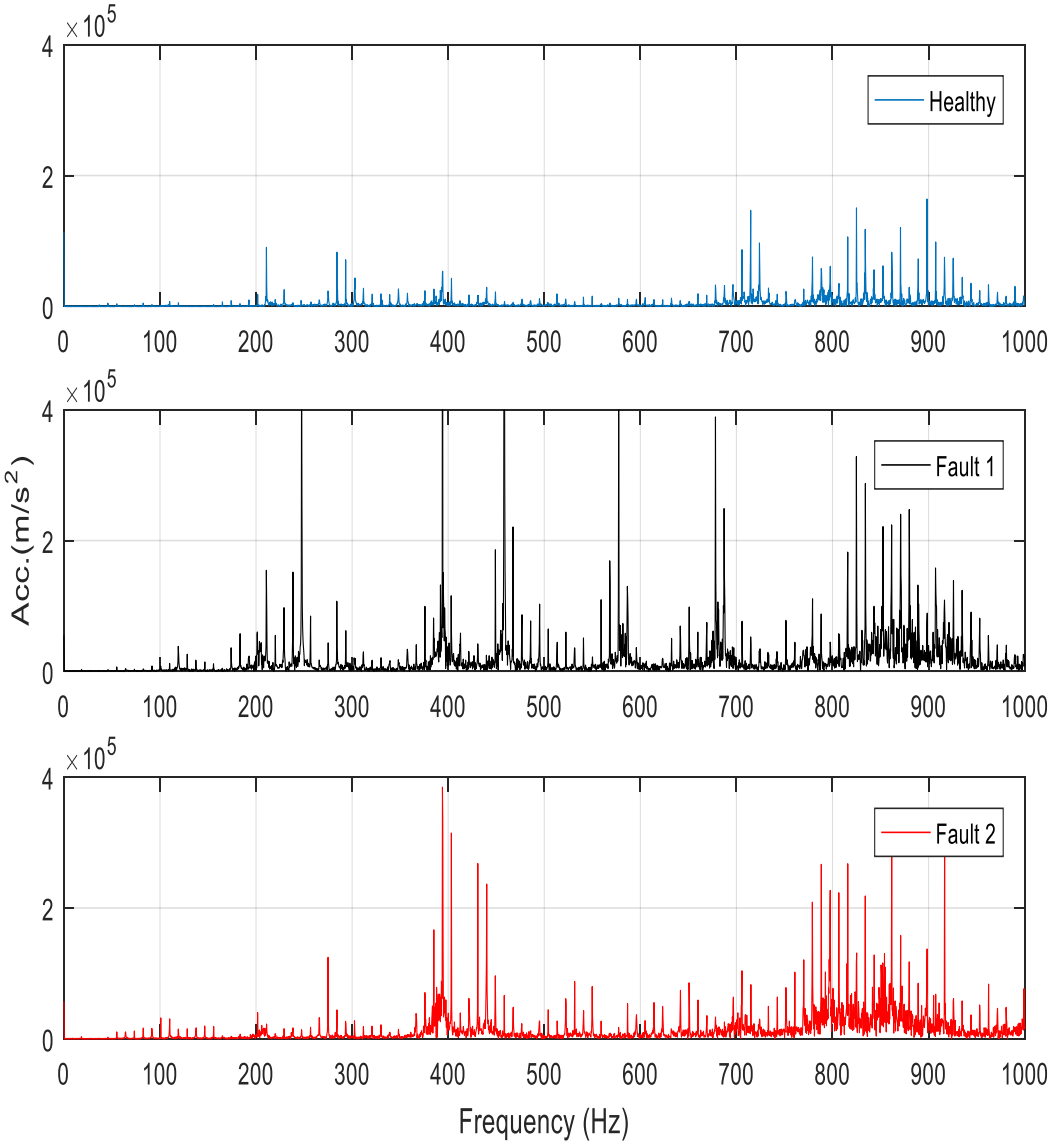

Figure 6-5 FFT for baseline and faulty signals for steel cover at 550 rpm, the blue line indicates the baseline condition, the black line is for the 25% tooth breakage and the red line is for 85%

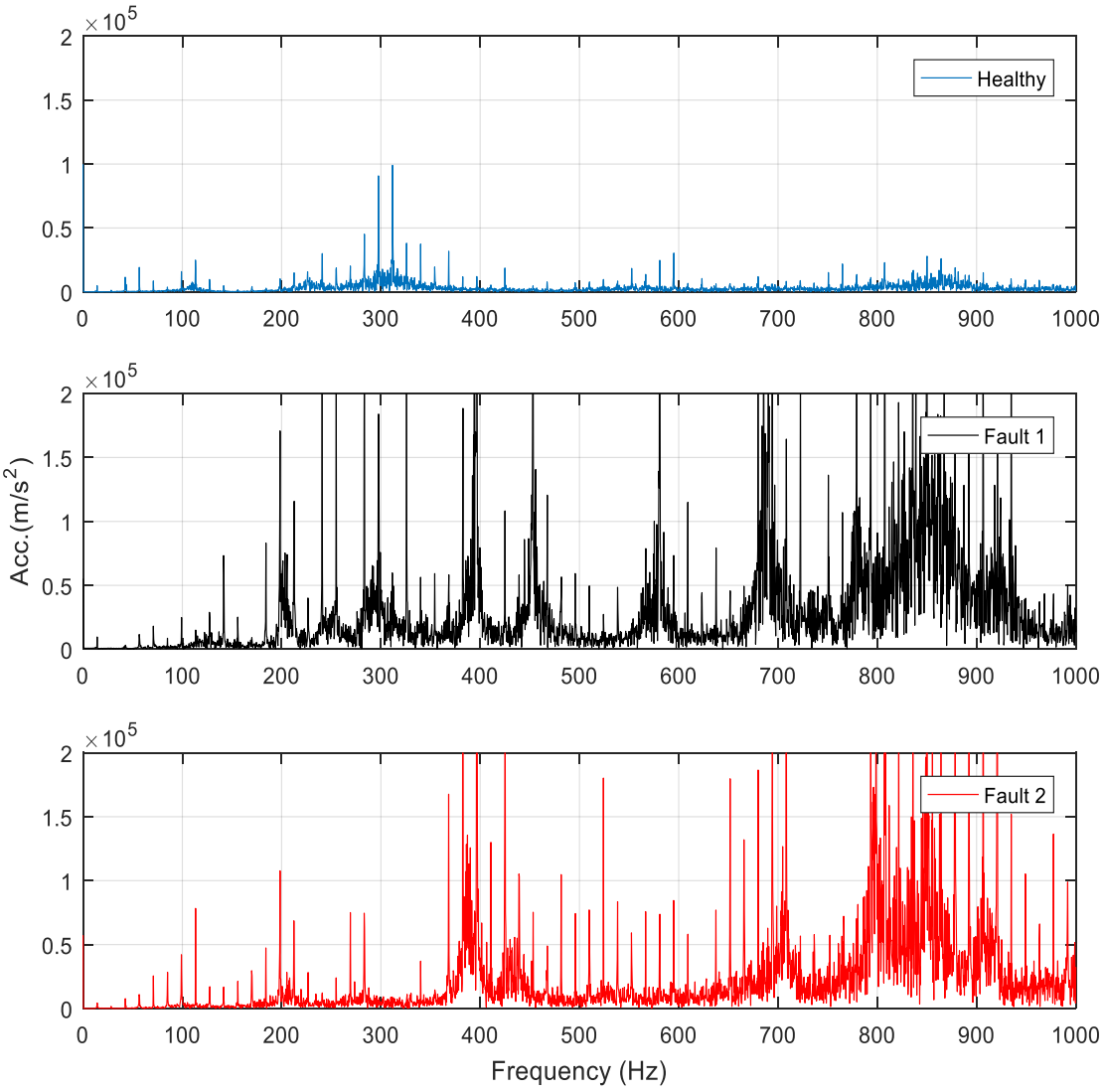

Figure 6-6 FFT for baseline and faulty signals for steel cover at 850 rpm, the blue line indicates the baseline condition, the black line is for the 25% tooth breakage and the red line is for 85%

The FFT has been used to transform the time-domain vibration signals of baseline and faulty signals to the frequency domain as shown in Figures (6.5) to (6.8). Unfortunately, although the figures show changes to the frequency spectrum with the tooth breakage faults, the changes did not appear consistent or significant. Additionally, the sidebands were absented from these signature signals. The reason is that the recorded signals are complex and their statistic characteristics vary with time and because of the effect of the housing as well.

The results show that the FFT did not provide consistent gear's condition related information. However, for that, the low pass filter has been applied to filter the signal above 1000 Hz as

mentioned in the section (4.5) and some statistical parameters were applied to filtered signals as in the following section.

6.9 Comparison of statistical metrics

In this work, statistical parameters were applied to filtered signals to determine the condition of the machine, i.e. whether it is baseline or a fault is present.

Figures (6.7) and (6.8) show values of statistical parameters for the initial and modified assemblies at two rotational speeds, 550 and 850 rpm. The abscissa values of 1, 2 and 3 correspond to the baseline, 25% and 85% tooth removal, respectively. Results indicate that the statistical parameters all vary with defect length, although not all of them in a consistent way for either the aluminium or the steel housing.

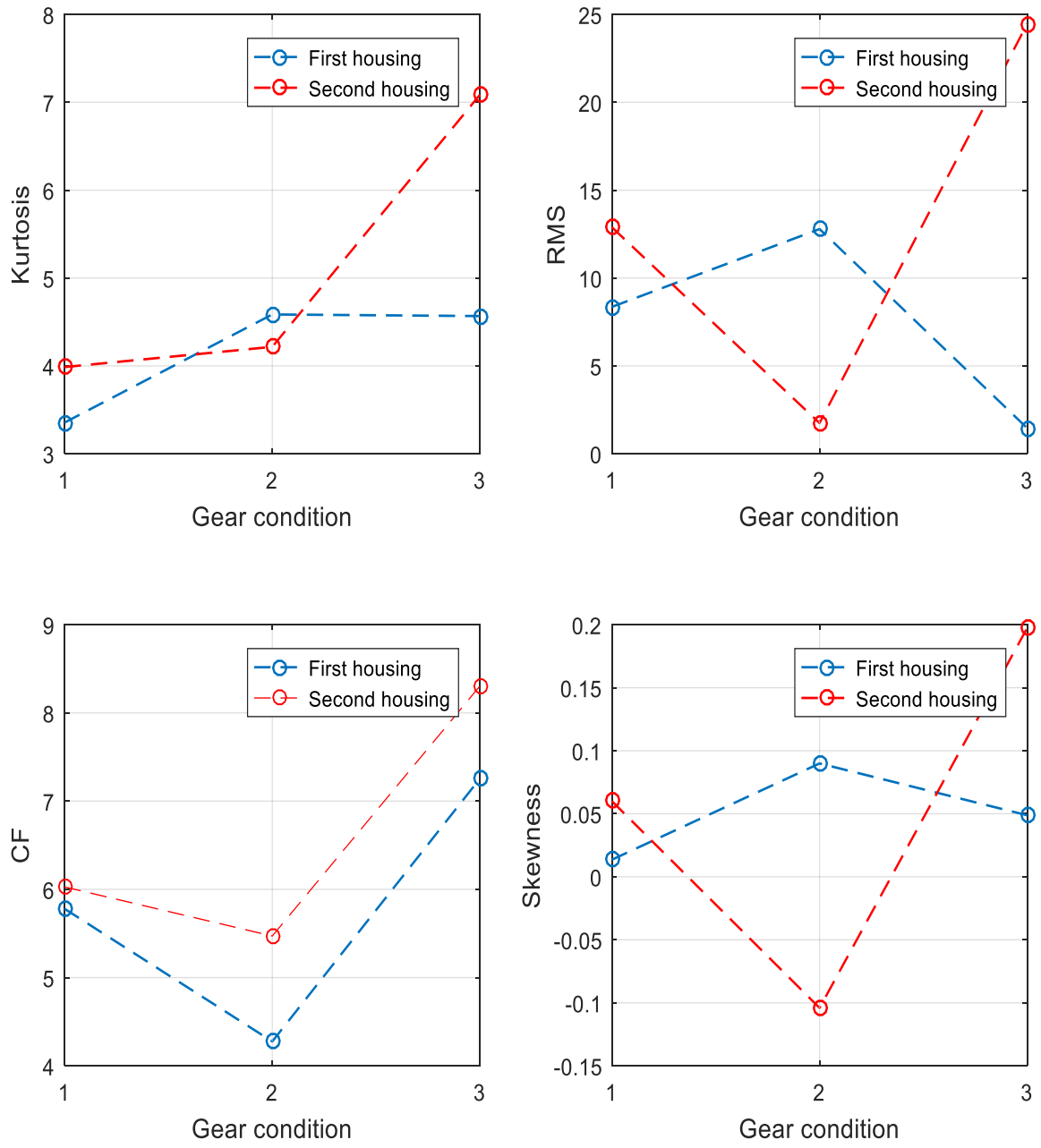

Figure 6-7 Statistical parameters for acceleration signals using aluminium and steel covers. 1, 2 and 3 refer to baseline and faulty conditions of the machine at 550 rpm

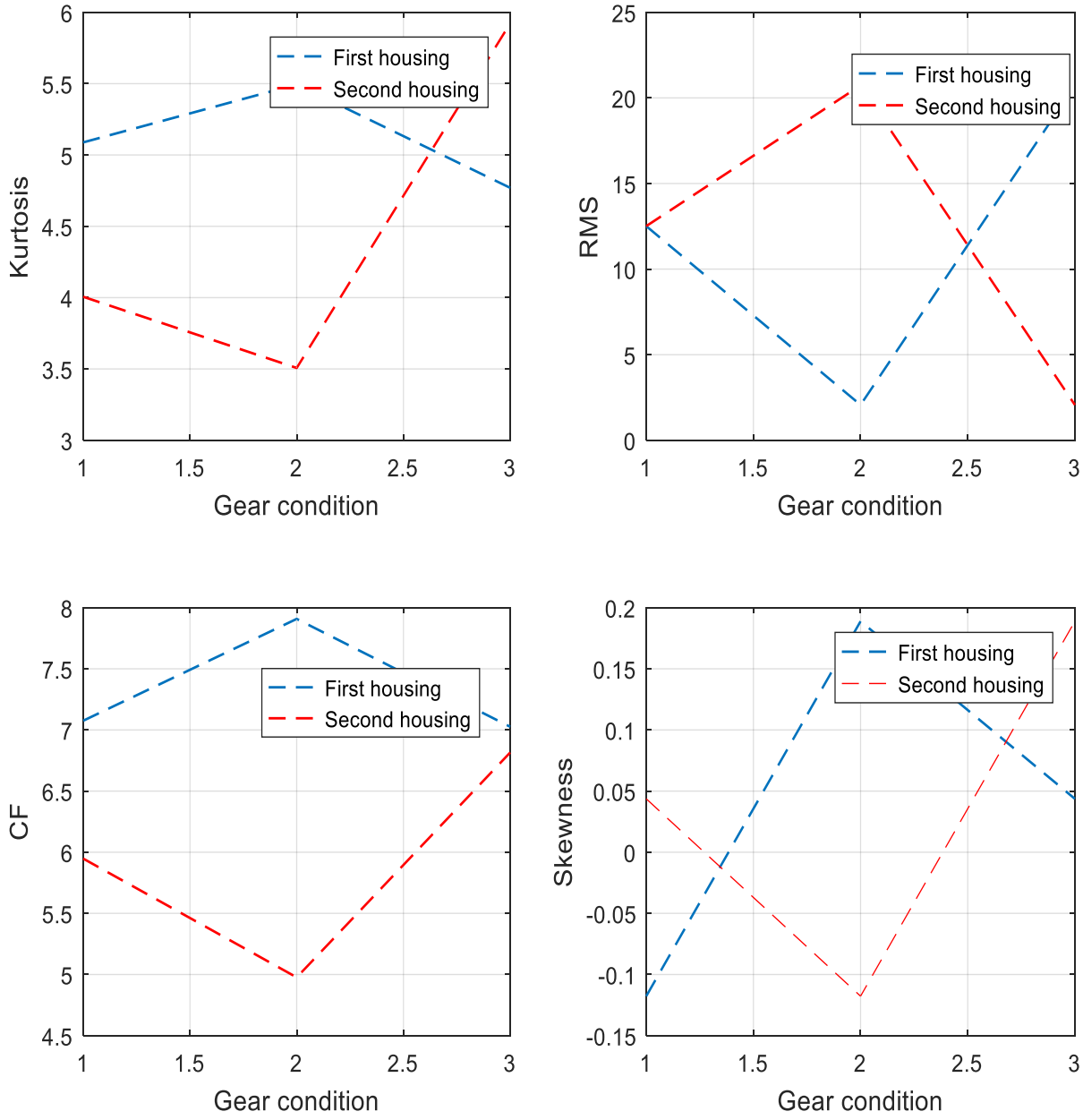

Figure 6-8 Statistical parameters for acceleration signals using aluminium and steel covers. 1, 2 and 3 refer to baseline and faulty conditions of the machine at 850 rpm

It can be clearly seen that the values of kurtosis for a second assembly at the speed 550 rpm, have been increased rapidly for healthy and faulty condition, while for the first housing, there was no consistent trend shown. However, for other parameters, there are no consistent trends have been obtained, which indicated that even though we used the filter, they did not show significant trends for all values, which means that the effect of the housing has not been completely removed. At the speed 850 rpm, the values of all parameters shown that there were

no consistent trends, which means that the effect of the housing may be remain. For that, the more advanced methods have been applied as in the following section.

6.10 Advanced CM techniques

This section begins by introducing methods for analysis of non-linear and non-stationary signal such as total energy (TE) and empirical mode decomposition (EMD). Data analysis is an essential part of the transition from pure research to application. Theory usually begins with linear and stationary processes, which are relatively easy to analyse, but many real-world problems, particularly in CM, are non-linear and non-stationary.

6.11 The performance of EMD on experimental vibration data

EMD method was used to decompose vibration signals collected from the experiments into a number of signals, the IMFs. Each IMF represents a different vibration source. Figures (6.9) to (6.12) show the decomposed signals for the baseline gear for both housings at rotational speeds 550 and 850 rpm. The analysis of these baseline data is used as guide for faulty conditions. However, decomposed signals for faulty data can be seen in Appendix C.

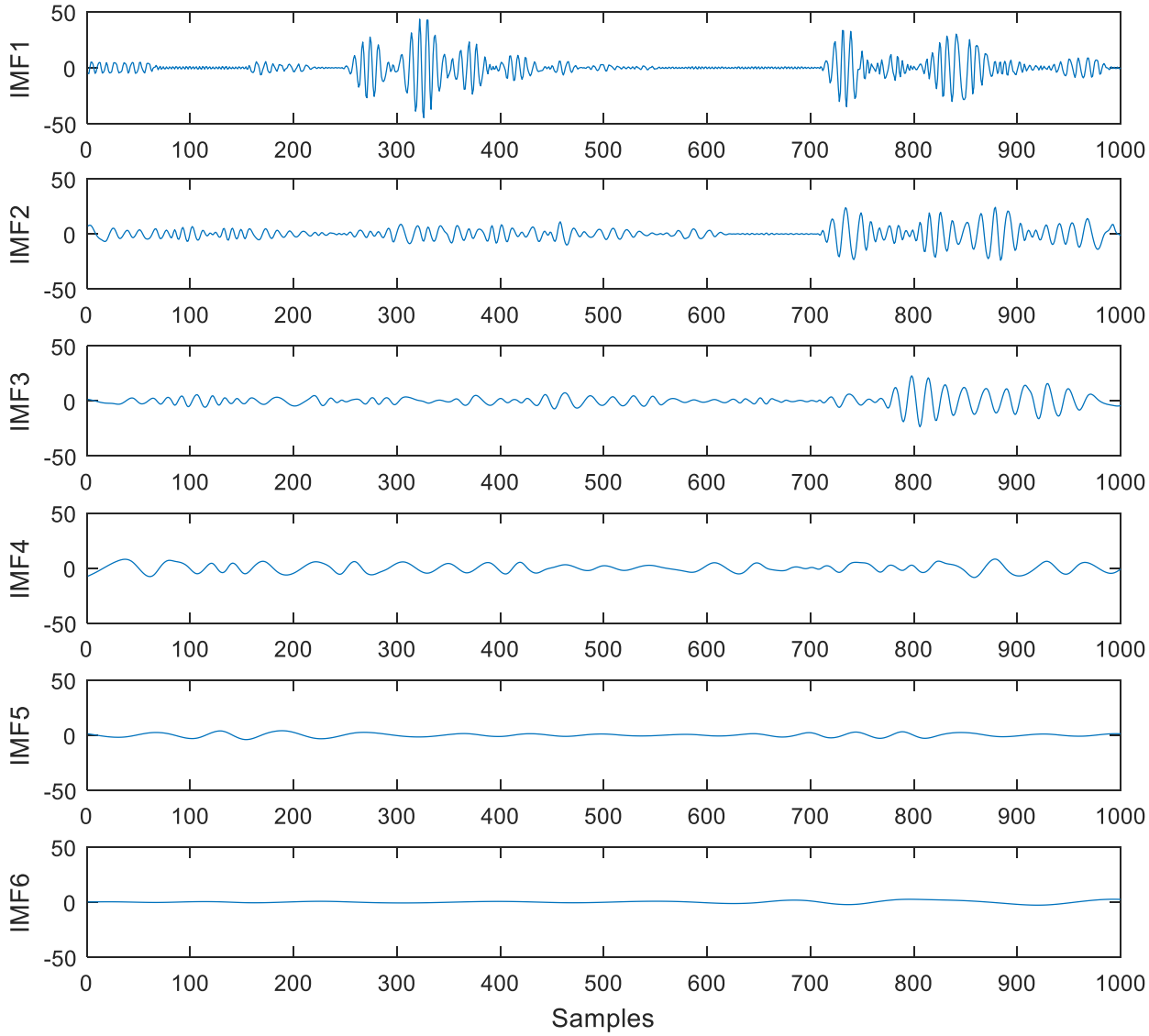

Figure 6-9 Decomposition of experimental gear vibration signal into intrinsic mode functions for baseline condition using aluminium cover at 550 rpm

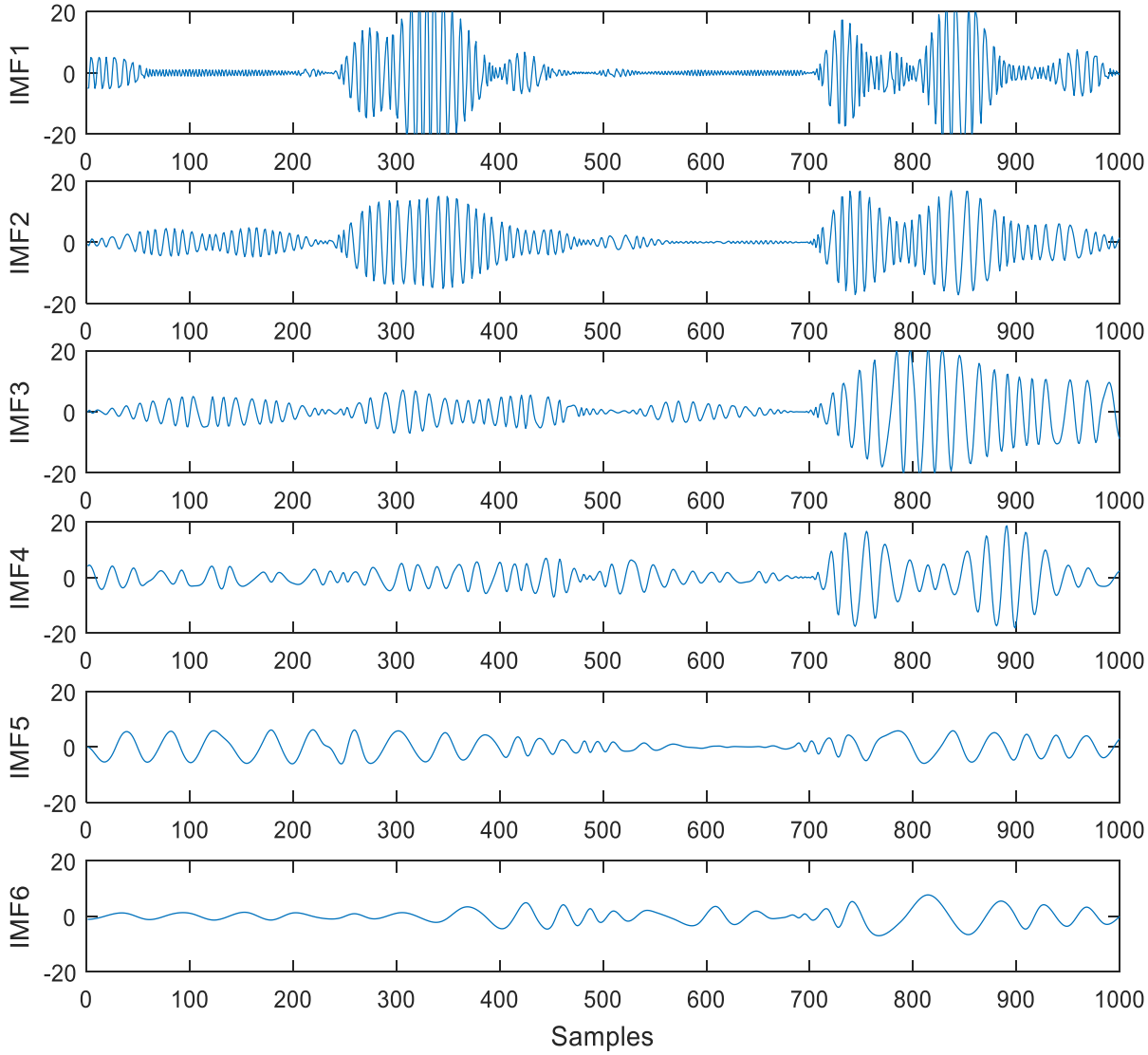

Figure 6-10 Decomposition of experimental gear vibration signal into intrinsic mode functions for baseline condition using aluminium cover at 850 rpm

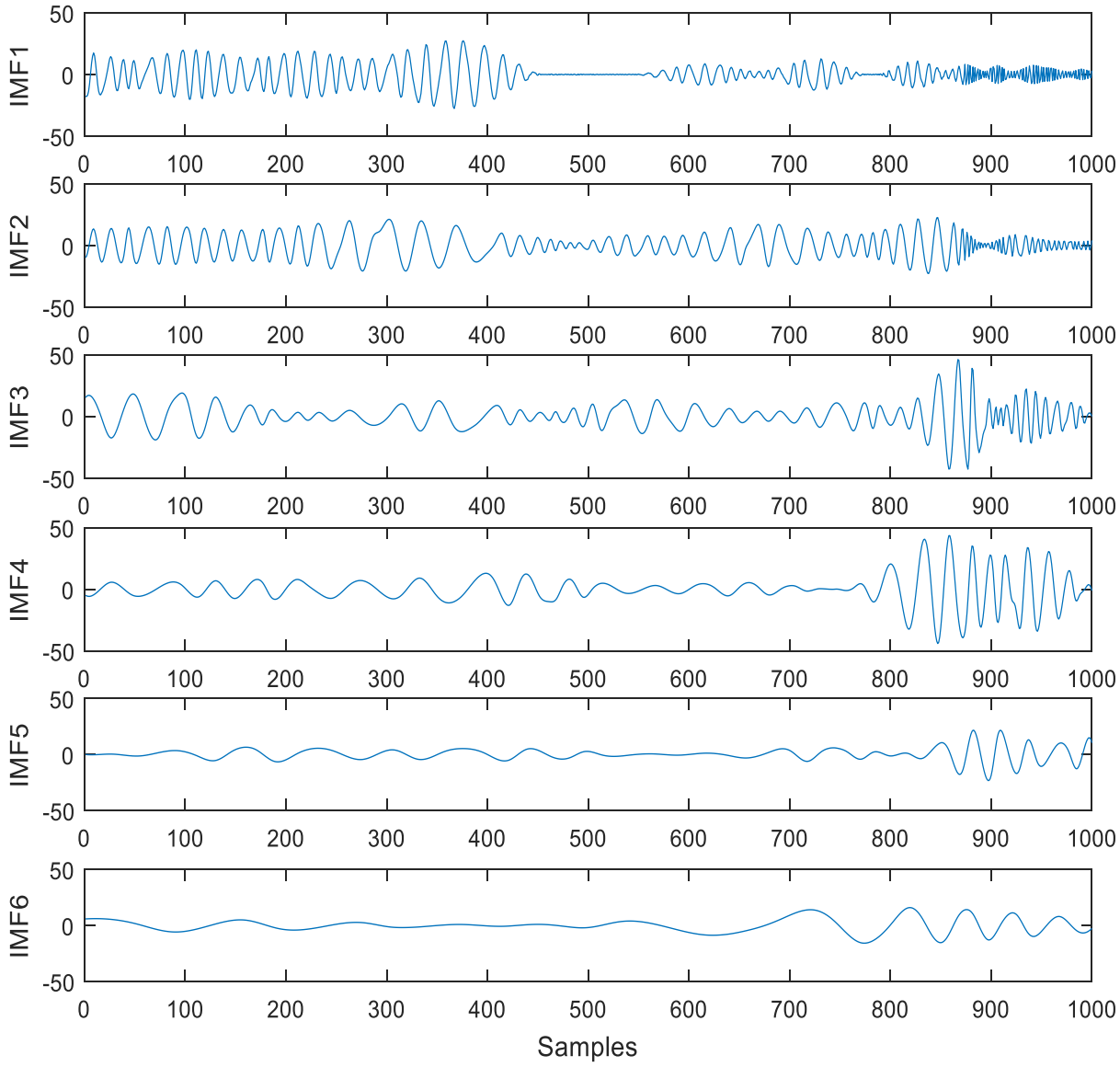

Figure 6-11 Decomposition of experimental gear vibration signal into intrinsic mode functions for baseline condition using steel cover at 550 rpm

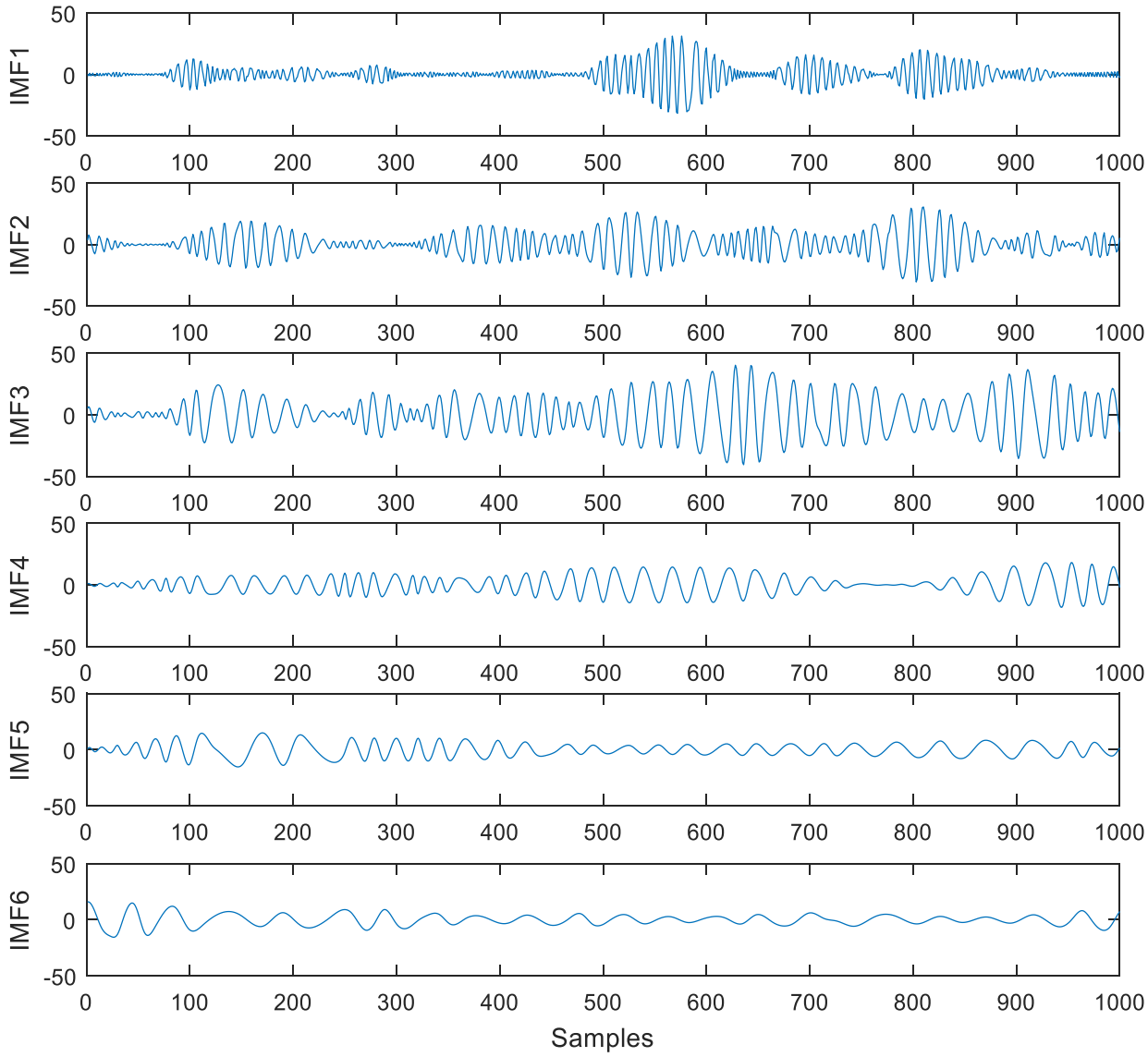

Figure 6-12 Decomposition of experimental gear vibration signal into intrinsic mode functions for baseline condition using steel cover at 850 rpm

The decomposition separates modes according to their frequencies, and it is assumed that the results in the first IMF1 are completely corrupted by noise, whilst low frequency modes IMF2, IMF3 and IMF4 are related to components such as gears, bearings and shafts. However, from Figures (6.9) to (6.12), it was impossible to identify which mode contains the mesh frequency or shaft frequency.

A FFT was applied to each IMF in turn to produce the spectra shown in Figures (6.13) to (6.16). In these figures, the signals show the high and low frequencies produced by the different sources such as gears, shafts, bearings as affected by the housing (resonances).

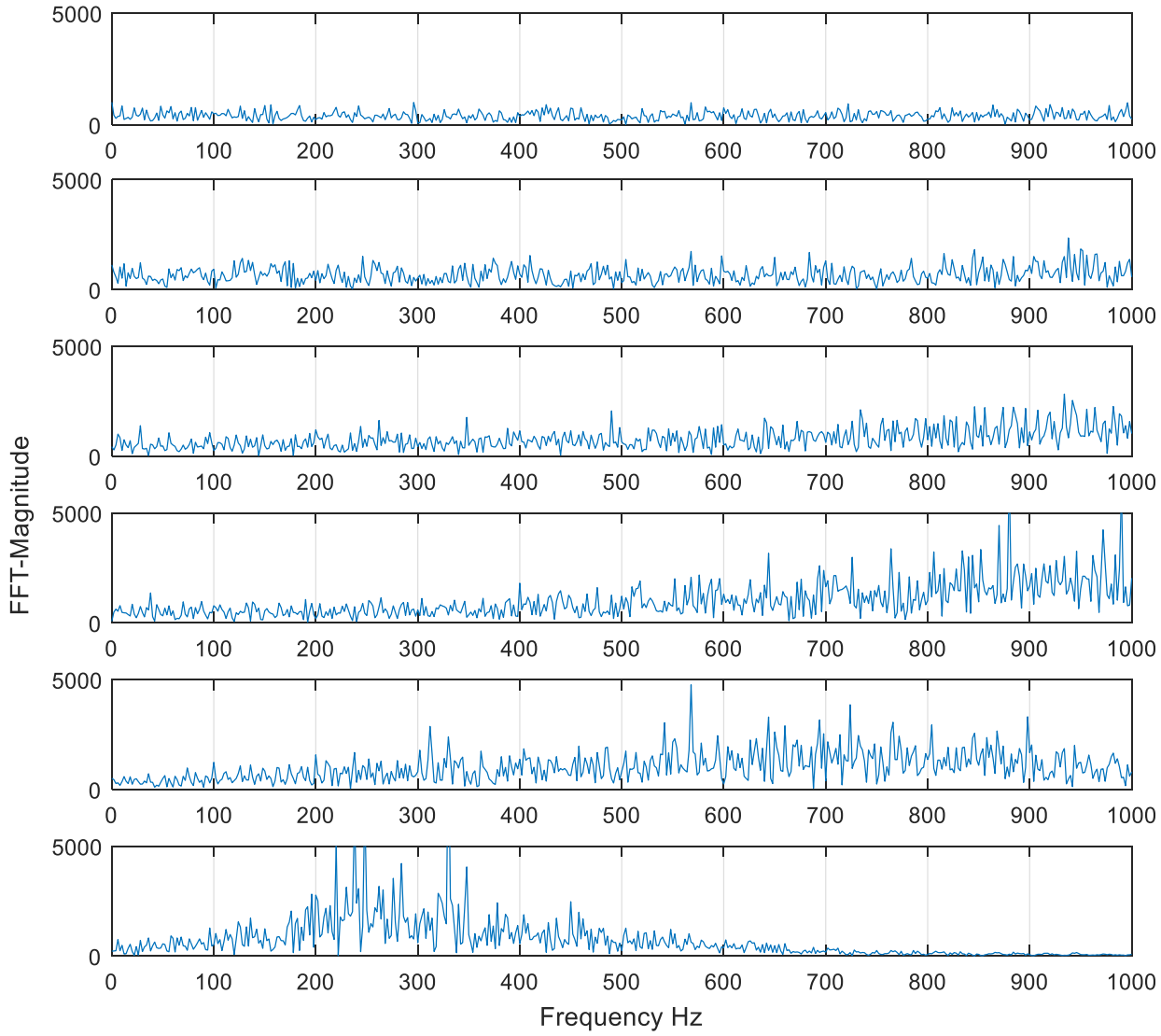

Figure 6-13 Fast Fourier transform applied on each IMF; aluminium cover at 550 rpm

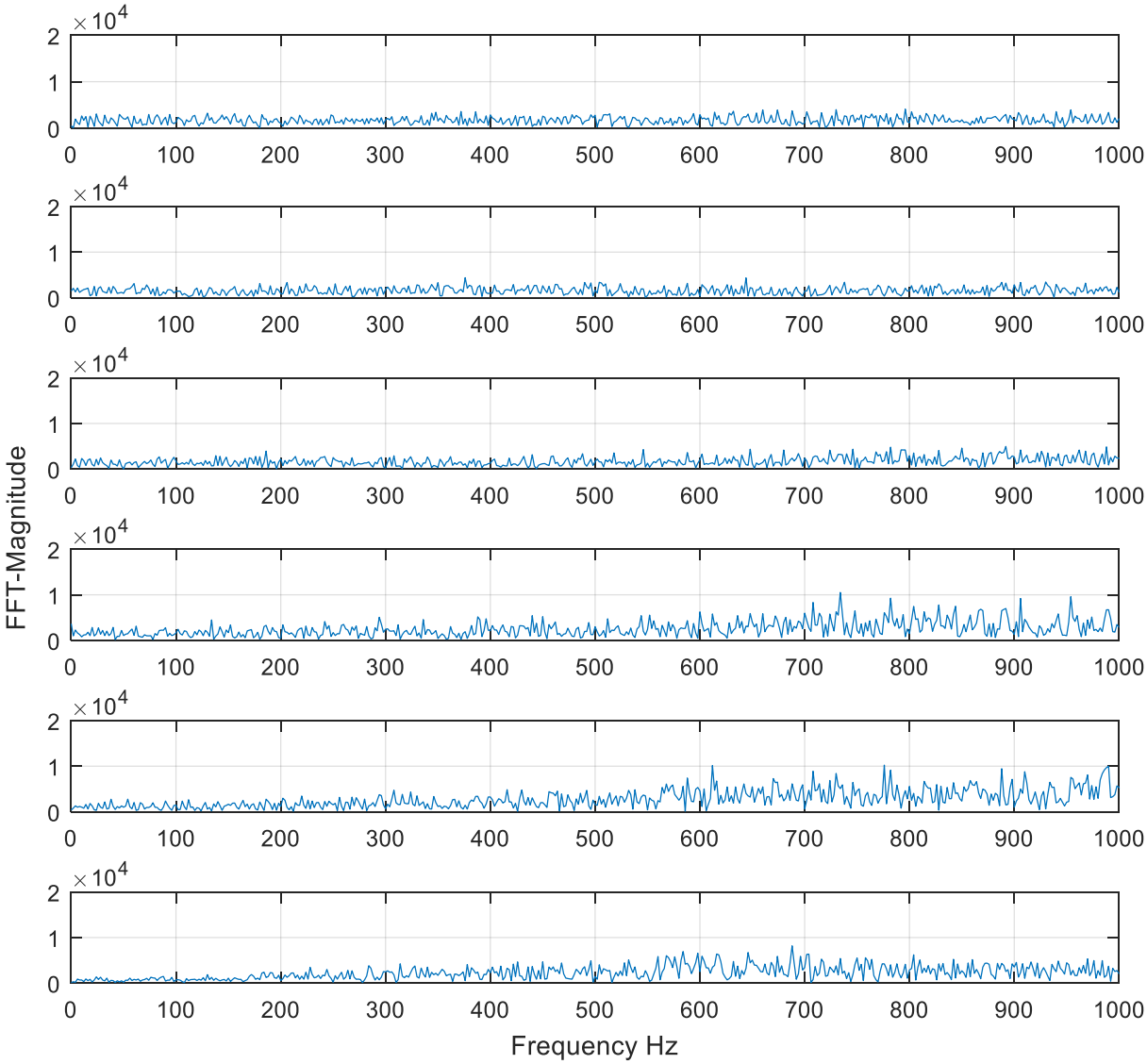

Figure 6-14 Fast Fourier transform applied on each IMF; aluminium cover at 850 rpm

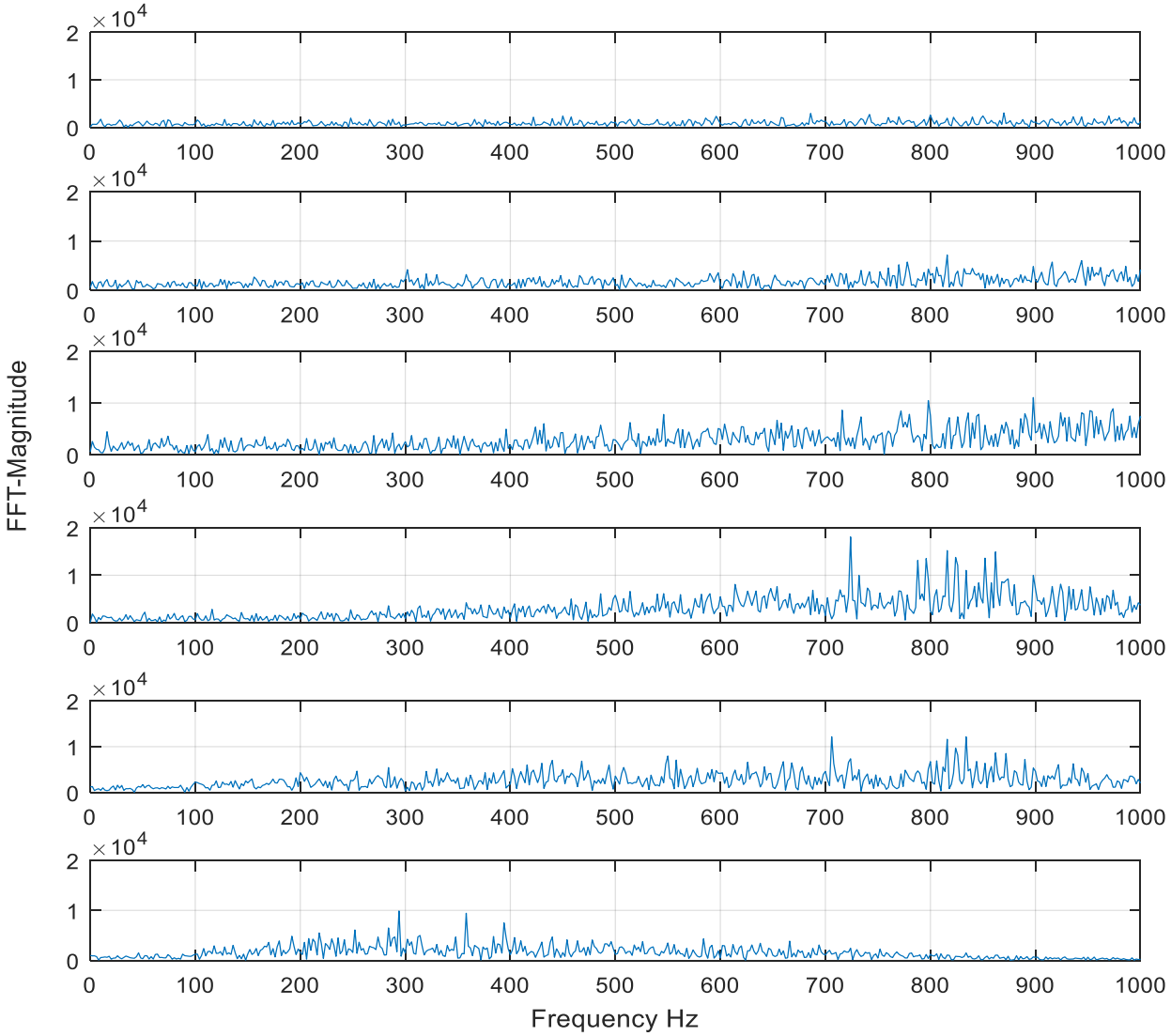

Figure 6-15 Fast Fourier transform applied on each IMF; steel cover at 550 rpm

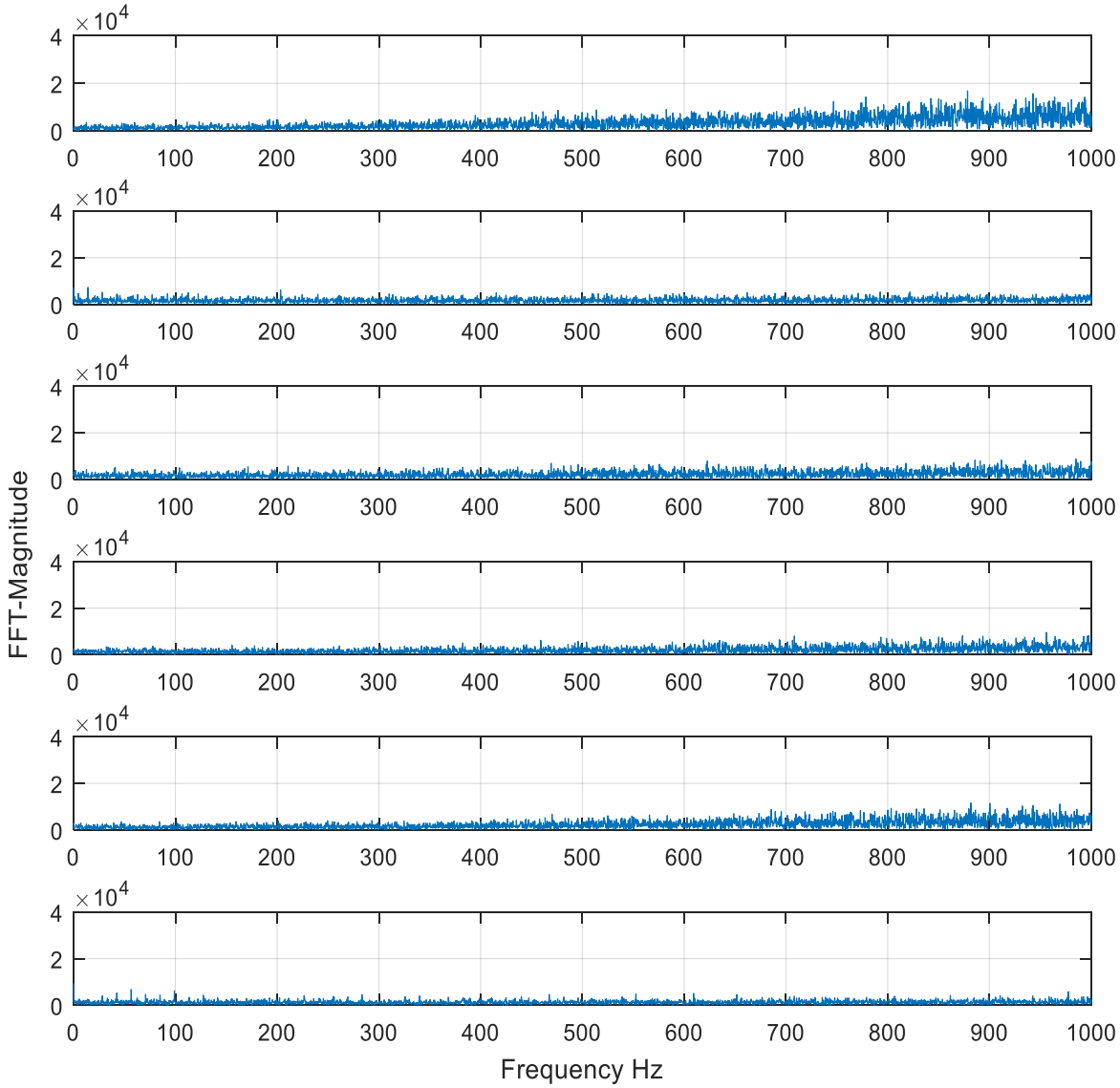

Figure 6-16 Fast Fourier transform applied on each IMF; steel cover at 850 rpm

Referring to Figures (6.13) to (6.16), which were simplified by considering only the baseline case, it was impossible to determine which signal (mode) is consistently related to the gear mesh frequency or shaft frequencies. See Appendix C for FFT for faulty cases.

Figures (6.17) and (6.18) represent the total energy plots obtained using the TE method for baseline gear and gear suffering from tooth breakage of 25 and 85% for the two different housings and rotational speeds 550 and 850 rpm. As can be seen, there is no consistent growth in energy from baseline with fault condition for two covers.

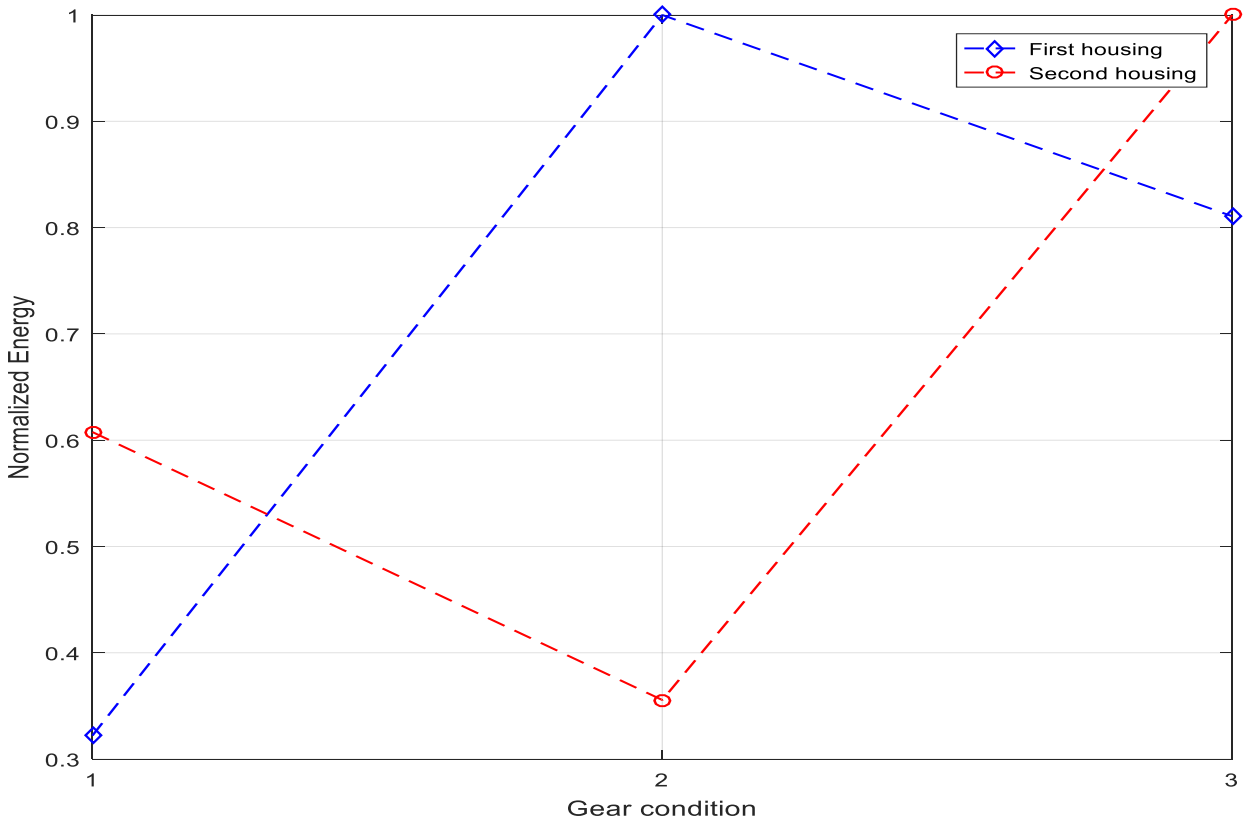

Figure 6-17 Normalized feature intensity level of experimental signals using aluminium cover at 550 rpm; 1,2,3 are indicated the condition of the gear

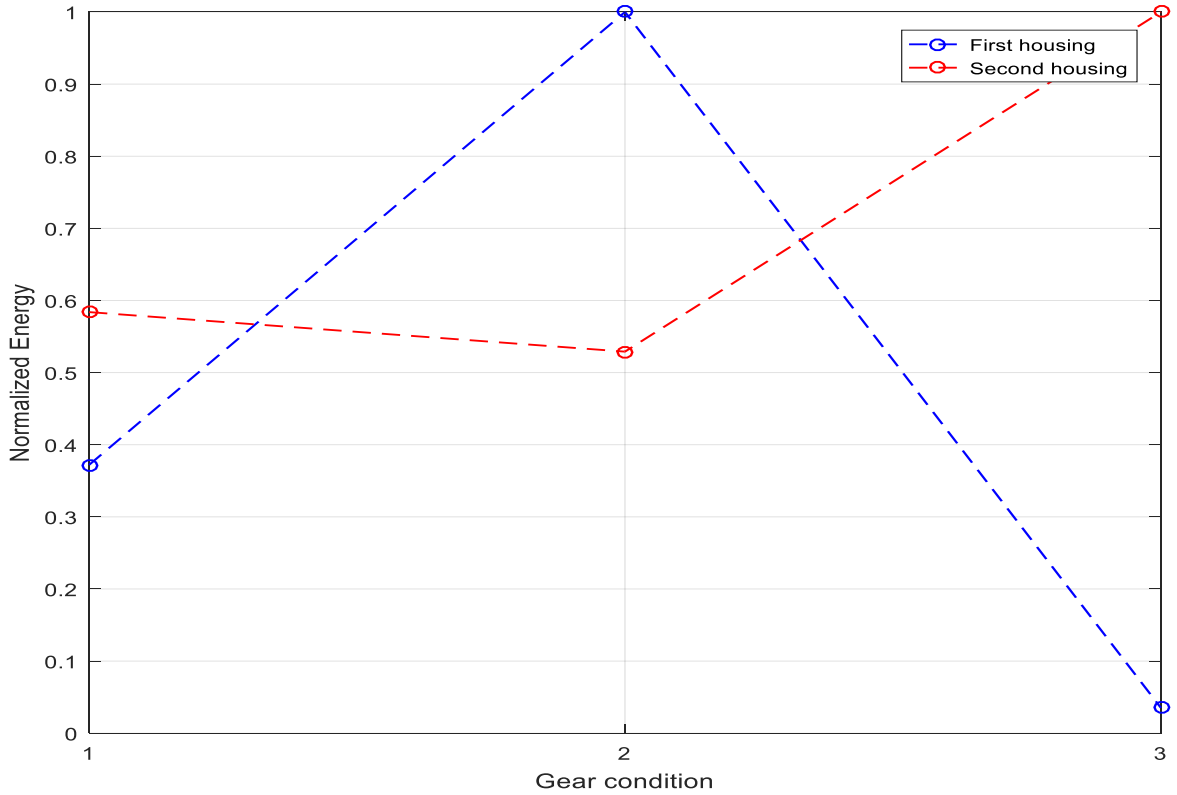

Figure 6-18 Normalized feature intensity level of experimental signals using steel cover at 850 rpm; 1,2,3 are indicated the condition of the gear

The energy levels were calculated for the test rig (machine) at the two drive speeds. There was a decrease in TE with the introduction of the first fault for both covers at 550 and 850 rpm but, as can be seen in the figures, the TE then increase slightly for the second fault. Even though total energy and EMD have provided the possibility of online CM for detecting crack initiation in wind turbine blades [5, 145], no clear relationship is shown between gear fault severity and the energy levels in the vibration signals from the gears in our test rig. This method appears not to provide the possibility of a useful maintenance strategy for detecting defects in a gear based on conventional signal measurement (at least for this case).

6.12 Summary

In general, failure detection using frequency domain analysis can be achieved by monitoring two parameters in the spectrum. The first is variation in the amplitude of a particular frequency

such as the appearance of the characteristic frequencies associated with bearing faults and the second is changes in the structure of sidebands in the spectrum.

FFT has been applied to transform the signal into time domain and to determine the frequency of each component. As can be seen from Figures (6.3) to (6.6), the FFT does not show frequencies related to components such as shaft and gear, and their side bands because these frequencies may be hidden due to noise. The FFT approach does not appear to be able to distinguish the spectral responses between the different signals.

However, low pass filter has been used in frequency domain to filter the signal, after which the signals transformed to time domain and subjected to statistical parameters. The results show that kurtosis could be effective for the one housing and not for another which means that the effect of the housing may have not been removed. Thus, other parameters are not likely to be effective for fault detection.

The statistical analysis of the time-domain signal (after filtered) from baseline and faulty gearboxes shows that for the statistical parameters used, there is limited information that could be extracted about the condition of the spur gear from the vibration signal time domain waveform. More advanced signal processing EMD and TE were also applied to the measured signal to detect the gear defects. However, the result of the combination between EMD and TE methods was shown that they are unlikely to be able to detect and diagnose broken tooth gear faults.

The condition of the spur gear was assessed using various vibration signal analysis techniques including statistical measures and advanced methods. The results, however, show that there is no correlation between the severity of the fault and the parameters for the aluminium and steel housings. This lock of the correlation could be because of the effect of the housing. To overcome this problem, the inverse approach (blocked force) will be introduced and used. The

following chapter will test this approach in order to determine whether it has the potential to be effective for CM purposes.

Chapter 7

Fault identification based on gear mesh blocked forces

In the previous chapter, acceleration signals were used in an attempt to identify the most suitable signal processing method for determining the faults in gears. In this chapter, instead of the direct acceleration signals, indirect signals are used for identifying the presence of a fault. The statistical parameters kurtosis and crest factor as well as the more advanced method (total energy) are applied to these indirect signals. The results are compared to those obtained from the direct acceleration signals in the previous chapter.

7.1 Introduction

The signals normally measured for CM purposes originate from internal forces, such as gear mesh forces, bearing forces etc. which generate the initial disturbance somewhere inside the machine housing. As previously explained these forces cannot, generally, be measured directly which means the measured signals initiated by the internal forces will be modified by the properties of the housing, particularly housing resonances which may be considered to contaminate the signal of interest. For example, consider the same gears installed in two housings of different materials such as aluminium and steel; different vibration signals will be measured from sensors placed on the housings, but the differences are due the housing properties and not the source that generated them. Different monitoring points on the same housing will also yield different signals for the same source. We can argue, therefore, that we would obtain more direct information about the fault if the effect of the housing could be removed. The resulting signal could then be analysed by any convenient signal processing method.

The blocked force represents the force required to constrain a mechanical interface such that its velocity is zero. It was shown by Moorhouse, et al., [105] that blocked force signals may be obtained in-situ through an inverse method, similar to that used in standard inverse force identification [110]. Hence, in this chapter we investigate the potential for using an approach based on blocked force signals rather than acceleration. The approach will be used in conjunction with conventional signal features such as kurtosis and crest factor, in order to help identify faults in the gear.

The aim of this chapter is to employ the same approach for the indirect measurement of blocked forces at the gear mesh point in a gearbox and, to use the acquired blocked force signals in the identification of seeded faults.

The flowchart in Figure (7.1) shows the process of the experimental tests for blocked force measurements for CM. It should be noted that all processing should be done in the frequency domain to calculate the BF signal. Once the obtained blocked force signal has been validated, it is filtered using low pass filter in frequency domain as mentioned in section 4.5. After that, the signal is transformed to the time domain and elementary statistical parameters (kurtosis and crest factor) used to assess the signal. Subsequently a more advanced parameter (total energy) is applied.

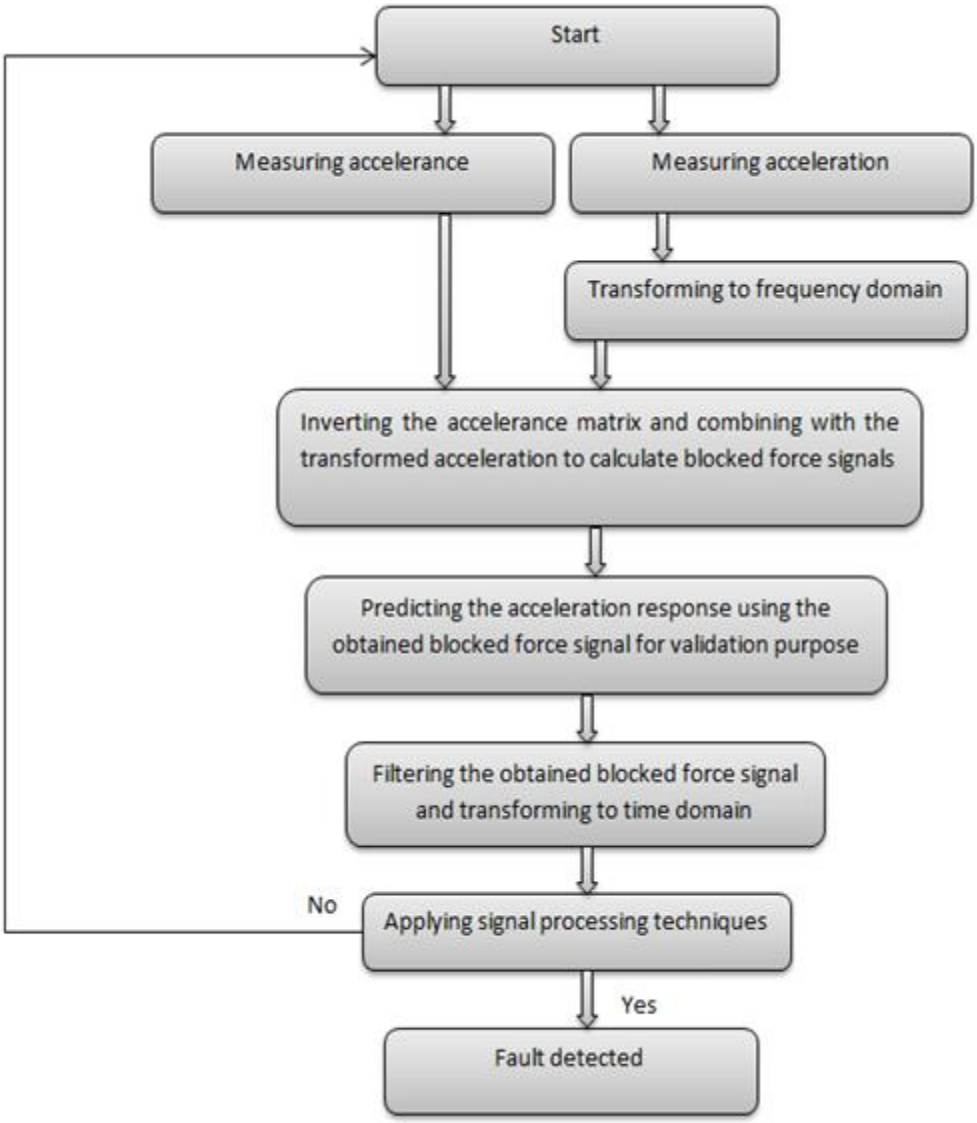

Figure 7-1 Scheme flowchart of the inverse process. Some signal processing techniques are applied to the obtained blocked force signals (Yes indicates that the fault has been detected, No indicates that the fault has not been detected, so, process starts again)

7.2 Case study

The aim of this work is to apply blocked force signals to identify faults in a gear. To do this we will first acquire the blocked forces at the gear mesh using the inverse procedure described in Chapter 4. However, before applying this method as a CM technique, there needs to be an assessment of the quality of the blocked forces to make sure they are suitable. As this was done using the on-board validation procedure described in Chapter 5, more experiments will be conducted using two different housings and same speeds to calculate and validate blocked force for second housing. Following this, the obtained blocked force signals are filtered using the low pass filter and then CM techniques are applied to blocked force signals and comparisons made against conventional methods. The proposed approach will be applied at two rotational speeds (550 rom and 850 rpm) for a baseline assembly, with no seeded gear faults, and assemblies where 25% and 85% of a gear tooth was removed, as in Figure (4.4).

The experimental data was collected using the test rig described in Chapter 4 and two covers were used to provide two housings as in Figure (4.6). In this chapter, the procedure for blocked force measurement is different to the acceleration measurement. As mentioned previously, to obtain the blocked force signal, a two-stage measurement procedure must be conducted.

It was shown in Chapter 5 that the blocked forces of a gearbox test rig (vibration source) could be obtained whilst it is coupled to a receiver with no need to dismantle the source-receiver assembly. This was done by exciting the contact points to gain the accelerance matrix at the mesh points whilst the operational acceleration of the source was measured while the source is still assembled to receiver but the accelerometers mounted on the interface were removed. The idea here is to extend the measurement to calculate and validate the blocked force using different covers (to provide two different housing) and different speeds.

7.3 Blocked force measurement

As mentioned in section (5.6) two-stage measurement procedure has been conducted to obtain the blocked force signal using different assemblies, see figure (5.12). The accelerance and acceleration were measured using the same procedure which done for first assembly.

Again, the measured acceleration signals are transformed into the frequency domain and multiplied by the inverse accelerance matrix to calculate the blocked force, as per Eqs.(3.25). As explained previously it is well known that inverse methods, such as the blocked force characterisation, are notoriously sensitive to the effects of ill conditioning. Having obtained blocked force in frequency domian, low pass filter is applied to filter the signal above 1000 Hz. After filtered the obtained blocked force signal, it is then transformed into time domain and parameters namely, Kurtosis, crest factor and total energy applied.

It is thus important to assess the quality of the acquired blocked forces before applying any CM methods using different housing. This may be done using on-board validation, see Sections 5.3.4, 5.5.3 and 5.6.3.

7.3.1 On-board validation

The on-board validation of blocked force involves predicting a reference operational response (using the acquired blocked force), and comparing it against the directly measured reference response. This comparison, such as presented in Figures (5.14) and (5.15), allows for a visual assessment of the blocked forces predictive capabilities and indicates the quality of the blocked forces themselves.

To further assess the quality of the acquired blocked force, the aluminium housing cover was replaced by the steel cover and the blocked force for the latter was obtained and validated using the same inverse procedure.

Having calculated the blocked force, Eq. (3.26) is used to obtain the predicted acceleration.

For completeness, two sets of blocked forces are used, one from the original test rig, and the other from the test rig modified by using a different top cover on the housing.

Figures (7.2) and (7.3) present the on-board validations for the initial test rig running at 550 and 850 rpm, respectively. As can be seen, there is a good level of agreement across the majority of the frequency range. This suggests that most of the contributing DoF have been accounted for.

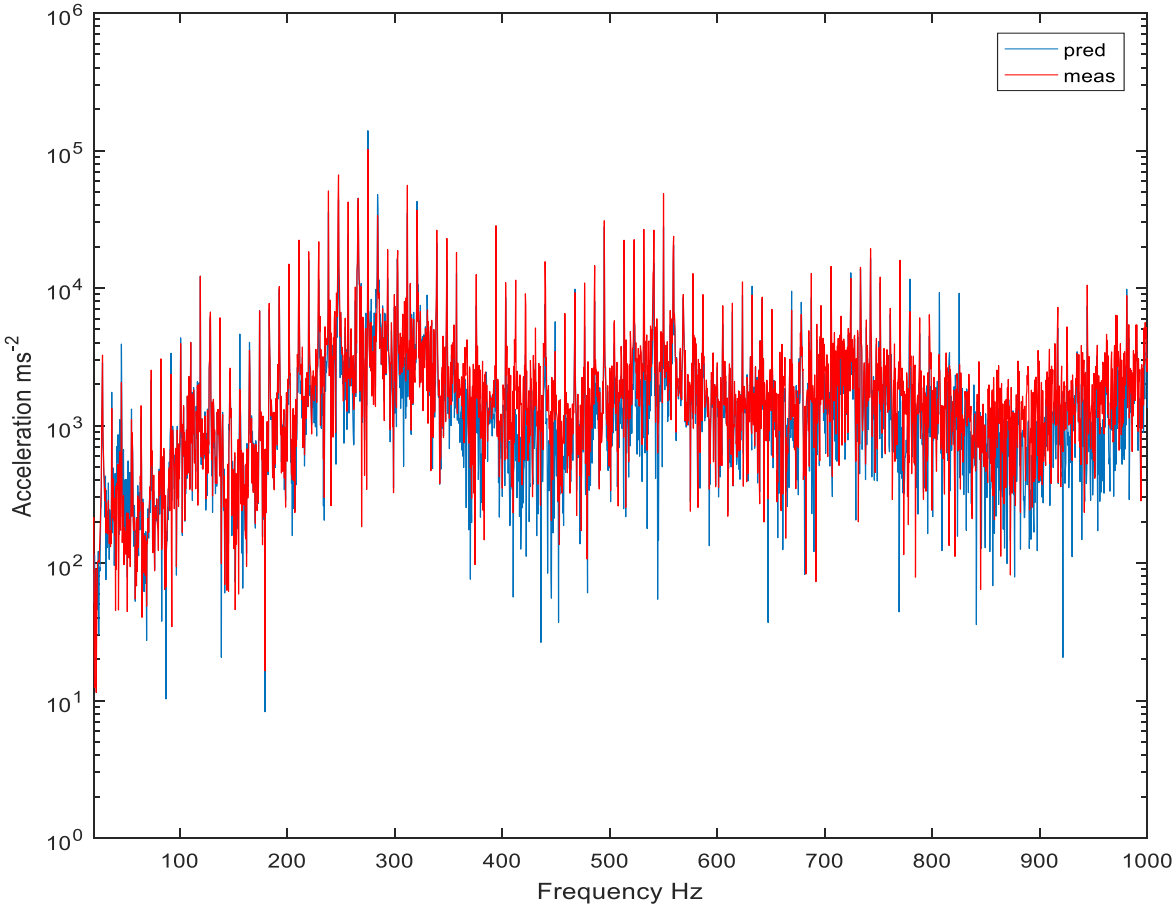

Figure 7-2 On-board validation results of two blocked forces using aluminium cover. The blue line is the predicted acceleration. Red line is the measured acceleration at 550 rpm

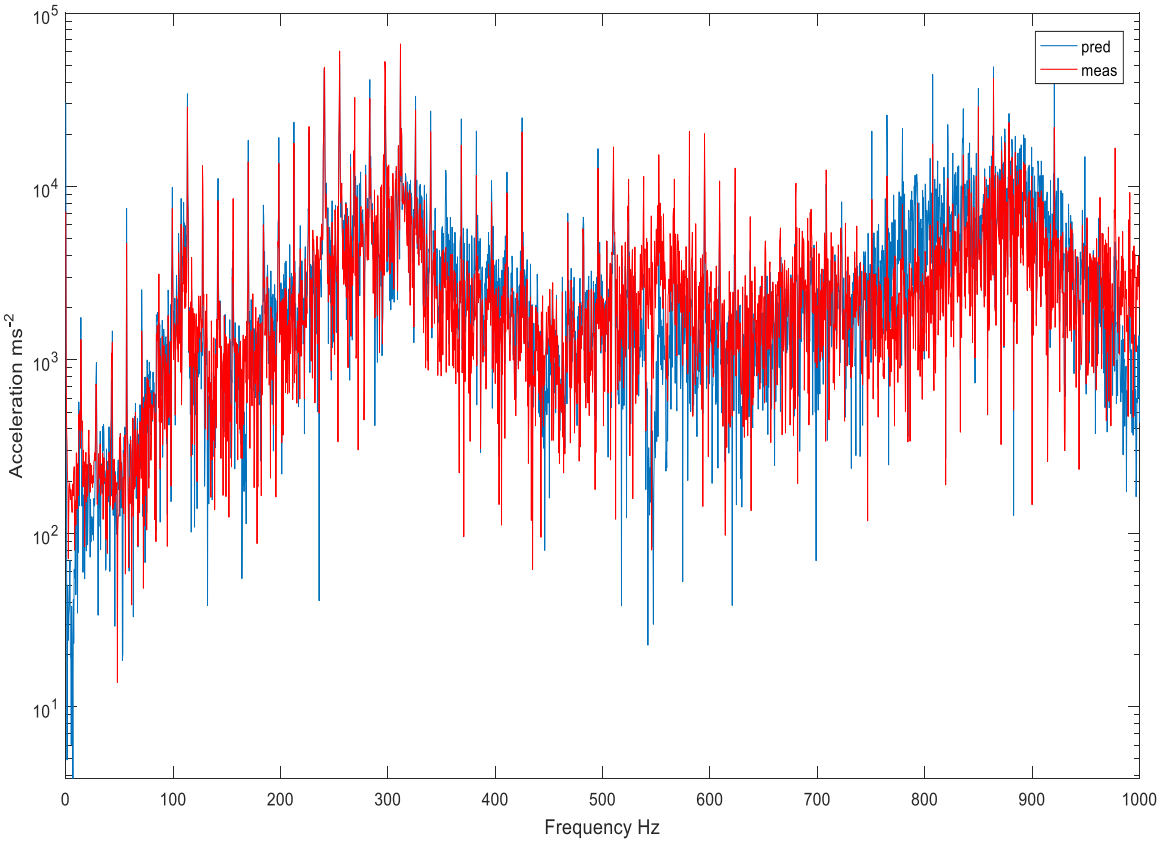

Figure 7-3 On-board validation results of two blocked forces using steel cover. The blue line is the predicted acceleration. Red line is the measured acceleration at 850 rpm

Consider an active component, such as a gear, which develops a fault when installed in a specific housing. The forces generated by the component contain the effects of the fault, which can be picked up in the housing vibration signature. However, even if the fault component signal can be separated from those of other active components, the fault signature is still coloured by the dynamic properties of the housing.

Having obtained the blocked force signal, whether for baseline or faulty conditions, it is then filtered and transformed to the time domain subjected to parameters (Kurtosis, crest factor and total energy) to identify the condition of the machine. In the following sections, statistical parameters and TE are applied to filtered obtained BF signals after transforming them into time domain to detect faults.

7.4 Blocked force time domain signals

For illustrative purposes, the time domain blocked force signals for baseline and faulty conditions at a speed of 550 rpm are shown in Figure (7.4). Such signals are representative of those typically encountered in CM and highlight the need for statistical identification methods.

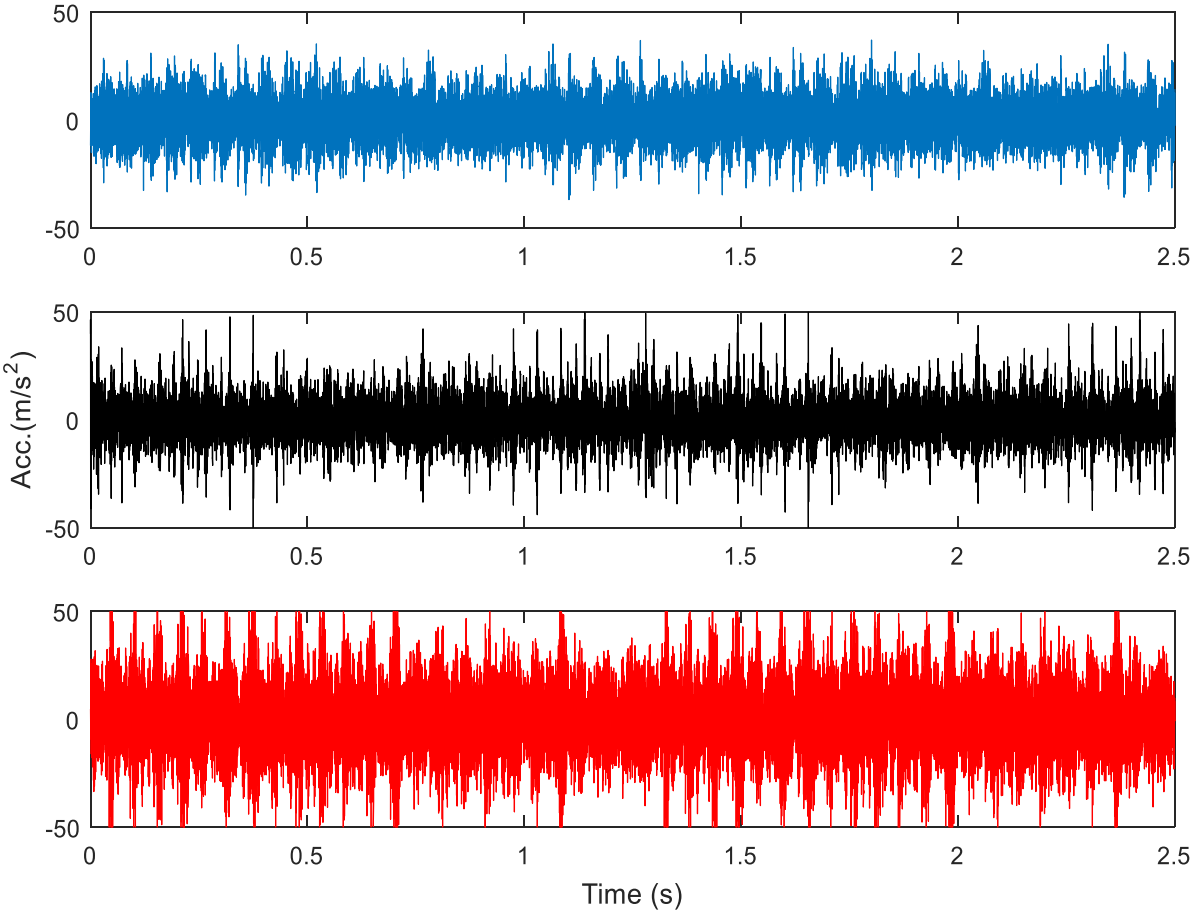

Figure 7-4 Blocked force time-domain signals. Blue is the baseline signal, black is for 25% tooth fault and red is for 85% tooth fault. All at 550 rpm

7.5 Comparison of statistical features

In this section, the kurtosis and crest factor were applied to the obtained blocked force signal at the gear mesh region. The same methods were adopted as when these measures are part of standard CM procedures applied to operational measurements.

7.5.1 Kurtosis and crest factor result based on blocked force signals

Figures (7.5) and (7.6) show the kurtosis values for the time domain blocked force signals for the aluminium ‘‘First housing’’ and steel ‘‘Second housing’’ housings at 550 and 850 rpm. As can be seen, this parameter varies with defect length in a consistent way compared to the results for kurtosis shown in Figures (6.7) and (6.8).

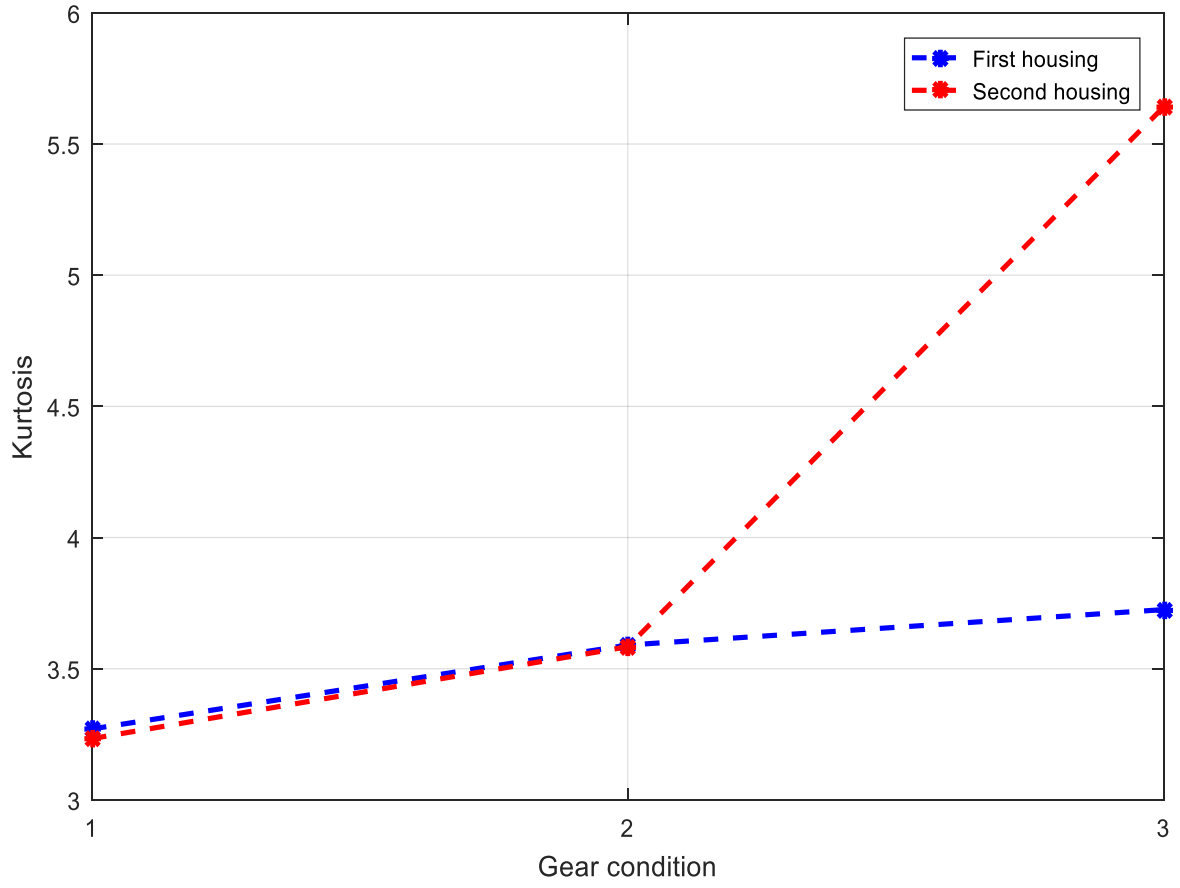

Figure 7-5 Kurtosis for blocked force signals using two aluminium and steel covers. 1, 2 and 3 are referred to baseline, 25% tooth fault and 85% tooth fault respectively. The blue line is for the aluminium cover and the red for the steel cover, at 550 rpm

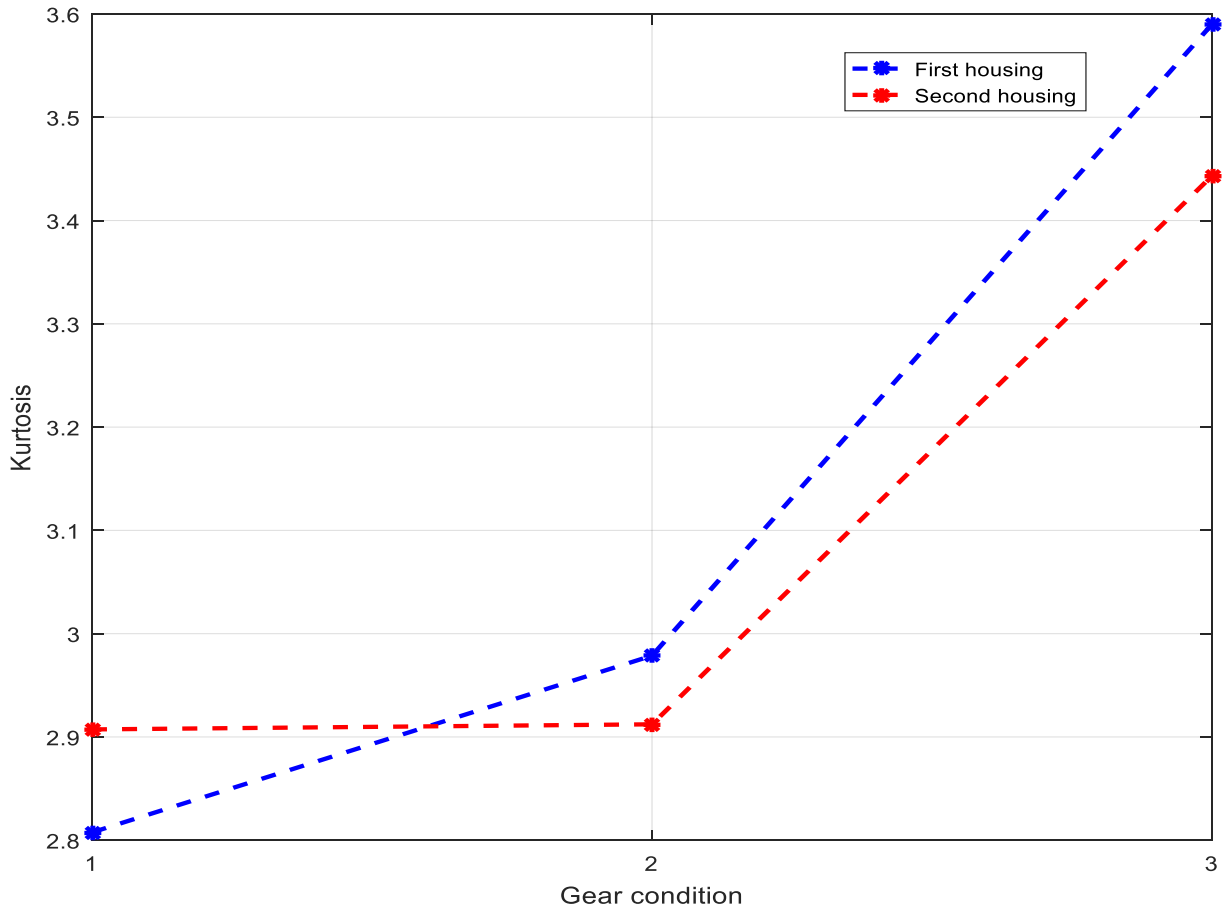

Figure 7-6 Kurtosis for blocked force signals using two aluminium and steel covers. 1, 2 and 3 are referred to baseline, 25% tooth fault and 85% tooth fault respectively. The blue line is for the aluminium cover and the red for the steel cover, at 850 rpm

However, figures (7.5) and (7.6) show that the effect of the housing has been almost removed which means that the blocked force method can be used to remove what the low pass filter could not do.

Figures (7.7) and (7.8) show the values for the crest factor for both housings at speeds 550 and 850 rpm, respectively. Again, a consistent and increasing trend can be observed which suggests that CF is likely to be useful for detecting tooth defects in gears; at least for blocked force signals.

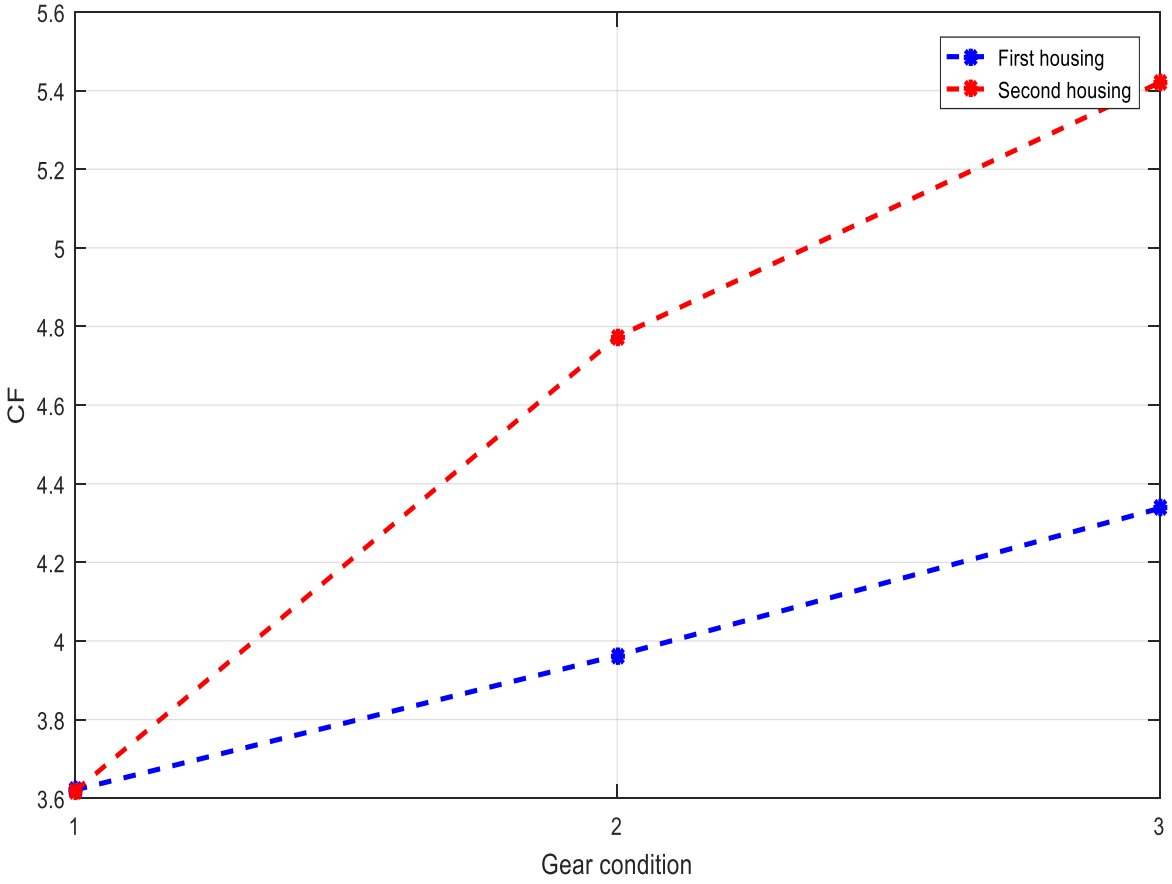

Figure 7-7 CF for blocked force signals using aluminium and steel covers. 1, 2 and 3 are referred to baseline, 25% tooth fault and 85% tooth fault respectively. The blue line is for the aluminium cover and the red for the steel cover, at 550 rpm

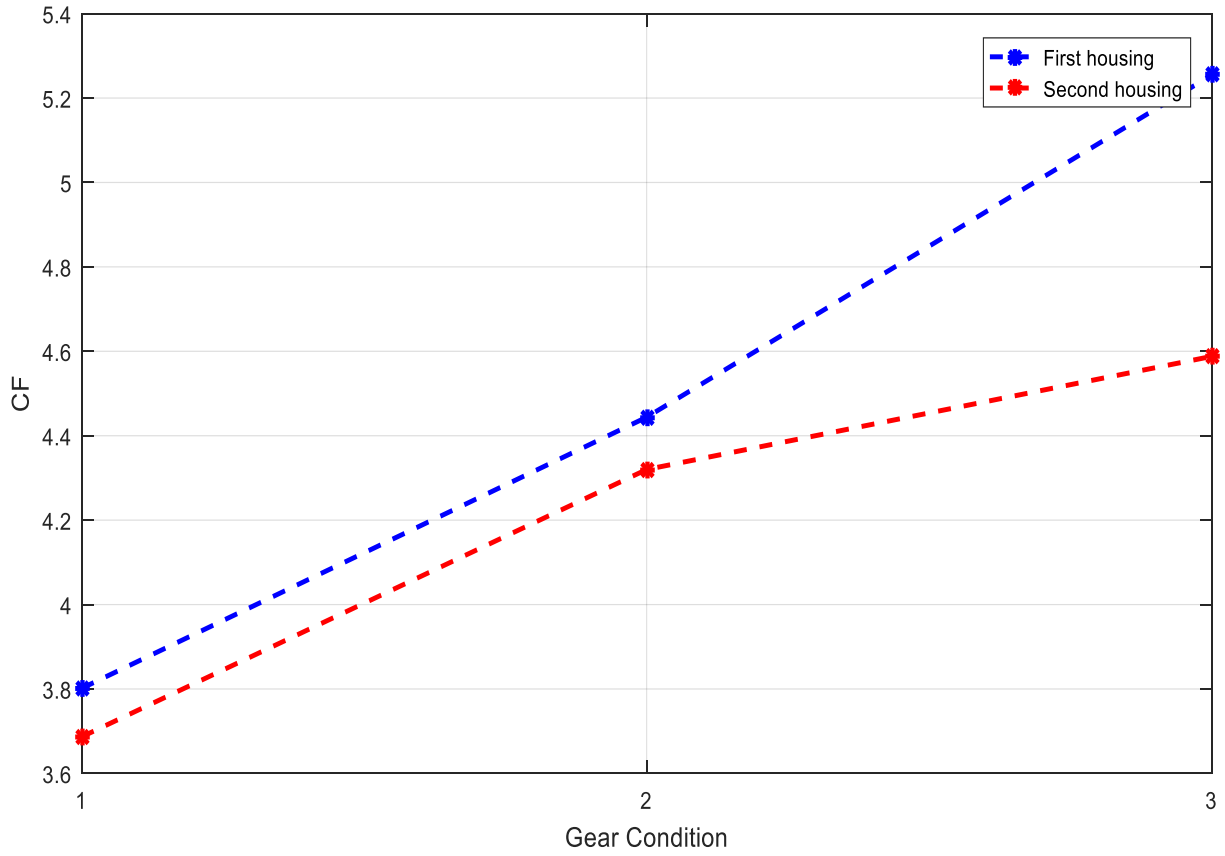

Figure 7-8 CF for blocked force signals using aluminium and steel covers. 1, 2 and 3 are referred to baseline, 25% tooth fault and 85% tooth fault respectively. The blue line is for the aluminium cover and the red for the steel cover, at 850 rpm

The results presented in Figures (7.5) to (7.8) suggest that kurtosis and crest factor are more likely to be effective in diagnosing gear system defects when used with blocked force signals, as opposed to standard acceleration signals. This is thought to be because the effect of the housing is removed, leaving behind a signal which describes more closely the fault. It should be noted that in the comparison between the blocked force kurtosis and crest factor with the kurtosis and crest factor obtained directly from the housing acceleration, the former is more consistent with what we would expect for an increasing magnitude of defect, which suggests that they would be an effective diagnostic. This suggests that the kurtosis and crest factor applied to blocked force are likely to be effective in diagnosing gear system defects, at least for this case. The above results are summarized in Table 7.1 where the kurtosis and crest factor of blocked force and acceleration signals are given for the different levels of fault.

Table 7-1 Comparison between values of statistical parameters for baseline and faulty gears based on acceleration and BF signals.

Parameter	Condition of gear (% tooth removed)	values of statistical parameters form acceleration & Blocked force signals							
		Acceleration		BF		Acceleration		BF	
		Alum	Steel	Alum	Steel	Alum	Steel	Alum	Steel
		550 rpm	550 rpm	550 rpm	550 rpm	850 rpm	850 rpm	850 rpm	850 rpm
	Baseline	5.1	3.9	3.3	3.2	5.1	4	2.8	2.9
	25%	4.5	4.2	3.6	3.5	5.5	3.5	2.9	2.9
	85%	4.6	7.1	3.7	5.6	4.8	5.9	3.6	3.4
	Baseline	7.8	6	3.6	3.6	7.1	5.9	3.8	3.7
	25%	5.6	5.5	3.9	4.7	7.9	4.9	4.4	4.3
	85%	5.4	8.3	4.3	5.4	7	6.8	5.3	4.6

The tables 7.2 and 7.3 show the ratio of kurtosis and crest factor based on acceleration and BF signals using two assemblies.

Table 7-2 Ratio of kurtosis values for baseline and faulty gears based on acceleration and BF signals for two different assemblies (Ka and Ks are kurtosis of the aluminium and the steel housing result).

Kurtosis		**Ratio of Acceleration Ka/Ks**	**Ratio of BF Ka/Ks**
	Baseline	1.3	1
	25%	1.1	1
	85%	0.65	0.7
Average		1	1
	Baseline	1.3	0.9
	25%	1.5	1
	85%	0.81	1
Average		1.2	1

Table 7-3 Ratio of crest factor values for baseline and faulty gears based on acceleration and BF signals for two different assemblies (CFa and CFs are crest factor of the aluminium and the steel housing result).

CF		Ratio of Acceleration CFa/CFs	Ratio of BF CFa/CFs
	Baseline	1.3	1
	25%	1	0.8
	85%	0.65	0.8
Average		0.9	0.9
	Baseline	1.2	1
	25%	1.6	1
	85%	1	1.2
Average		1.3	1

In theory, the fault is a property of the gear not the assembly. Thus, the BF should be the same from the different assemblies. Considering the assumption applied and experimental uncertainties, we would not expect it to be prefect straight line, but the fact that it is more linear than acceleration signals suggests that the fault has been independently characterised. It shows the independent property of assemblies and identifying the fault without the effect of the housing. Furthermore, the variation in the BF kurtosis and crest factor, between different assemblies, is less than in the acceleration signals.

To confirm the advantages of using the in-situ blocked force for CM, especially for detection of tooth faults, more advanced parameter (total energy) was used.

7.6 Total energy result based on blocked force signals

In this section, more advanced method has been applied to further investigate the result obtained above using kurtosis and crest factor. Figures (7.9) and (7.10) represent total energy for baseline gear and gear suffering tooth breakage of 25% and 85% for rotational speeds 550 and 850 rpm, based on blocked force signals.

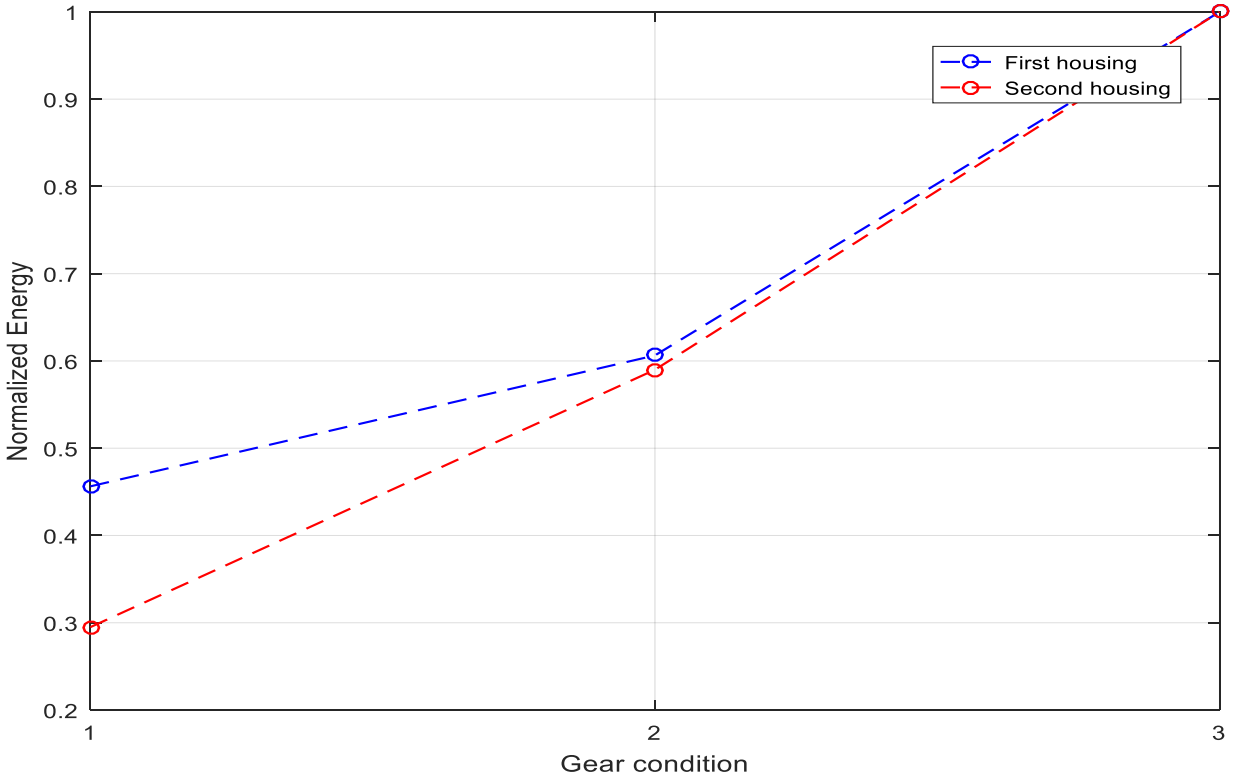

Figure 7-9 Total energy method for blocked force signals using aluminium and steel covers at speed 550

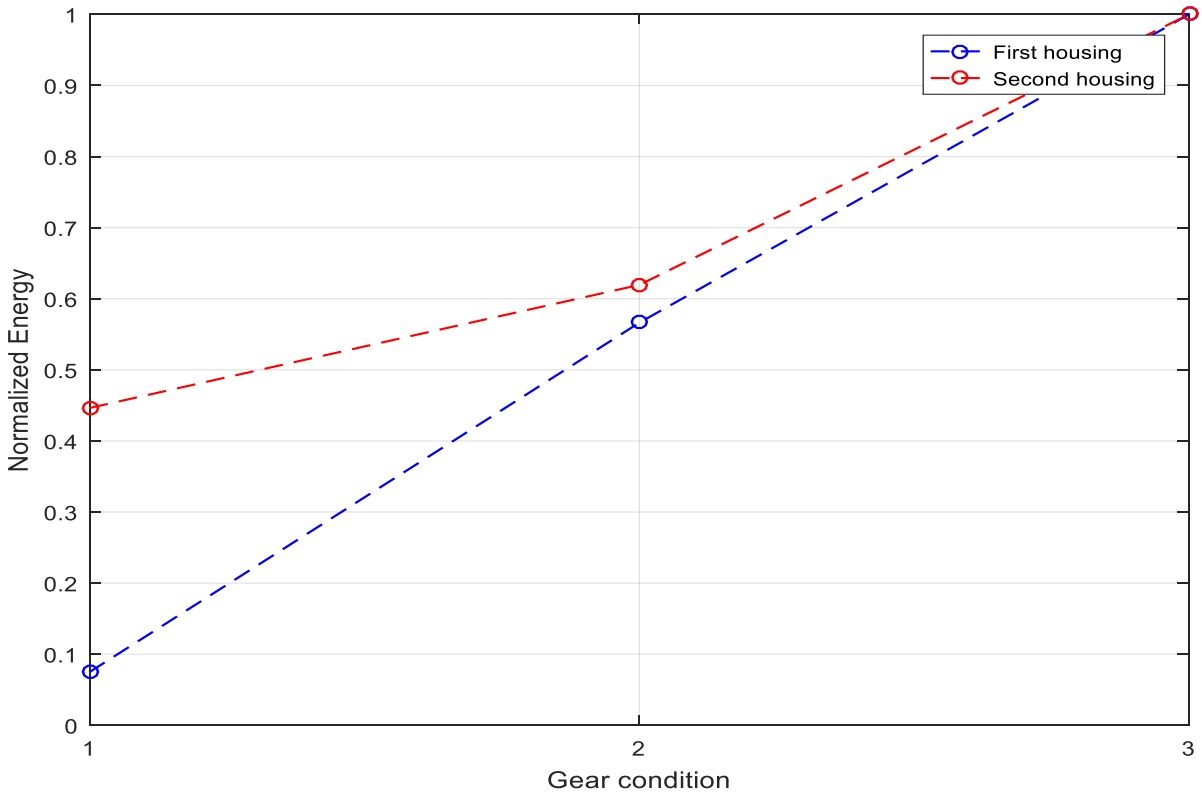

Figure 7-10 Total energy method for blocked force signals using aluminium and steel covers at speed 850 rpm

As can be seen, there is a clear trend in the relationship between the fault severity and the energy levels for both housings at 550 and 850 rpm. The curve gradually rises as more of the tooth is removed. This method appears to provide a possibly of detecting defects in a gear, based on the inverse signal (blocked force signal). The results show that total energy applied to BF signals is suitable for diagnosing faults in gears, at least for this case study.

7.7 Summary

This chapter has investigated the potential of use of inversely determined blocked force in condition monitoring of gears for the detection of broken tooth faults. Experimental work was carried out using a baseline spur gear and one suffering from 25% and 85% tooth removal for a single tooth.

This study has produced a promising approach that could be used to help with detecting and, possibly, diagnosing tooth breakage in a spur gear. The approach is to use the inversely

acquired in-situ blocked force which requires a two-stage measurement procedure to obtain the blocked force signal.

The acquired blocked forces were assessed through an on-board validation procedure for the second assembly, the results of which suggested that they were sufficiently precise. Obtained blocked force signals were filtered (using low pass filter as described in section 4.5) and then transformed into the time domain and subjected to the parameters kurtosis, crest factor and total energy.

The agreement in the blocked forces obtained with both aluminium and steel housings (which theoretically should be the same) was good and much more similar than the directly measured accelerations. Blocked force values were also more consistent and in agreement with what would be expected from increased tooth damage. The results show that the kurtosis, crest factor and total energy applied to blocked force signals are more likely to be sensitive and effective in diagnosing a faulty gear compared to result obtained for same parameters applied directly to the measured acceleration after using the filter.

Chapter 8

Contribution to knowledge, Achievements, Conclusions and Recommendations

This chapter presents the contributions to knowledge made by this thesis. It summarises the achievements of the research project and explains how the objectives stated in Section 1.8 were attained. The chapter concludes the study with recommendations for further work.

8.1 Introduction

Here, before concluding, we refer back to the aim of this work, which is testing the use of the blocked force method to determine if it has a significant advantage over acceleration measured directly on machine housing for CM purposes, specifically the detection of fault signals from a gearbox.

Seeded faults in a gear generated vibration; the vibration signature carried useful information about the health of the gearbox and was used in this project to identify the presence of a defect in the test rig spur gear. However, the vibration signal will also contain information concerning structural (housing) resonances, bearings and gear meshing frequencies as well as random noise. Different techniques were used to detect the presence of the seeded gear faults in these distorted and noisy signals;

- Time domain methods including statistical analysis of the signal,
- Frequency domain techniques including FFT, and
- Empirical mode decomposition and total energy.

This project included the design and construction of a test rig that allowed the simulation of different severities of a given defect in a spur gear. Signals from this test rig were analysed using time and frequency domain tools. A new approach, the so-called in-situ blocked force is presented. The obtained blocked force signals for baseline and faulty conditions were validated and the same analytical techniques were applied as to the time domain signals. The different sets of results have been compared to ones obtained from the direct signals.

8.2 Contribution to knowledge

The contributions to knowledge made by this research project are:

The first contribution is the demonstration of the use of in-situ blocked force to characterize gear mesh interactions. A measured characteristic of the source independent of its surroundings can be acquired using this blocked force approach.

The second contribution is to have successfully used this blocked force to provide a (blocked force) signal for the effective detection of broken gear tooth faults. This method has the great advantage that it removes the effect of the housing and transmission paths on the signal, and provides a more reliable signal for condition monitoring.

8.3 Conventional measurement

This study presents vibration-based fault detection for a spur gear using simple statistical parameters. Advanced signal processing methods (a combination of EMD-Total energy of the meshing frequency band) were also used to extract features from the experimental data collected. A practical vibration measurement system consisting of accelerometers and data recorders was employed.

FFT was applied to transform the time signal into frequency domain. After that, the low pass filter has been applied to filtered signal (see section 4.5). The filter has been used in frequency domain and then the filtered signal was transformed to time domain. The statistical parameters kurtosis, crest factor, RMS and skewness were then applied to filtered time domain signal to detect varying degrees of tooth breakage. These parameters may be used on their own for fault detection; however, their sensitivity has been shown to be poor for the given fault conditions. Even though the kurtosis shown good trends for the one assembly and one speed, they did not change or create a trend that would indicate failure in the stages of faults and were unable to provide any reliable diagnostic information. Moreover, the noise might be removed or reduced but the effect of the housing seems to be remains. Thus, the more advanced methods were applied.

EMD was used to decompose the signal into IMFs, and the FFT was applied to produce the spectra of each IMF, and total energy was calculated for the meshing frequency and its sidebands. The results show, at least for this case study, these methods were not effective in detecting defects in the gear, neither at a stage (25% removed) nor when fully developed (85%) when using the directly measured acceleration.

8.4 Inverse measurement

In order to achieve the aim of the thesis, inverse measurements were necessary. To begin with, accelerance was measured and verified for each measurement as described in Chapter 5. After that, the acceleration was measured in frequency domain using the hammer as in section (5.5), after which the measured 'acceleration' was combined with accelernace to calculate blocked force signal. For second step, the acceleration was measured by operating the moor as in section (5.6) and in this case, the acceleration was transformed into the frequency domain and combined with the inverse accelerance matrix to calculate the blocked force signal. Once obtained the blocked force signal for first case, it is then used to predict acceleration for validation purposes. For section case, the obtained blocked force signal is filtered and then transformed into the time domain. The simple and advanced parameters were then applied to investigate the use of the inverse measurement for CM purposes.

Kurtosis, crest factor and total energy were applied to the filtered blocked force time domain signals and compared to the results obtained based on acceleration signals. It was shown that parameters applied to the BF signals are more effective in showing clear trends of detecting the faults in gear than applied to the acceleration signal.

8.5 Summary

It should be noted that this study has demonstrated that an inverse method, combined with conventional use of statistical features of the signal, provided clearer trends than the same parameters based on acceleration signals (filtered signals).

A method is proposed that can substantially reduce, or even remove the effect of the housing along the transmission path and which contaminates the source signal. The vibration that is measured on the machine housing will be a combination of the characteristics of the source signal (which contains the fault information) and the characteristics of the elements forming the transmission path and, of course, the housing on which the sensors were placed.

If these unwanted effects are removed from the accelerometer signal, such that the blocked force is specific to a source, then the signal processing techniques might more reliably detect and even diagnose the faults for specific component.

This research has demonstrated that vibration parameters such as TE, kurtosis or crest factor based on the filtered blocked force signals are more reliable and robust for the detection of developing tooth breakage. These results have shown the possibility of using an inverse method for rotating machinery condition monitoring.

8.6 Conclusions

This research has described the application of blocked force signals to the condition monitoring of gears for the detection of faults.

For the noise contaminated vibration signals collected from the test rig, simple statistical parameters (kurtosis and crest factor) were insufficient for fault detection. This study has introduced a promising new approach to detect tooth breakage in a spur gear. The proposed approach makes use of the blocked force to remove the effect of housing resonances.

A two-stage measurement was used to obtain the blocked force signals. The blocked force signals were filtered and transformed into the time domain and subject to the parameters (kurtosis, crest factor and total energy). One of the main aims achieved is that a way of obtaining the blocked forces for a gear mesh has been developed and implemented.

Blocked force CM gave kurtosis, crest factor and TE values that were more consistent and in agreement with what would be expected from increased tooth damage. The results of these parameters based on the blocked force show promise for use in the field of CM for fault detection.

8.7 Recommendations (Future Work)

The result presented in this thesis show that kurtosis, crest factor and total energy applied to the blocked force signals are promising tools for fault detection, at least for gearboxes. However, there is a need to determine whether the inverse method is suitable for detecting faults in other items of interest such as motor, bearings, etc.

It is worth to mention here that the method has been tried out in small gearbox in the lab while in theory same measurement can be applied in the field in large structures. Other need practical difficulties which may expect you will need to open the machine and put the accelerometers inside to measure FRF while it is shut down which means that everything should be quiet to perform this work.

Moreover, there are some difficulties which should be considered: the measurements process is longer and the amount of the required equipment for performing the measurements such as the number of the accelerometers, the NetdB software, the type of hammer and others. However, before applying this method in large structures (machines), it is necessary to apply it with consideration on the following suggestions.

Possible future work that could improve condition monitoring and fault detection in rotating machine systems based on inverse measurement.

The suggestions are:

- Having tested the method in the laboratory on small gearbox, would be to apply it to a real machine.

- Additional and different faults should be introduced into the gear and other components.
- The focus of the research could be extended to include all rotating machine parts.
- Vary the load on the gearbox.
- Use high speed gearboxes.
- Use combinations of faults.

References

1. Thompson, S. (2000). Tribology Solutions: Section 1.
2. Scheffer, C., & Girdhar, P. (2004). Practical machinery vibration analysis and predictive maintenance. Elsevier.
3. Davies, A. (Ed.). (2012). Handbook of condition monitoring: techniques and methodology. Springer Science & Business Media.
4. Al-Arbi, S. (2012). Condition monitoring of gear systems using vibration analysis (Doctoral dissertation, University of Huddersfield).
5. Ibrahim, G. R. (2011). Design and implementation of gearboxes vibration based condition monitoring system (Doctoral dissertation, The Manchester Metropolitan University).
6. Wang, L., & Gao, R. X. (Eds.). (2006). Condition monitoring and control for intelligent manufacturing. Springer Science & Business Media.
7. Albarbar, A., Pietruszkiewicz, R., & Starr, A. (2007). Towards the implementation of integrated multimeasurand wireless monitoring system. In Proceedings 2nd World Congress on Engineering Asset Management (WCEAM) June.
8. Baydar, N. (2000). The Vibro-acoustic Monitoring of Gearboxes. University of Manchester.
9. Harris, C. M., & Piersol, A. G. Harris shock and vibration handbook, 2002. Norwich, NY: Knovel.
10. Barron, D. R. (Ed.). (1996) Engineering condition monitoring: practice, methods and applications. Longman.
11. Marwala, T. (2012). Condition monitoring using computational intelligence methods: applications in mechanical and electrical systems. Springer Science & Business Media.
12. Saeed, A. (2008). on line condition monitoring system for wind turbine.
13. Cheng, H. (2007). Implementation strategies and tools for condition based maintenance at nuclear power plants. International Atomic Energy Agency, Vienna.
14. Alhouli, Y., Alkhaledi, A., Alzayedi, A., Alardhi, M., & Abed, A. I. (2016). Study of Diesel Engine Vibration Condition Monitoring. Global Journal of Research In Engineering.
15. Welbourn, D. B. (1979). Fundamental knowledge of gear noise: a survey (No. IMechE-C117/79).
16. Randall, R.B., 1982. A new method of modeling gear faults. Journal of Mechanical Design, 104(2), pp.259-267.
17. Fair, C. (1998). Synchronous sampling sideband orders from helical planetary gear sets (Doctoral dissertation, Virginia Tech).
18. Tom, K. F. (2010). Survey of Diagnostic Techniques for Dynamic Components (No. ARL-TR-5082). Army research lab Adelphi MD sensors and electron devices directorate.
19. Moorhouse, A. (2012). Vibro-acoustic measurement methods in condition monitoring, in CM / MFPT. London.
20. Morris, R.a.P., F., 1994. The Reliability Based Maintenance Strategy: A Vision for Improving Industrial Productivity. Computational Systems Incorporated (CSI).
21. Elliott, A., Moorhouse, A., & Pavic, G. (2007, September). Characterisation of a structure-borne sound source using independent and in-situ measurement. In ICA 19.
22. Elliott, A. S. (2009). Characterisation of structure borne sound sources in-situ (Doctoral dissertation, University of Salford).
23. Höller, C. (2013). Indirect methods of obtaining activity and mobility of structure-borne sound sources (Doctoral dissertation, University of Liverpool).
24. Ghodake, M. S. B., Mishra, A. K., & Deokar, A. V. A Review on Fault Diagnosis of Gear-Box by Using Vibration Analysis Method.

25. Cuc, A. I. (2002). Vibration-based techniques for damage detection and health monitoring of mechanical systems (Doctoral dissertation, University of South Carolina).
26. Dhamande, L. S., & Chaudhari, M. B. An Overview of Fault Detection Methods for Transmission System Components using Vibration Analysis.
27. Hoshi, T. (2006). Damage monitoring of ball bearing. CIRP Annals-Manufacturing Technology, 55(1), 427-430.
28. Fahrenberg, J. BIBLIOGRAPHY Ambulatory Assessment. Ethology, Ecology & Evolution, 4, 401-416.
29. Kotta, A. (2015). Condition Monitoring: Using Computational intelligence methods.
30. Shin, J. H., & Jun, H. B. (2015). On condition based maintenance policy. Journal of Computational Design and Engineering, 2(2), 119-127.
31. Kim, H. E. (2010). Machine prognostics based on health state probability estimation (Doctoral dissertation, Queensland University of Technology).
32. Peng, Y., Dong, M., & Zuo, M. J. (2010). Current status of machine prognostics in condition-based maintenance: a review. The International Journal of Advanced Manufacturing Technology, 50(1-4), 297-313.
33. Sikorska, J. Z., Hodkiewicz, M., & Ma, L. (2011). Prognostic modelling options for remaining useful life estimation by industry. Mechanical Systems and Signal Processing, 25(5), 1803-1836.
34. Yu, J. (2011). A hybrid feature selection scheme and self-organizing map model for machine health assessment. Applied Soft Computing, 11(5), 4041-4054.
35. Kan, M. S., Tan, A. C., & Mathew, J. (2015). A review on prognostic techniques for non-stationary and non-linear rotating systems. Mechanical Systems and Signal Processing, 62, 1-20.
36. Wang, W. J., & McFadden, P. D. (1995). Application of orthogonal wavelets to early gear damage detection. Mechanical Systems and Signal Processing, 9(5), 497-507.
37. Stander, C. J., Heyns, P. S., & Schoombie, W. (2002). Using vibration monitoring for local fault detection on gears operating under fluctuating load conditions. Mechanical Systems and Signal Processing, 16(6), 1005-1024.
38. Martin, H. R., & Ismail, F. (1989). Review of gear damage monitoring techniques. In International Machinery Monitoring and Diagnostic Conference, 1stUnion College; Electric Power Research Institute; Machinery Failure Prevention Group; and others.
39. Liu, X., Ma, L., & Mathew, J. (2009). Machinery fault diagnosis based on fuzzy measure and fuzzy integral data fusion techniques. Mechanical Systems and Signal Processing, 23(3), 690-700.
40. Lebold, M. (2004). Development of distributed wireless smart sensors for gearbox prognostic application. In Proceedings of the 58th Meeting of the Society for Machinery Failure Prevention Technology.
41. Stevens, P. W., Hall, D., & Smith, E. (1996, June). A multidisciplinary research approach to rotorcraft health and usage monitoring. In Proc. Annual Forum, American Helicopter Society (Vol. 2, pp. 1732-1751).
42. Norton, M. P., & Karczub, D. G. (2003). Fundamentals of noise and vibration analysis for engineers. Cambridge university press.
43. Stewart, R. M. (1977). Some useful data analysis techniques for gearbox diagnostics. University of Southampton.
44. McFadden, P. D. (1987). Examination of a technique for the early detection of failure in gears by signal processing of the time domain average of the meshing vibration. Mechanical systems and signal processing, 1(2), 173-183.
45. Sohn, H., & Farrar, C. R. (2001). Damage diagnosis using time series analysis of vibration signals. Smart materials and structures, 10(3), 446.

46. Inalpolat, M., & Kahraman, A. (2009). A theoretical and experimental investigation of modulation sidebands of planetary gear sets. Journal of Sound and Vibration, 323(3-5), 677-696.
47. El Badaoui, M., Guillet, F., & Daniere, J. (2004). New applications of the real cepstrum to gear signals, including definition of a robust fault indicator. Mechanical Systems and Signal Processing, 18(5), 1031-1046.
48. Ashnibha, R. A. (2012). An investigation into current and vibration signatures of three phase induction motors (Doctoral dissertation, Manchester Metropolitan University.
49. Abouhnik, A. A. (2012). An Investigation into Vibration Based Techniques for Wind Turbine Blades Condition Monitoring(Doctoral dissertation, Manchester Metropolitan University).
50. Lei, Y., Lin, J., He, Z., & Zuo, M. J. (2013). A review on empirical mode decomposition in fault diagnosis of rotating machinery. Mechanical Systems and Signal Processing, 35(1-2), 108-126.
51. Antoniadou, I., Manson, G., Dervilis, N., Barszcz, T., Staszewski, W., & Worden, K. (2012, July). Condition monitoring of a wind turbine gearbox using the empirical mode decomposition method and outlier analysis. In 6th European Workshop on Structural Health Monitoring. Proceedings available online at http://www. ewshm2012. Com/Proceedings. aspx.
52. Li, H., Zheng, H., & Tang, L. (2010). Gear fault detection based on Teager-Huang transform. International Journal of Rotating Machinery, 2010.
53. Antoniadou, I., Manson, G., Dervilis, N., Barszcz, T., Staszewski, W. J., & Worden, K. (2012). Use of the Teager-Kaiser energy operator for condition monitoring of a wind turbine gearbox. In International Conference on Noise and Vibration Engineering 2012, ISMA 2012, including USD 2012: International Conference on Uncertainty in Structure Dynamics (Vol. 6, pp. 4255-4268).
54. Antoniadou, I., Manson, G., Staszewski, W. J., Barszcz, T., & Worden, K. (2015). A time–frequency analysis approach for condition monitoring of a wind turbine gearbox under varying load conditions. Mechanical Systems and Signal Processing, 64, 188-216.
55. He, Q., Kong, F., & Yan, R. (2007). Subspace-based gearbox condition monitoring by kernel principal component analysis. Mechanical Systems and Signal Processing, 21(4), 1755-1772.
56. He, Q., Yan, R., Kong, F., & Du, R. (2009). Machine condition monitoring using principal component representations. Mechanical Systems and Signal Processing, 23(2), 446-466.
57. Žvokelj, M., Zupan, S., & Prebil, I. (2011). Non-linear multivariate and multiscale monitoring and signal denoising strategy using kernel principal component analysis combined with ensemble empirical mode decomposition method. Mechanical Systems and Signal Processing, 25(7), 2631-2653.
58. Vernekar, K., Kumar, H., & Gangadharan, K. V. (2014). Gear fault detection using vibration analysis and continuous wavelet transform. Procedia Materials Science, 5, 1846-1852.
59. Ibrahim, G. R. (2011). Design and implementation of gearboxes vibration based condition monitoring system (Doctoral dissertation, The Manchester Metropolitan University).
60. Childs, P. R. (2013). Mechanical design engineering handbook. Butterworth-Heinemann.
61. Dudley, D. W. (1962). Gear handbook: the design, manufacture, and application of gears. McGraw Hill Higher Education.
62. Spur gear. (2015). Retrieved 24 Feb, 2015, from: http://www.mechanicalbooster.com/2015/02/types-of-gears.html.
63. StuffWorks,Gears(2015).Retrieved July. 2015, from: http://science.howstuffworks.com/transport/engines-equipment/gear2.htm.
64. Worm Gear. (2016). Retrieved Nov. 2016, from: https://www.nord.com/content/worm-gear-applications.
65. Lin, J., & Zuo, M. J. (2003). Gearbox fault diagnosis using adaptive wavelet filter. Mechanical systems and signal processing, 17(6), 1259-1269.

66. Lucente, M. (2008). Condition monitoring system in wind turbine gearbox. Master's thesis, KTH in cooperation with NTNU, Stockholm.
67. Engineers, N. C (2016). Retrieved Feb. 2016, from: http://www.tribology.co.uk/services/investigate/g01-0.htm.
68. Petersen, T. S. (2017). Scaling infrared femtosecond optical parametric oscillators to high average powers. University of Rochester.
69. BAM, (2016). Retrieved Feb. 2016, from: http://www.go-fast.com/trs_drive_gear_failures.htm.
70. Maekawa, K., Obikawa, T., Yamane, Y., & Childs, T. H. C. (2003). Mechanical design. Elsevier.
71. Lubrication, M. Gear Adhasive Wear (2016). Retrieved Aug. 2016, from: http://www.machinerylubrication.com/Read/150/gear-failures.
72. Dalpiaz, G., Rivola, A., & Rubini, R. (2000). Effectiveness and sensitivity of vibration processing techniques for local fault detection in gears. Mechanical systems and signal processing, 14(3), 387-412.
73. Choy, F. K., Huang, S., Zakrajsek, J., Handschuh, R. F., & Townsend, D. P. (1996). Vibration signature analysis of a faulted gear transmission system. Journal of Propulsion and Power, 12(2), 289-295.
74. Stelzner, A. D., Kammer, D. C., & Milenkovic, P. (2001). A time domain method for estimating forces applied to an unrestrained structure. Journal of vibration and acoustics, 123(4), 524-532.
75. Parloo, E., Verboven, P., Guillaume, P., & Van Overmeire, M. (2003). Force identification by means of in-operation modal models. Journal of Sound and Vibration, 262(1), 161-173.
76. Leclere, Q., Pezerat, C., Laulagnet, B., & Polac, L. (2005). Indirect measurement of main bearing loads in an operating diesel engine. Journal of Sound and Vibration, 286(1-2), 341-361.
77. Thite, A. N., & Thompson, D. J. (2003). The quantification of structure-borne transmission paths by inverse methods. Part 1: Improved singular value rejection methods. Journal of Sound and Vibration, 264(2), 411-431.
78. Moorhouse, A. T., Elliott, A. S., & Evans, T. A. (2009). In situ measurement of the blocked force of structure-borne sound sources. Journal of Sound and Vibration, 325(4-5), 679-685.
79. Kammer, D. C., & Milenkovic, P. A Time Domain Method for Estimating Forces Applied to an Unrestrained Structure.
80. Jacquelin, E., Bennani, A., & Hamelin, P. (2003). Force reconstruction: analysis and regularization of a deconvolution problem. Journal of sound and vibration, 265(1), 81-107.
81. Leclere, Q., Pezerat, C., Laulagnet, B., & Polac, L. (2005). Indirect measurement of main bearing loads in an operating diesel engine. Journal of Sound and Vibration, 286(1-2), 341-361.
82. Thite, A. N., & Thompson, D. J. (2003). The quantification of structure-borne transmission paths by inverse methods. Part 2: Use of regularization techniques. Journal of Sound and Vibration, 264(2), 433-451.
83. Elliott, A. S., Moorhouse, A. T., Huntley, T., & Tate, S. (2013). In-situ source path contribution analysis of structure borne road noise. Journal of Sound and Vibration, 332(24), 6276-6295.
84. Lennström, D., Olsson, M., Wullens, F., & Nykänen, A. (2016). Validation of the blocked force method for various boundary conditions for automotive source characterization. Applied Acoustics, 102, 108-119.
85. Ishugah, T. F., Li, Y., Wang, R. Z., & Kiplagat, J. K. (2014). Advances in wind energy resource exploitation in urban environment: A review. Renewable and sustainable energy reviews, 37, 613-626.
86. Elliott, A. S., & Moorhouse, A. T. (2010). In-situ characterisation of structure borne noise from a building mounted wind turbine. PROCEEDINGS OF ISMA2010.

87. Moorhouse, A. T., Elliott, A. S., & Meggitt, J. W. R. (2017). Using Blocked Force Data for Vibro-Acoustic Prediction and Simulation. In Dynamics of Coupled Structures, Volume 4 (pp. 115-118). Springer, Cham.
88. Gardonio, P., & Brennan, M. J. (2002). On the origins and development of mobility and impedance methods in structural dynamics. Journal of Sound and vibration, 249(3), 557-573.
89. Klerk, D. D., Rixen, D. J., & Voormeeren, S. N. (2008). General framework for dynamic substructuring: history, review and classification of techniques. AIAA journal, 46(5), 1169-1181.
90. Meggitt. J. W, E., A. S., Moorhouse, A.T, Vibration assemblies and their use in the prediction of Vibro-acoustic responses.
91. Wang, D., Tsui, K. L., & Miao, Q. (2017). Prognostics and Health Management: A Review of Vibration based Bearing and Gear Health Indicators. IEEE Access.
92. Yang, M., & Makis, V. (2010). ARX model-based gearbox fault detection and localization under varying load conditions. Journal of Sound and Vibration, 329(24), 5209-5221.
93. He, Q., Liu, Y., & Kong, F. (2010). Machine fault signature analysis by midpoint-based empirical mode decomposition. Measurement Science and Technology, 22(1), 015702.
94. Randall, R. B., & Antoni, J. (2011). Rolling element bearing diagnostics—A tutorial. Mechanical systems and signal processing, 25(2), 485-520.
95. Shen, C., Wang, D., Kong, F., & Peter, W. T. (2013). Fault diagnosis of rotating machinery based on the statistical parameters of wavelet packet paving and a generic support vector regressive classifier. Measurement, 46(4), 1551-1564.
96. Elliott, A., & Moorhouse, A. T. (2008). Characterisation of structure borne sound sources from measurement in-situ. Journal of the Acoustical Society of America, 123(5), 3176.
97. Elliott, A., Moorhouse, A., & Pavic, G. (2007, September). Characterisation of a structure-borne sound source using independent and in-situ measurement. In ICA 19.
98. Rubin, S. (1964). Transmission matrices for vibration and their relation to admittance and impedance. Journal of Engineering for Industry, 86(1), 9-21.
99. Fulford, R. A., & Gibbs, B. M. (1999). Structure-borne sound power and source characterization in multi-point-connected systems, part 2: About mobility functions and free velocities. Journal of Sound and Vibration, 220(2), 203-224.
100. Evans, T. (2010). Estimation of uncertainty in the structure-borne sound power transmission from a source to a receiver (Doctoral dissertation, Salford: University of Salford).
101. Elliott, A. S. (2009). Characterisation of structure borne sound sources in-situ (Doctoral dissertation, University of Salford).
102. O'hara, G. J. (1967). Mechanical impedance and mobility concepts. The journal of the Acoustical Society of America, 41(5), 1180-1184.
103. Petersson, B. A. T., & Gibbs, B. M. (2000). Towards a structure-borne sound source characterization. Applied Acoustics, 61(3), 325-343.
104. Höller, C. (2010). Characterization of structure-borne sound sources in buildings (Doctoral dissertation, Diploma Thesis. Institut für Technische Akustik, RWTH Aachen University).
105. Moorhouse, A. T., Elliott, A. S., & Evans, T. A. (2009). In situ measurement of the blocked force of structure-borne sound sources. Journal of Sound and Vibration, 325(4-5), 679-685.
106. Tarantola, A. (1987). Inverse problem theory: Methods for data fitting and model parameter estimation. Elsevier, Netherlands, p. 386.
107. Wilkinson, J. H. (1971). Introduction to Part II, The Algebraic Eigenvalue Problem, Handbook for Automatic Computation, Vol II, Linear Algebra, JH Wilkinson and C. Reinsch.
108. Van Loan, C. F. (1996). Matrix computations (Johns Hopkins studies in mathematical sciences).
109. Reusken., W. (2008). Numerik für Ingenieure und Naturwissenschaftler. 2nd edition.

110. Höller, C. (2013). Indirect methods of obtaining activity and mobility of structure-borne sound sources (Doctoral dissertation, University of Liverpool).
111. Rakha, M. A. (2004). On the Moore–Penrose generalized inverse matrix. Applied Mathematics and Computation, 158(1), 185-200.
112. Penrose, R. (1955, July). A generalized inverse for matrices. In Mathematical proceedings of the Cambridge philosophical society (Vol. 51, No. 3, pp. 406-413). Cambridge University Press.
113. Bartlett, F. D., & Flannelly, W. G. (1979). Model verification of force determination for measuring vibratory loads. Journal of the American Helicopter Society, 24(2), 10-18.
114. Hillary, B. (1983). Indirect measurement of vibration excitation forces (Doctoral dissertation, Imperial College London (University of London)).
115. Powell, R. E. (1982). Multichannel inverse filtering of machinery vibration signals (Doctoral dissertation, Massachusetts Institute of Technology).
116. Dobson, B. J., & Rider, E. (1990). A review of the indirect calculation of excitation forces from measured structural response data. Proceedings of the Institution of Mechanical Engineers, Part C: Mechanical Engineering Science, 204(2), 69-75.
117. Blau, M. (2000, August). Inverse force synthesis: state of the art and future research. In Proceedings of Inter-Noise.
118. Roggenkamp, T. J. (1995). An investigation of the indirect measurement of broadband force spectra.
119. Elliot, A. S., & Moorhouse, A. T. (2012, April). A quarter vehcile transfer path analysis by in-situ measurement. In INTER-NOISE and NOISE-CON Congress and Conference Proceedings (Vol. 244, No. 1, pp. 807-813). Institute of Noise Control Engineering.
120. Lai, H. Y. (2012, August). Integrated reception-plate inverse-force test method for commercial airplane equipment structure-borne noise specification and qualification. In INTER-NOISE and NOISE-CON Congress and Conference Proceedings (Vol. 2012, No. 3, pp. 8469-8478). Institute of Noise Control Engineering.
121. Kohrs, T. and R. Kirchner (2012). Direct vs. in-situ structure-borne sound source characterization Effect of simplifications on power transmission for a typical railway vehicle source. In Proceedings of ICSV19, Vilnius.
122. Gajdatsy, P. (2011). Advanced transfer path analysis methods. KU Leuven, Department of Mechanical Engineering–PhD Thesis.
123. Blau, M. (1999). Indirect measurement of multiple excitation force spectra by FRF matrix inversion: influence of errors in statistical estimates of FRFs and response spectra. Acta Acustica united with Acustica, 85(4), 464-479.
124. Blau, M. (1998). Error considerations in inverse force synthesis: What is different with respect to sole measurements of FRFs and response spectra. In Proceedings of Euronoise(Vol. 98, pp. 405-410).
125. Fabunmi, J. A. (1986). Effects of structural modes on vibratory force determination by the pseudoinverse technique. AIAA journal, 24(3), 504-509.
126. Thite, A. N. (2003). Inverse determination of structure-borne sound sources (Doctoral dissertation, University of Southampton).
127. Thite, A. N., & Thompson, D. J. (2003). The quantification of structure-borne transmission paths by inverse methods. Part 1: Improved singular value rejection methods. Journal of Sound and Vibration, 264(2), 411-431.
128. Choi, H. G., Thite, A. N., & Thompson, D. J. (2006). A threshold for the use of Tikhonov regularization in inverse force determination. Applied Acoustics, 67(7), 700-719.
129. Choi, H. G., Thite, A. N., & Thompson, D. J. (2007). Comparison of methods for parameter selection in Tikhonov regularization with application to inverse force determination. Journal of Sound and Vibration, 304(3-5), 894-917.

130. Blau, M. (1997). Indirect force spectra identification by FRF matrix inversion: a reliable approach based on quantitative error models. In INTERNOISE (Vol. 3, pp. 1387-1390). Noise control foundation.
131. Zheng, S., Zhou, L., Lian, X., & Li, K. (2011). Coherence analysis of the transfer function for dynamic force identification. Mechanical Systems and Signal Processing, 25(6), 2229-2240.
132. Dally, J. W., Riley, W. F., & McConnell, K. G. (1984). Instrumentation for engineering measurements.
133. Ashnibha, R. A. (2012). An investigation into current and vibration signatures of three phase induction motors (Doctoral dissertation, Manchester Metropolitan University).
134. Mas, P., Sas, P., & Wyckaert, K. (1994, September). Indirect force determination based upon matrix inversion: A study on statistical and deterministic accuracy. In Proceedings of the International Conference on Noise and Vibration Engineering (pp. 1049-1065).
135. Stevens, P. W., Hall, D., & Smith, E. (1996, June). A multidisciplinary research approach to rotorcraft health and usage monitoring. In Proc. Annual Forum, American Helicopter Society (Vol. 2, pp. 1732-1751).
136. Forrester, B. D. (1996). Advanced vibration analysis techniques for fault detection and diagnosis in geared transmission systems (Doctoral dissertation, Swinburne University of Technology).
137. Lebold, M., McClintic, K., Campbell, R., Byington, C., & Maynard, K. (2000, May). Review of vibration analysis methods for gearbox diagnostics and prognostics. In Proceedings of the 54th meeting of the society for machinery failure prevention technology (Vol. 634, p. 16).
138. Tandon, N., & Choudhury, A. (1999). A review of vibration and acoustic measurement methods for the detection of defects in rolling element bearings. Tribology international, 32(8), 469-480.
139. Parey, A., El Badaoui, M., Guillet, F., & Tandon, N. (2006). Dynamic modelling of spur gear pair and application of empirical mode decomposition-based statistical analysis for early detection of localized tooth defect. Journal of sound and vibration, 294(3), 547-561.
140. Solé, J., Turiel, A., & Llebot, J. E. (2007). Using empirical mode decomposition to correlate paleoclimatic time-series. Natural Hazards and Earth System Science, 7(2), 299-307.
141. Huang, N. E., Wu, M. L. C., Long, S. R., Shen, S. S., Qu, W., Gloersen, P., & Fan, K. L. (2003, September). A confidence limit for the empirical mode decomposition and Hilbert spectral analysis. In Proceedings of the Royal Society of London A: Mathematical, Physical and Engineering Sciences (Vol. 459, No. 2037, pp. 2317-2345). The Royal Society.
142. Huang, N. E. (2014). Hilbert-Huang transform and its applications (Vol. 16). World Scientific.
143. Wu, Z., & Huang, N. E. (2004, June). A study of the characteristics of white noise using the empirical mode decomposition method. In Proceedings of the Royal Society of London A: Mathematical, Physical and Engineering Sciences(Vol. 460, No. 2046, pp. 1597-1611). The Royal Society.
144. Gao, Q., Duan, C., Fan, H., & Meng, Q. (2008). Rotating machine fault diagnosis using empirical mode decomposition. Mechanical Systems and Signal Processing, 22(5), 1072-1081.
145. Abouhnik, A., & Albarbar, A. (2012). Wind turbine blades condition assessment based on vibration measurements and the level of an empirically decomposed feature. Energy Conversion and Management, 64, 606-613.
146. Searle, S. R., & Khuri, A. I. (2017). Matrix algebra useful for statistics. John Wiley & Sons.

Appendix (A)

Review of matrix notation and properties

Review of matrix notation and properties is represented in this appendix. For a comprehensive treatment, see literature [146].

1. **Definitions**

   An mx1 column vector x is defined as:

$$\mathrm{x}_{mx1} = \begin{pmatrix} x_1 \\ \vdots \\ x_m \end{pmatrix}$$

An mxn matrix $\bar{\mathbf{H}}$ is defined as:

$$\bar{\mathbf{H}}_{mxn} = \begin{pmatrix} a_{11} & a_{12} & \dots & a_{1n} \\ a_{21} & a_{22} & \ddots & \vdots \\ \vdots & \vdots & \ddots & \vdots \\ a_{m1} & a_{m2} & \dots & a_{mn} \end{pmatrix}$$

Transposed matrix $\bar{\mathbf{H}}^{\mathbf{T}}$ and Hermitian transpose$\mathbf{H}^{\mathbf{H}}$**:**

$$\bar{\mathbf{H}}^{\mathbf{T}} = \begin{pmatrix} a_{11} & a_{12} & \dots & a_{1n} \\ a_{21} & a_{22} & \ddots & \vdots \\ \vdots & \vdots & \ddots & \vdots \\ a_{m1} & a_{m2} & \dots & a_{mn} \end{pmatrix} \quad \bar{\mathbf{H}}^{\mathbf{H}} = (\bar{\mathbf{H}}^{*})^{\mathbf{T}} = \begin{pmatrix} a^{*}{}_{11} & a^{*}{}_{12} & \dots & a^{*}{}_{1n} \\ a^{*}{}_{21} & a^{*}{}_{22} & \ddots & \vdots \\ \vdots & \vdots & \ddots & \vdots \\ a^{*}{}_{m1} & a^{*}{}_{m2} & \dots & a^{*}{}_{mn} \end{pmatrix}$$

Identity matrix I and diagonal matrix S:

$$\mathbf{I}_{nxn} = \begin{pmatrix} 1 & 0 & \dots & 0 \\ 0 & 1 & \ddots & \vdots \\ \vdots & \vdots & \ddots & \vdots \\ 0 & 0 & \dots & 1 \end{pmatrix} \quad \mathbf{S}_{nxn} = \begin{pmatrix} \sigma_{11} & 0 & \dots & 0 \\ 0 & \sigma_{22} & \ddots & \vdots \\ \vdots & \vdots & \ddots & \vdots \\ 0 & 0 & \dots & \sigma_{nn} \end{pmatrix}$$

Symmetric matrix:

$$\bar{\mathbf{H}} = \bar{\mathbf{H}}^{\mathbf{T}}$$

Orthogonal matrix:

$$\bar{\mathbf{H}} = \bar{\mathbf{H}}^{-\mathbf{T}}$$

Unitary matrix:

$$\bar{\mathbf{H}} = (\bar{\mathbf{H}}^{*})^{-\mathbf{T}}$$

The inverse $\bar{\mathbf{H}}^{-\mathbf{1}}$ of an nxn matrix $\bar{\mathbf{H}}$ is defined such that

$$\bar{\mathbf{H}}^{-\mathbf{1}}\bar{\mathbf{H}} = \bar{\mathbf{H}}\bar{\mathbf{H}}^{-\mathbf{1}} = \mathbf{I}$$

The norm of a vector or matrix is a measure of their length or size. Various definitions exist; one of the most important is the p-norm:

$$\|x\|_{\mathrm{p}} = \left(\sum_{i=1}^{n} |x_i|^p\right)^{1/p}$$

$$\|\mathrm{H}\|_{\mathrm{p}} = \max_{x \neq 0} \frac{\|\mathrm{H}x\|_{\mathrm{p}}}{\|x\|_{\mathrm{p}}}$$

Setting p=2 give the Euclidean vector norm and the spectral matrix norm:

$$\|x\|_2 = \sqrt{\mathrm{x}^{\mathrm{H}}\mathrm{x}} = \sqrt{|x_1|^2 + \cdots |x_n|^2}$$

$$\|\mathrm{A}\|_2 = \sqrt{\lambda_{max\left(\mathrm{A}^{\mathrm{H}}\mathrm{A}\right)}} = \sigma_{malx}(\mathrm{H})$$

The **rank** of a matrix indicates the number of linearly independent rows or columns

A. 2 matrix identities

Matrices must conform for multiplication:

$$\bar{\mathbf{H}}_{\mathrm{mxn}}\, \mathrm{z}_{\mathrm{nxp}} = \mathrm{C}_{\mathrm{mxp}}$$

Some important relationships regarding inverse and transposed matrices [146]:

$$(\mathbf{Hz})^{-} = \mathbf{z^{-1}}\, \bar{\mathbf{H}}^{\mathbf{-1}}$$

$$(\bar{\mathbf{H}}\mathbf{zC})^{-} = \mathbf{C^{-1}z^{-1}}\, \bar{\mathbf{H}}^{\mathbf{-1}}$$

$$(\bar{\mathbf{H}}^{\mathbf{T}})^{\mathbf{-1}} = (\bar{\mathbf{H}}^{\mathbf{-1}})^{\mathbf{T}}$$

$$(\bar{\mathbf{H}} + \mathbf{z})^{\mathbf{T}} = \bar{\mathbf{H}}^{\mathbf{T}} + \mathbf{z}^{\mathbf{T}}$$

$$(\bar{\mathbf{H}}\mathbf{z})^{\mathbf{T}} = \mathbf{z}^{\mathbf{T}}\, \bar{\mathbf{H}}^{\mathbf{T}}$$

$$(\bar{\mathbf{H}}\mathbf{zC})^{\mathbf{T}} = \mathbf{C}^{\mathbf{T}}\mathbf{z}^{\mathbf{T}}\, \bar{\mathbf{H}}^{\mathbf{T}}$$

$$(\bar{\mathbf{H}}^{\mathbf{-1}} + \mathbf{z}^{\mathbf{-1}})^{\mathbf{-1}} = \bar{\mathbf{H}}(\bar{\mathbf{H}} + \mathbf{z})^{\mathbf{-1}}$$

$$= \mathbf{z}(\bar{\mathbf{H}} + \mathbf{z})^{\mathbf{-1}}\bar{\mathbf{H}}$$

Appendix (B)

Blocked forces based on an artificial excitation

Figures below show the reciprocities of some accelrances

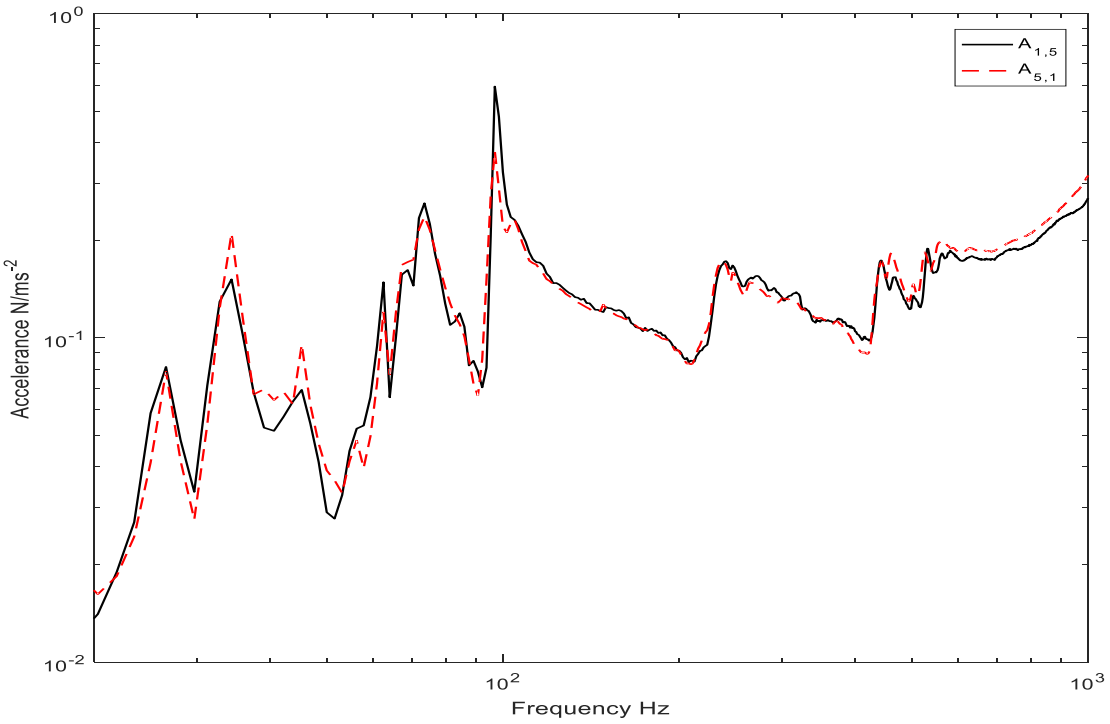

Reciprocity of two accelerances $A_{1,5}$ and $A_{5,1}$

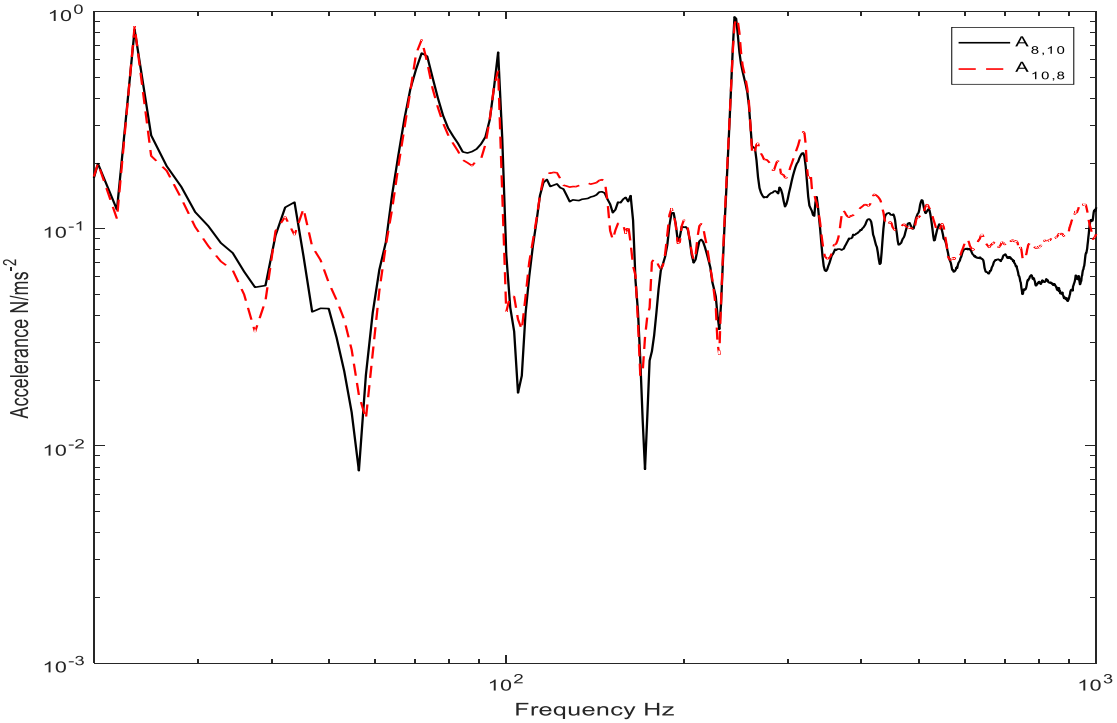

Reciprocity of two accelerances $A_{8,10}$ and $A_{10,8}$

Blocked forces based on real operational data

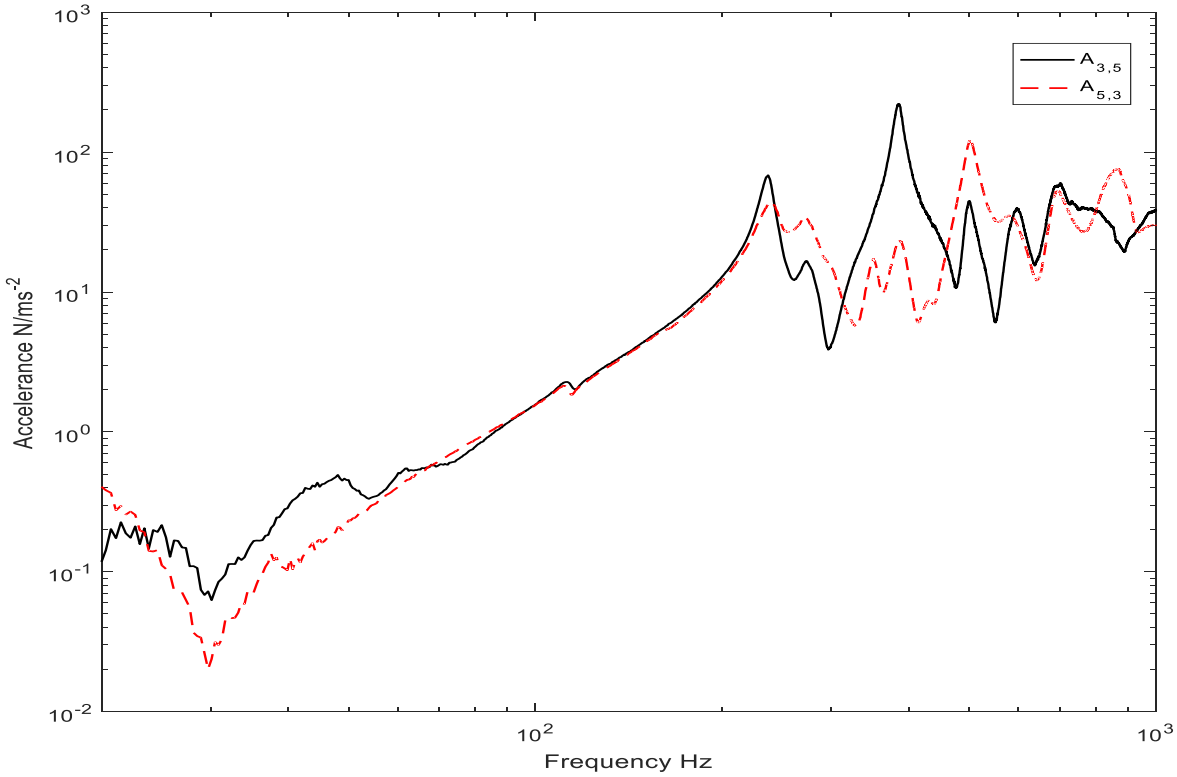

Reciprocity of two accelerances $A_{3,5}$ and $A_{5,3}$

Appendix (C)

The following figures show the Decomposed signals for first and second fault using the aluminium cover at 550 rpm and FFT plots of each IMF.

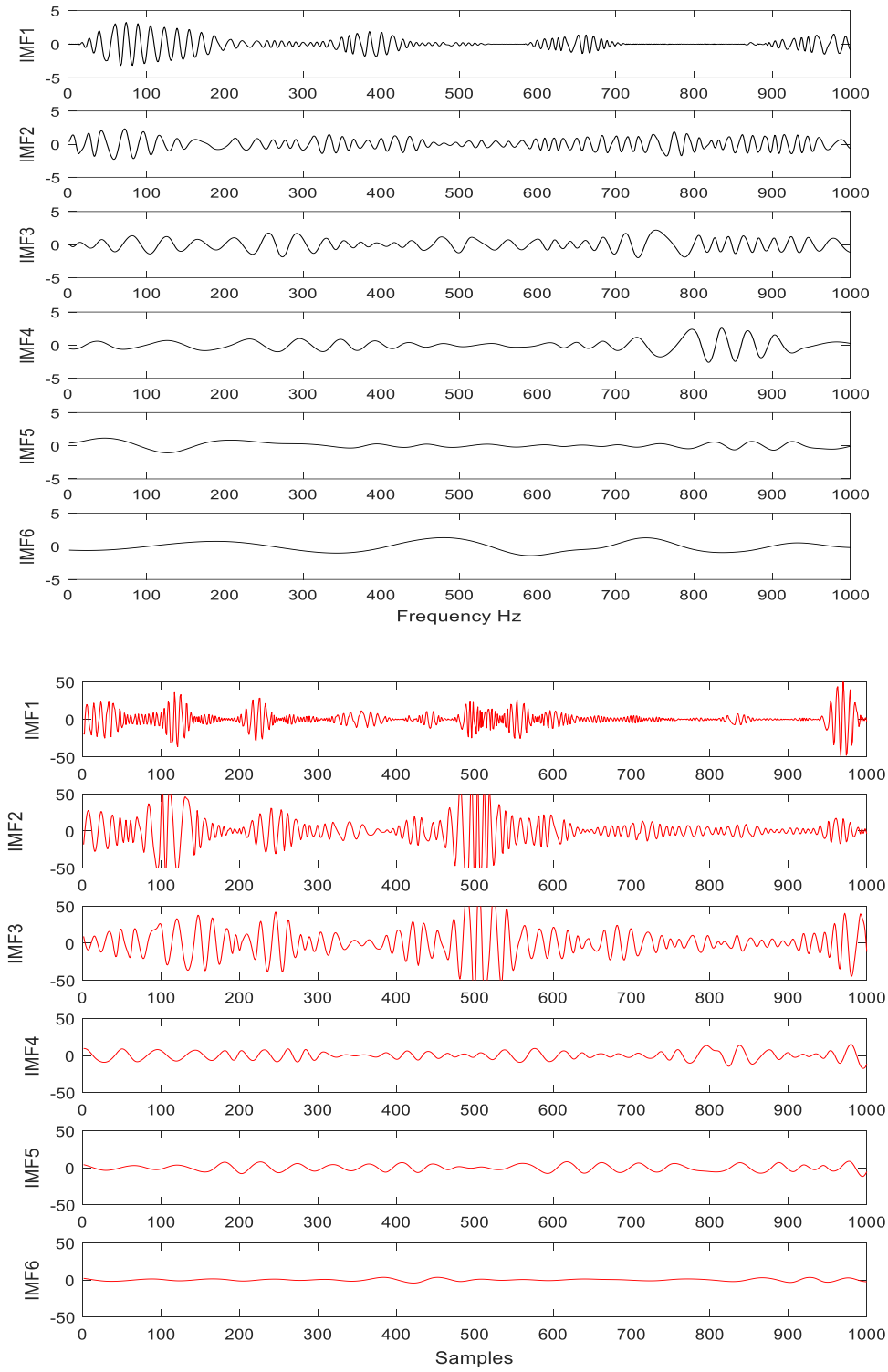

Decomposition of experimental gear vibration signal into intrinsic mode functions for faulty condition using aluminium cover at 550 rpm

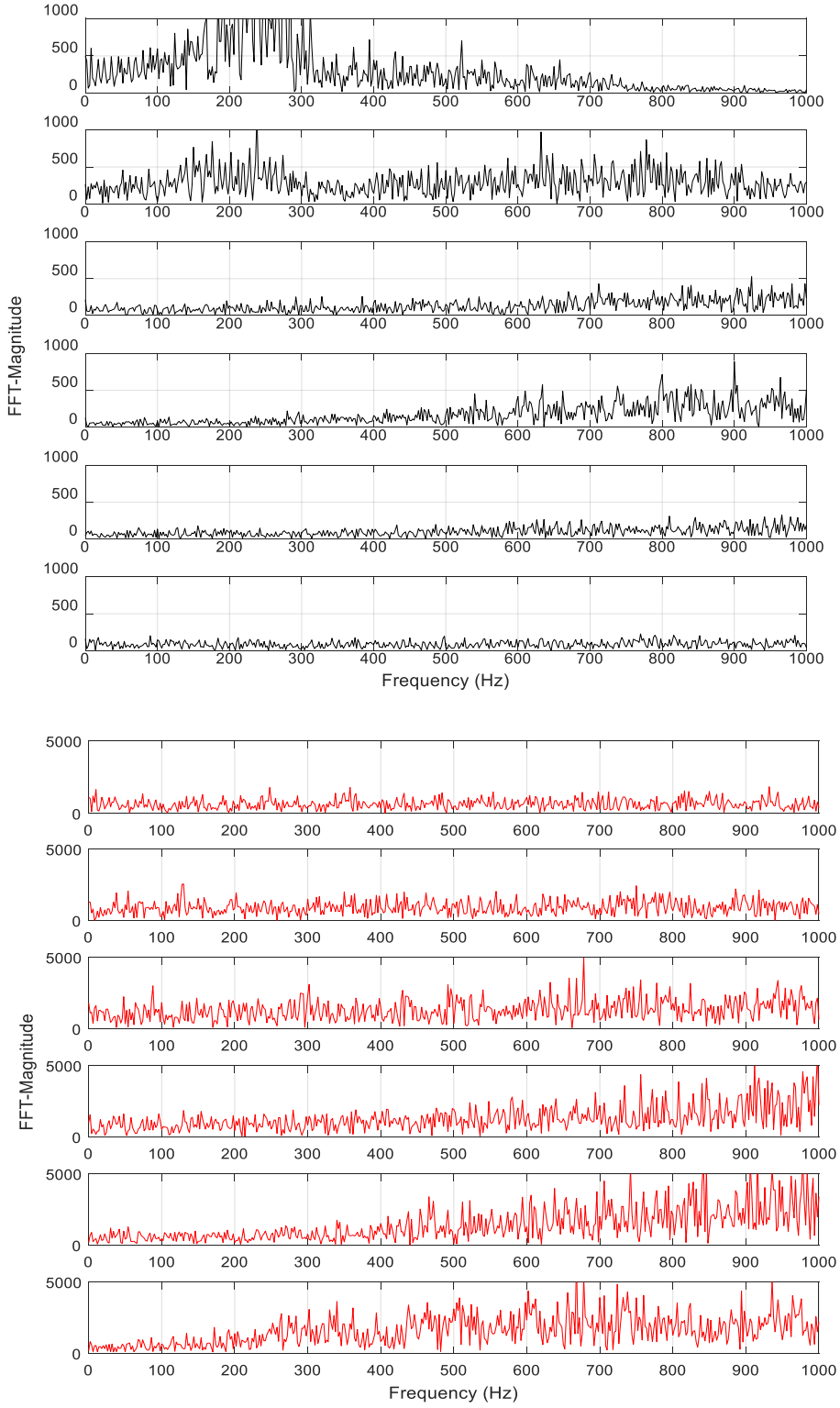

Fast Fourier transform applied on each IMF; aluminium cover, for first and second fault respectively at 550 rpm

The following figures show the Decomposed signals for first and second fault using the aluminium cover at 850 rpm and FFT plots of each IMF.

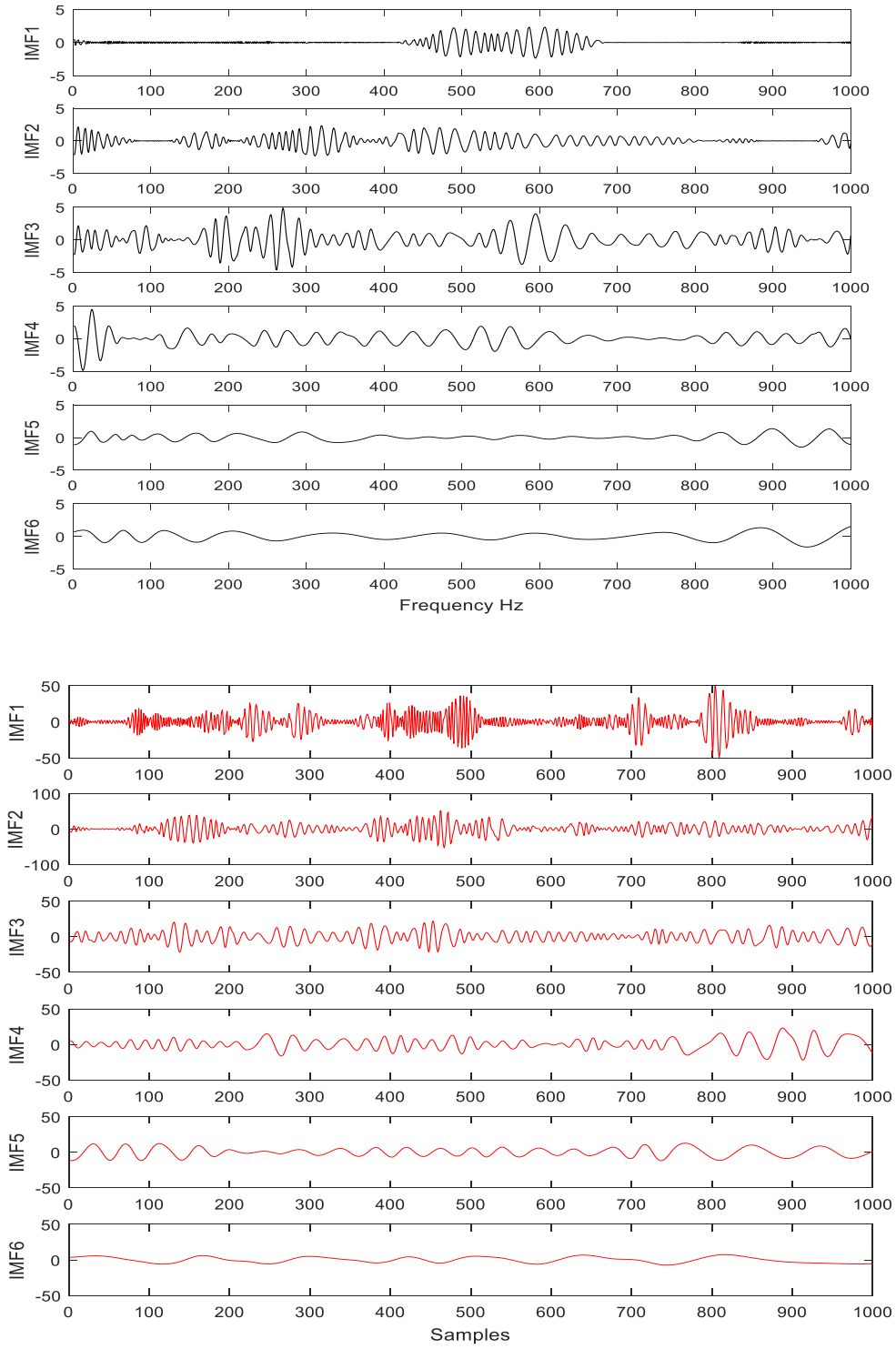

Decomposition of experimental gear vibration signal into intrinsic mode functions for faulty condition using aluminium cover at 850 rpm

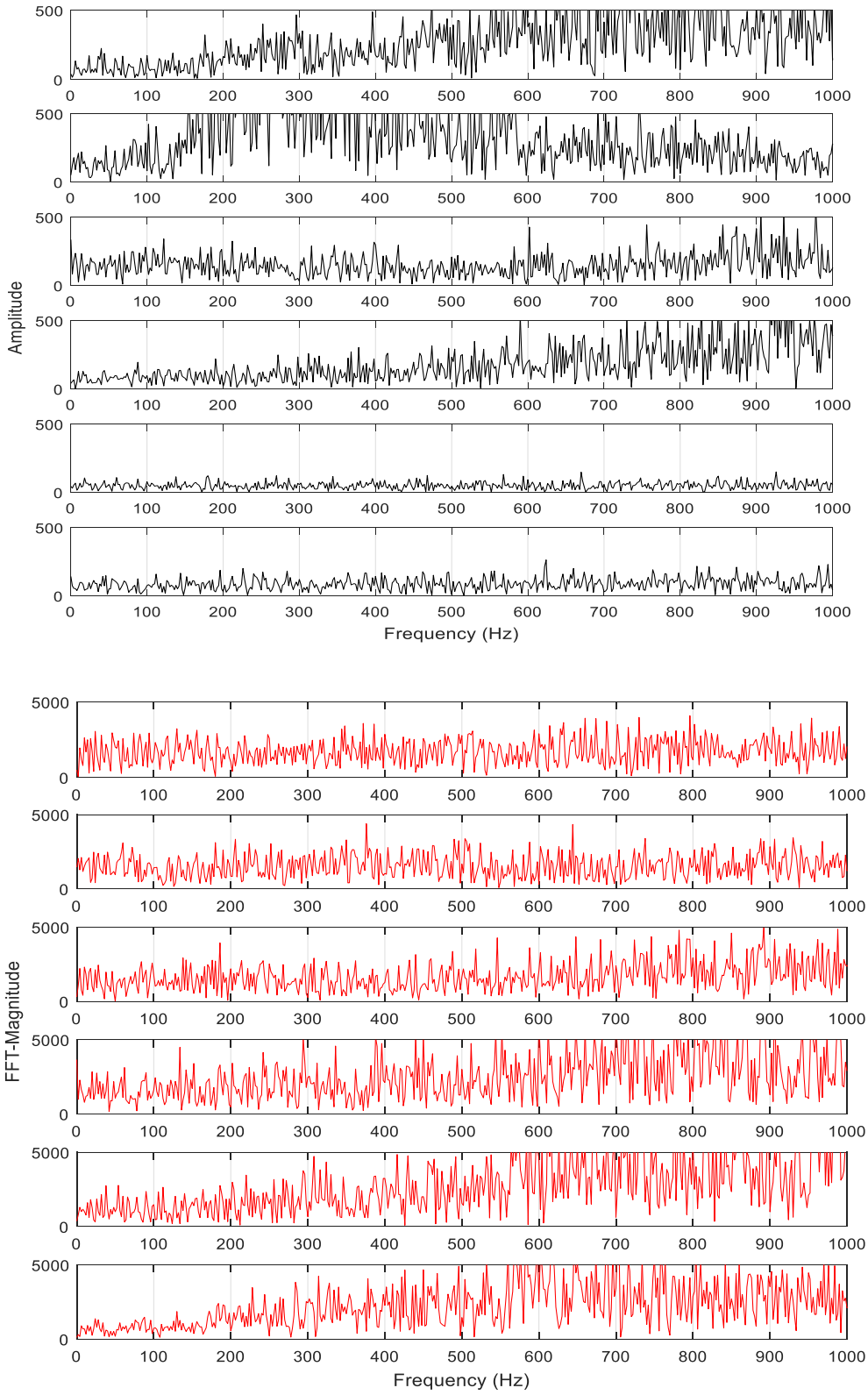

Fast Fourier transform applied on each IMF; aluminium cover, for first and second fault respectively at 850 rpm

The following figures show the Decomposed signals for first and second fault using the steel cover at 550 rpm and FFT plots of each IMF.

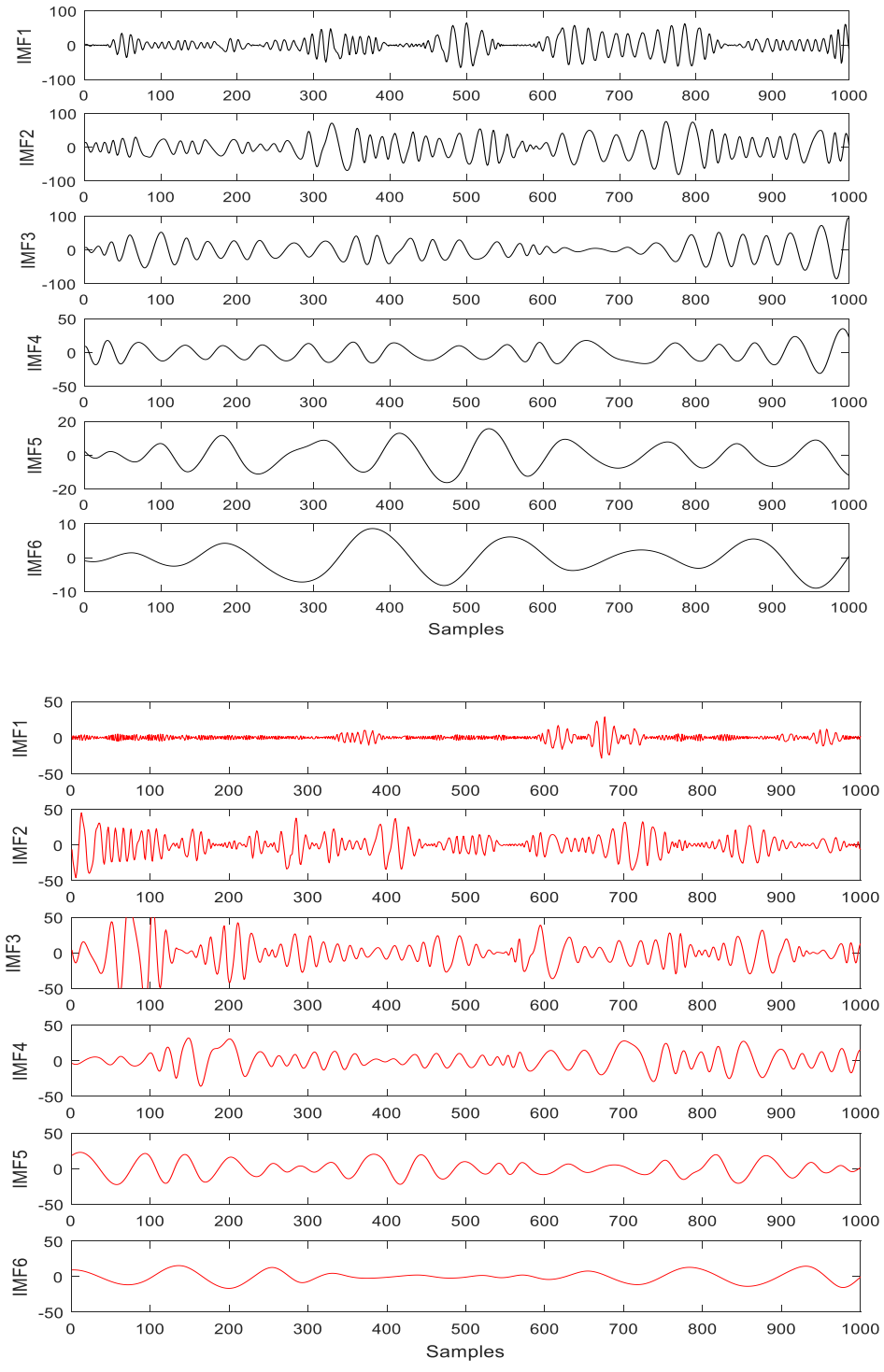

Decomposition of experimental gear vibration signal into intrinsic mode functions for faulty condition using steel cover at 550 rpm

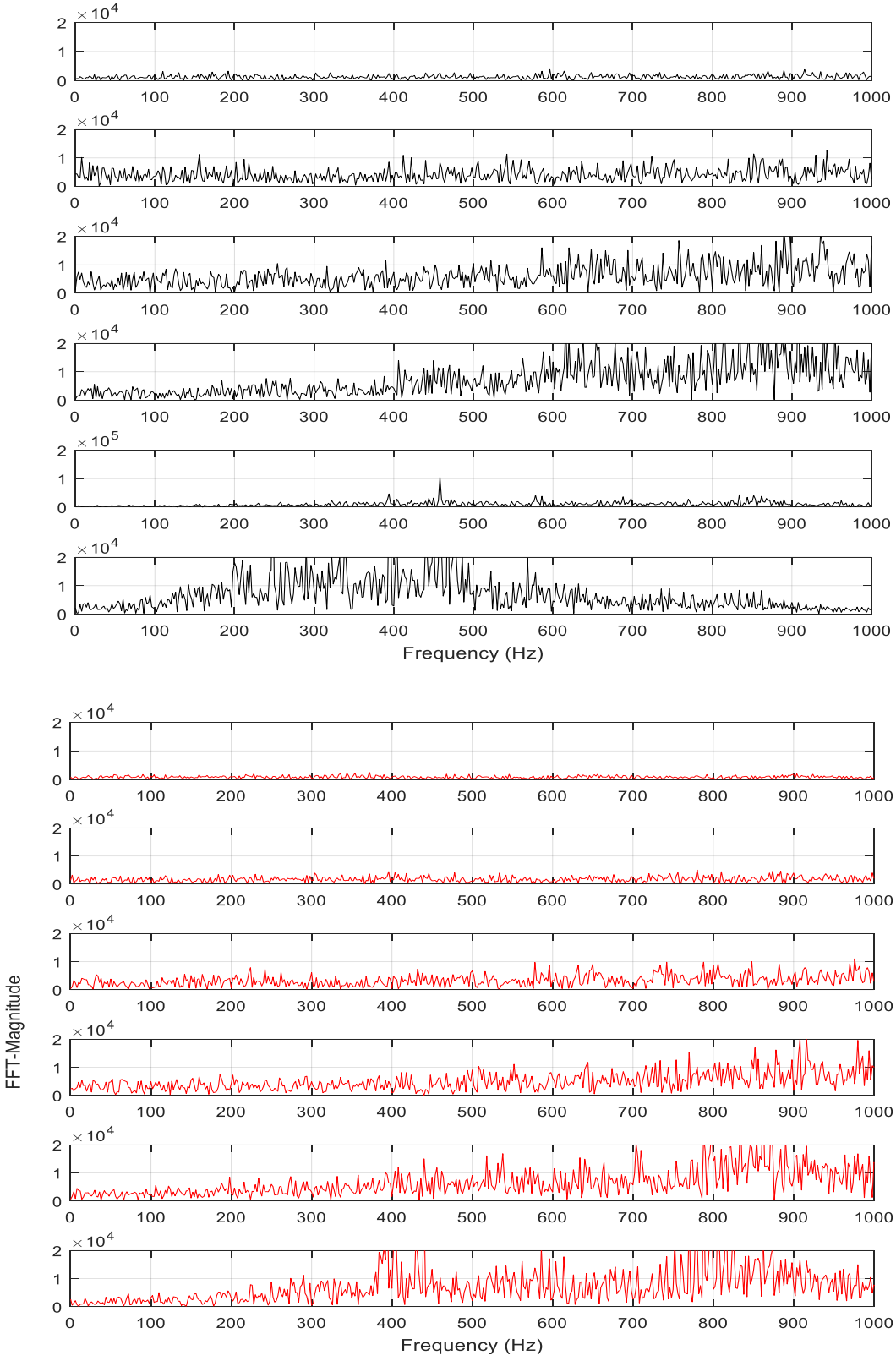

Fast Fourier transform applied on each IMF; steel cover, for first and second fault respectively at 550 rpm

The following figures show the Decomposed signals for first and second fault using the steel cover at 850 rpm and FFT plots of each IMF.

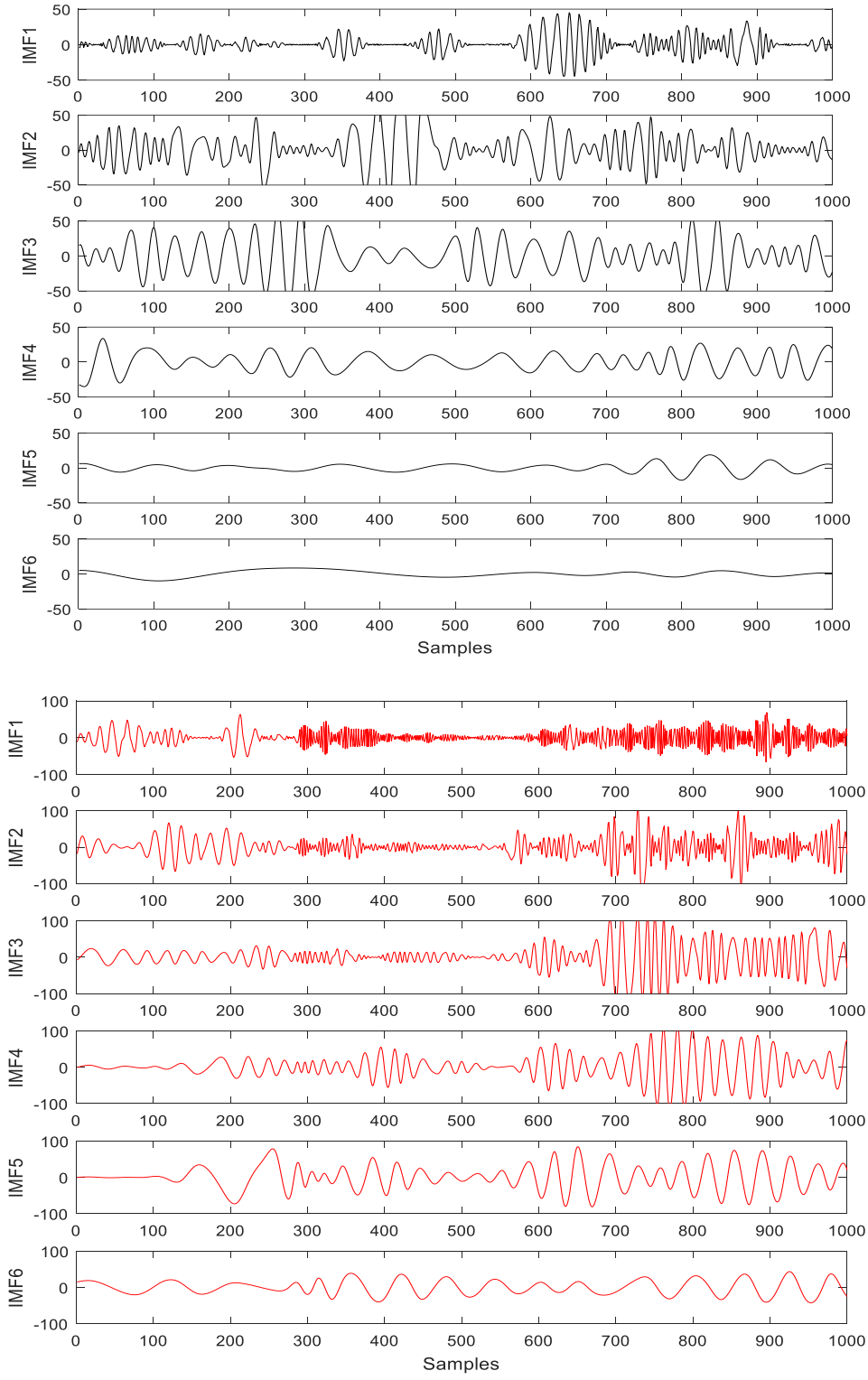

Decomposition of experimental gear vibration signal into intrinsic mode functions for faulty condition using steel cover at 850 rpm

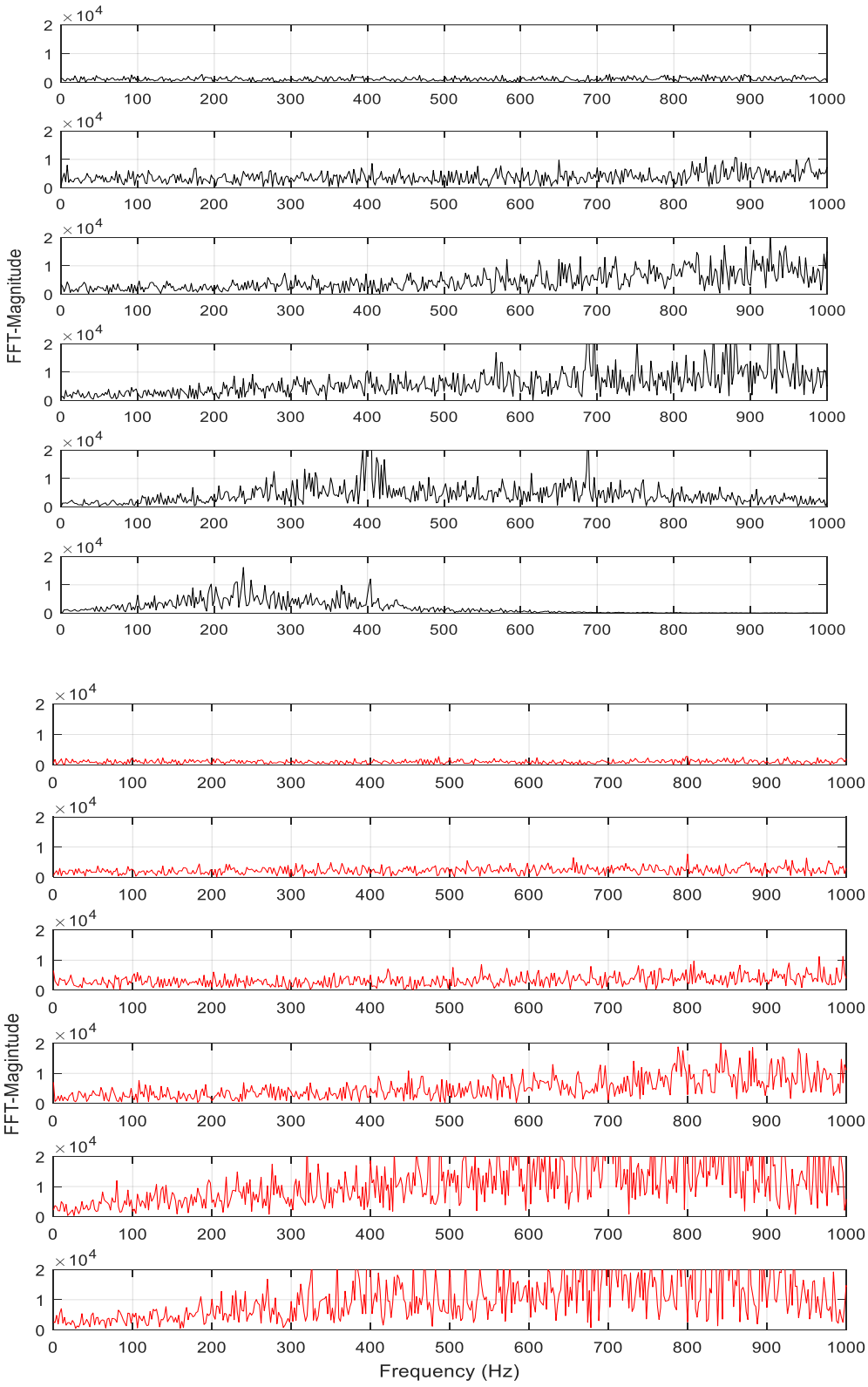

Fast Fourier transform applied on each IMF; steel cover, for first and second fault respectively at 850 rpm

The figures show the Blocked force signals for first assembly and at two different speeds (550 and 850rpm)

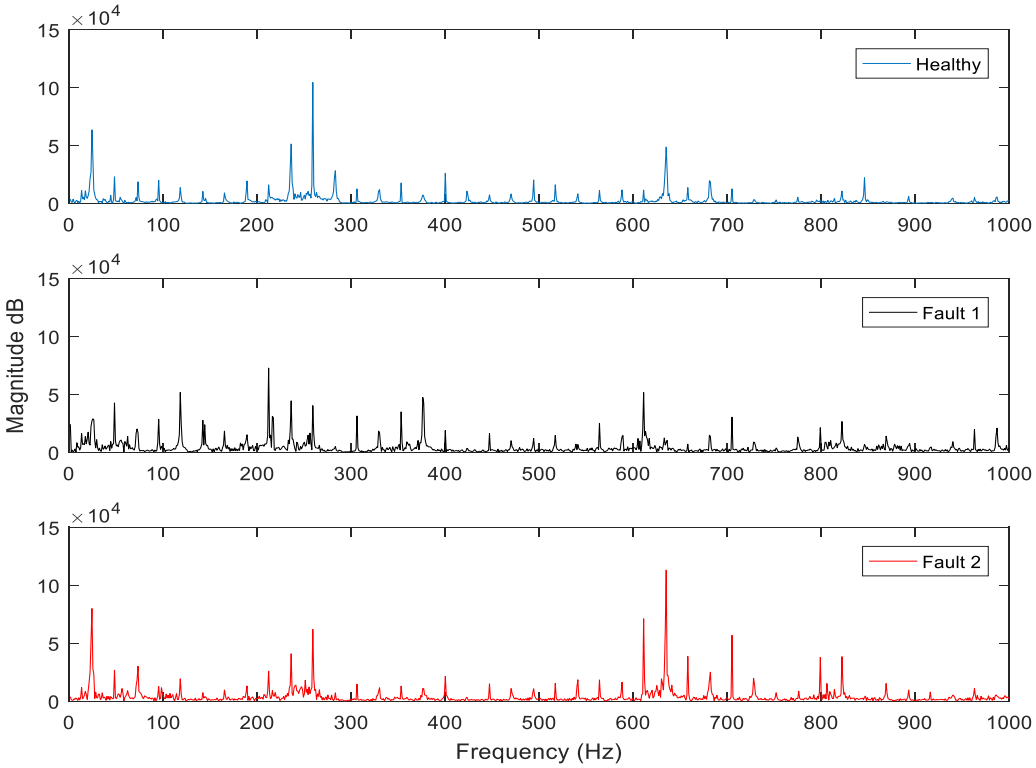

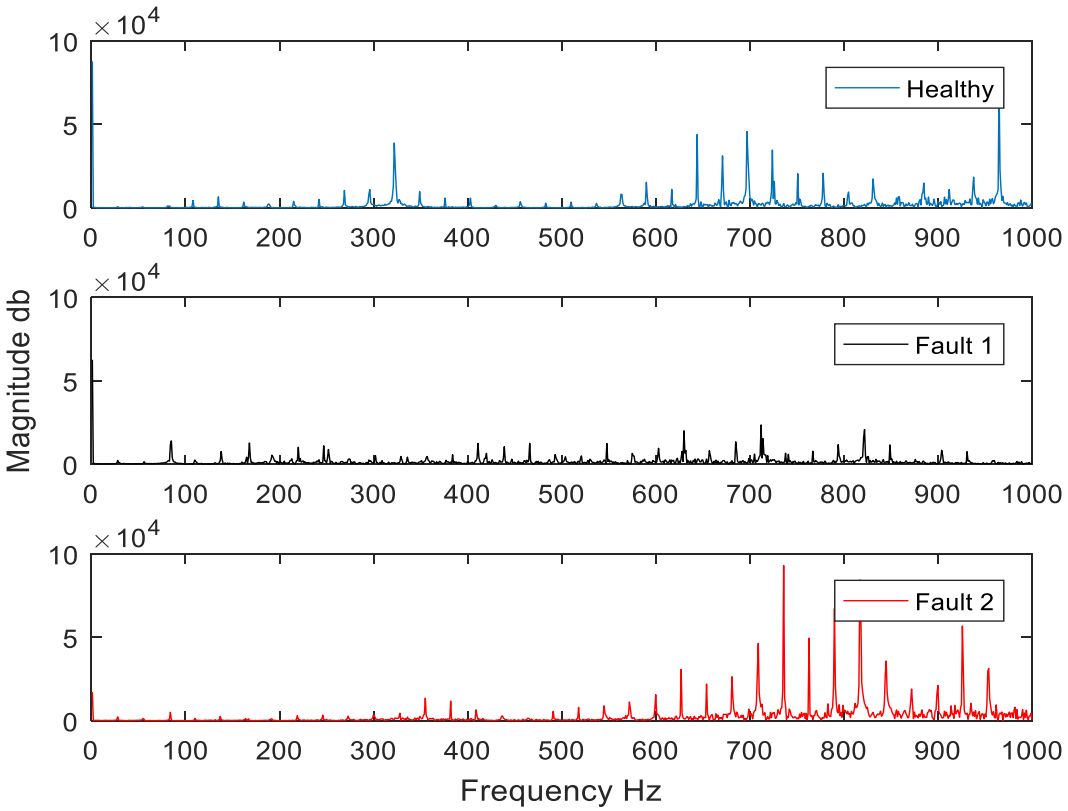

The figures show the Blocked force signals for the second assembly and at two different speeds (550 and 850rpm)

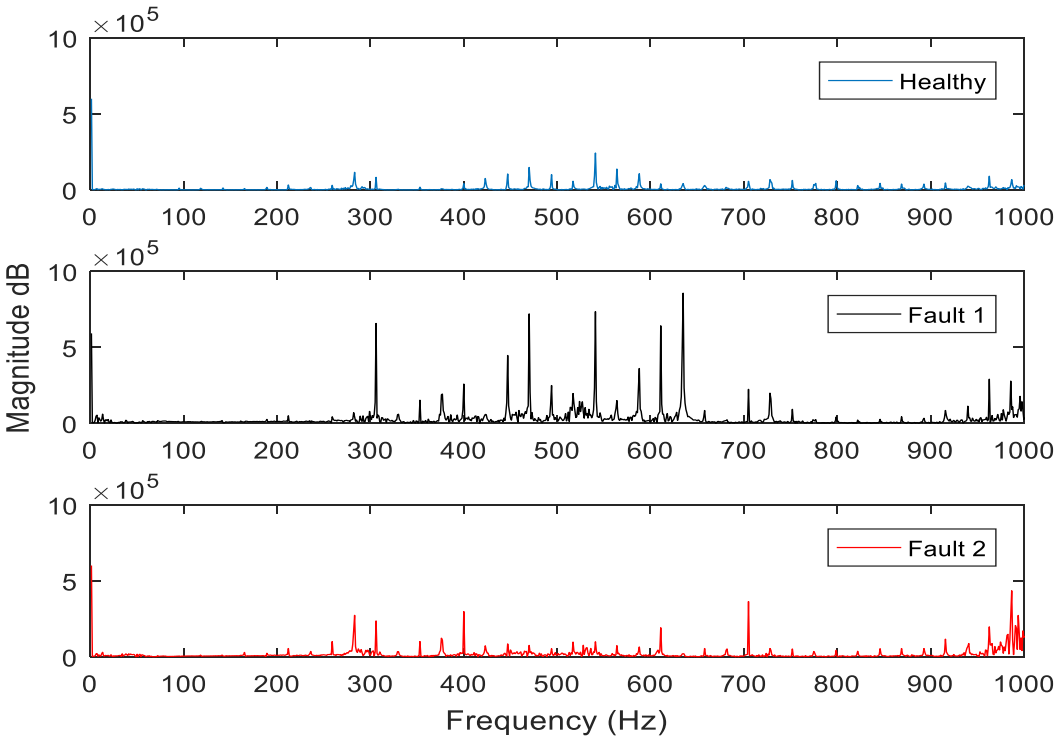

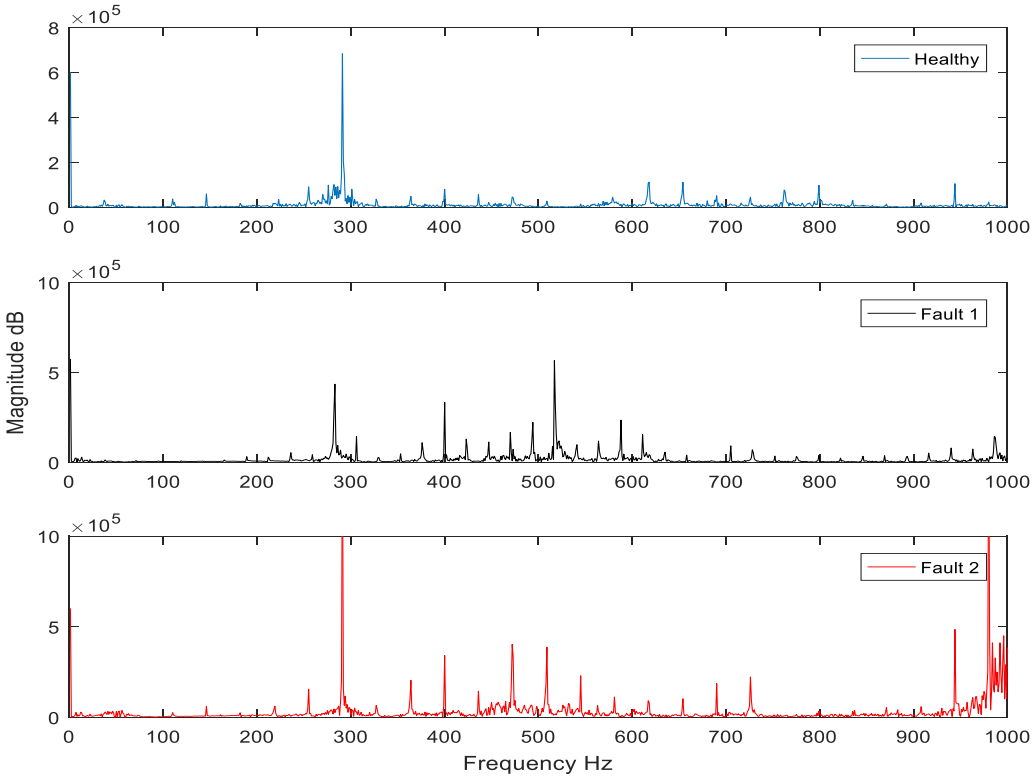
×10^5
Healthy
Fault 1
Fault 2
Magnitude dB
Frequency Hz
0
100
200
300
400
500
600
700
800
900
1000
2
4
5
6
8
10